

ISHAM, LINCOLN & BEALE
COUNSELORS AT LAW

DOCKETED
USNRC

THREE FIRST NATIONAL PLAZA
CHICAGO, ILLINOIS 60602
TELEPHONE 312 558-7500
TELEX 2-5288

'83 SEP 15 A11:19

EDWARD S. ISHAM 1872-1902
ROBERT T. LINCOLN 1872-1889
WILLIAM G. BEALE 1885-1923

WASHINGTON OFFICE
1120 CONNECTICUT AVENUE, N.W.
SUITE 840
WASHINGTON, D.C. 20036
202 833-9730

OFFICE OF SECRETARY
DOCKETING & SERVICE
BRANCH

September 13, 1983

In the Matter of)
)
CONSUMERS POWER COMPANY) Docket Nos. 50-329-OM
) 50-330-OM
) 50-329-OL
(Midland Plant, Units 1) 50-330-OL
and 2))

Charles Bechhoefer, Esq.
Atomic Safety & Licensing
Board Panel
U.S. Nuclear Regulatory Com-
mission
Washington, D. C. 20555

Dr. Jerry Harbour
Atomic Safety & Licensing
Board Panel
U.S. Nuclear Regulatory Com-
mission
Washington, D. C. 20555

Dr. Frederick P. Cowan
6152 N. Verde Trail
Apt. B-125
Boca Raton, Florida 33433

Dear Administrative Judges:

Enclosed is Volume IV of the Seismic Margin
Review, which deals with the Service Water Pump Structure.

Sincerely,

Philip P. Steptoe

PPS:es

enc.

cc Service List



**Consumers
Power
Company**

Frederick W Buckman
Executive Manager
Midland Project Office

General Offices: 1945 West Parnall Road, Jackson, MI 49201 • (517) 788-1933

September 2, 1983

Harold R Denton, Director
Office of Nuclear Reactor Regulation
US Nuclear Regulatory Commission
Washington, DC 20555

MIDLAND ENERGY CENTER
MIDLAND DOCKET NOS 50-329, 50-330
SEISMIC MARGIN REVIEW REPORT
FILE: B3.7.1 SERIAL: 25494

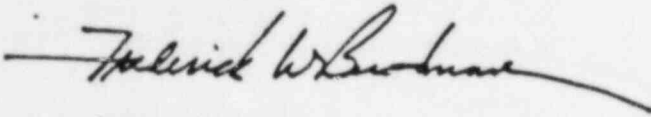
ENCLOSURE: VOLUME IV - SERVICE WATER PUMP STRUCTURE (25 COPIES)

REFERENCE: LETTER FROM J W COOK TO H R DENTON
SERIAL 21010, DATED FEBRUARY 4, 1983

As an attachment to our letter, Serial 21010, dated February 4, 1983, we submitted the criteria for the Seismic Margin Review, Volume I, for the Staff's review and it was subsequently discussed in a meeting on February 8, 1983 in Bethesda. The firm of Structural Mechanics Associates (SMA) of Newport Beach, CA, under the direction of Dr R P Kennedy, was assigned the task of performing the Seismic Margin Review per the criteria in Volume I. Volume IV, dealing with the evaluation of the Seismic Margins in the Service Water Pump Structure (SWPS) is submitted for the Staff's review as an attachment to this letter.

Volume IV of the Seismic Margin Review Report titled, "Service Water Pump Structure" describes in detail the method of analysis and the resulting seismic margins. The underpinning walls of the SWPS were included in this evaluation for their margins. This evaluation shows that there is still a considerable amount of margin in the design. The lowest margin identified for the underpinning walls was conservatively estimated at 3.7 with respect to code allowables. The lowest margin identified in the rest of the structure was conservatively estimated at 1.6 with respect to code allowables.

Future volumes of the Seismic Margin Review Report dealing with structures and systems will be submitted as they become available.



FWB/BFH/bjw

CC RJCook, Midland Resident Inspector
JGKeppler, Administrator, NRC Region III
DSHood, NRC
FRinaldi, NRC
GHarstead, Harstead Engineering

CONSUMERS POWER COMPANY
Midland Units 1 and 2
Docket No 50-329, 50-330

Letter Serial 25494 Dated September 2, 1983

At the request of the Commission and pursuant to the Atomic Energy Act of 1954, and the Energy Reorganization Act of 1974, as amended and the Commission's Rules and Regulations thereunder, Consumers Power Company submits Volume IV of the Seismic Margin Review titled, "Service Water Pump Structure".

CONSUMERS POWER COMPANY

By /s/ F W Buckman
F W Buckman, Executive Manager
Midland Project Office

Sworn and subscribed before me this 2nd day of September, 1983

/s/ Pamela J Griffin
Notary Public
Jackson County, Michigan

My Commission Expires Sept 8, 1984

NRC LICENSING CORRESPONDENCE - RECORD SUMMARY

DATE: September 2, 1983

DOCKET NUMBERS 50-329, 50-330
MIDLAND UNITS 1 & 2

SUMMARY: (State why letter is written)

Submits Volume IV "Service Water Pump Structure" of the Seismic Margin Review for NRC review.

COMMITMENTS MADE: (LCP items will be made for these items by Safety & Licensing;
Site commitments will be identified separately).

No LCP or Site commitments made

PREVIOUS NRC/CPCO CORRESPONDENCE
(References)

J W Cook to H R Denton, 2/4/83
Serial 21010

File/UFI NO.

B3.7.1

INDIVIDUALS PROVIDING INFORMATION
(Including Consultants)

Dr R P Kennedy (SMA)

CONCURRENCES (normally name of
section or department head and name
of any site personnel who concurred)

DTPerry
TRThiruvengadam

ORIGINATOR (Preparer)

BFHenley
DASommers

SPECIAL DISTRIBUTION

US Mail ☒

Federal Express ☐

Telecopy ☐

To Whom: MAMiller (USNRC)

INDIVIDUALS ASSIGNED RESPONSIBILITY
FOR IMPLEMENTING COMMITMENTS:

N/A

LCP item(s) or SER open item(s) this
correspondence closes:

N/A

Attachments or Enclosures?

Yes ☒

How Many: 25

No ☐

SMA 13701.05R003 (VOLUME IV)

DOCKETED
ENRC

'83 SEP 15 A11 23

OFFICE OF SECRETARY
DOCKETING & SERVICE
BRANCH

SEISMIC MARGIN REVIEW

VOLUME IV

SERVICE WATER PUMP STRUCTURE MARGIN EVALUATION

prepared for

CONSUMERS POWER COMPANY
Jackson, Michigan

August, 1983



STRUCTURAL
MECHANICS
ASSOCIATES
A Calif. Corp.

5160 Birch Street, Newport Beach, Calif. 92660 (714) 833-7552

SEISMIC MARGIN REVIEW

VOLUME IV

SERVICE WATER PUMP STRUCTURE MARGIN EVALUATION

by

D. A. Wesley
R. P. Kennedy
R. H. Kincaid
P. S. Hashimoto
W. H. Tong
R. D. Thrasher

Approved:

R. P. Kennedy
R. P. Kennedy
President

Approved:

Thomas R. Kipp
T. R. Kipp
Manager of
Quality Assurance

prepared for

CONSUMERS POWER COMPANY
Jackson, Michigan

August, 1983



STRUCTURAL
MECHANICS
ASSOCIATES
A Calif. Corp.

REVISIONS

Document Number SMA 13701.05R003(VOL. IV)

Title SEISMIC MARGIN REVIEW

VOLUME IV

SERVICE WATER PUMP STRUCTURE

MARGIN EVALUATION

Rev.	Description	QA	Project Manager
A 6/1983	Draft for Review	<i>Thomas R. Kipp</i> 6/29/83	<i>DA Wesley</i> 6/29/83
B 8/1983	2nd Draft for review incorporating initial comments	<i>Thomas R. Kipp</i> 8/24/83	<i>for DA Wesley</i> 8-24-83
Rev. 0 8/1983	Initial Issue	<i>Thomas R. Kipp</i> 8/26/83	<i>Raymond H. Hirsch</i> for <i>D.A. Wesley</i> 8/26/83

SEISMIC MARGIN REVIEW
MIDLAND ENERGY CENTER PROJECT

TABLE OF CONTENTS

<u>VOLUME NO.</u>	<u>TITLE</u>
I	METHODOLOGY AND CRITERIA
II	REACTOR CONTAINMENT BUILDING
III	AUXILIARY BUILDING
IV	SERVICE WATER PUMP STRUCTURE
V	DIESEL GENERATOR BUILDING
VI	BORATED WATER STORAGE TANK
VII	ELECTRICAL, CONTROL, INSTRUMENTATION AND MECHANICAL EQUIPMENT
VIII	NSSS EQUIPMENT AND PIPING
IX	BALANCE-OF-PLANT CLASS 1, 2 AND 3 PIPING, PIPE SUPPORTS AND VALVES
X	MISCELLANEOUS SUBSYSTEMS AND COMPONENTS

TABLE OF CONTENTS

<u>Section</u>	<u>Title</u>	<u>Page</u>
1	INTRODUCTION	IV-1-1
	1.1 Description of Structure	IV-1-2
	1.2 Ground Motion	IV-1-2
	1.3 Soil Properties	IV-1-3
2	SEISMIC ANALYSIS	IV-2-1
	2.1 Structure Dynamic Model	IV-2-1
	2.2 Soil-Structure Interaction	IV-2-2
	2.2.1 Layered Site Analyses	IV-2-2
	2.2.2 Energy Entrapment Due to Layering	IV-2-5
	2.2.3 Development of Lower Bound and Upper Bound Soil Case Effective Soil Shear Moduli	IV-2-6
	2.2.4 Development of Global Soil Stiffnesses and Dashpots	IV-2-10
3	SEISMIC RESPONSE	IV-3-1
	3.1 Modal Characteristics	IV-3-1
	3.2 Composite Modal Damping	IV-3-2
	3.3 Structure Seismic Response	IV-3-5
	3.3.1 Effects of Soil Conditions on Seismic Loads	IV-3-6
	3.3.2 Comparison of SMR and FSAR Design Loads	IV-3-7
	3.3.3 Element Loads	IV-3-7
4	CODE MARGINS	IV-4-1
	4.1 Shear Wall Capacity of Existing Structure	IV-4-2
	4.2 Diaphragm Capacity of Existing Structure	IV-4-10
	4.3 Effects of Reinforcement Bar Cutting	IV-4-11
	4.4 Underpinning Wall Capacities	IV-4-13
	4.5 Soil Bearing and Structure Stability Capacity	IV-4-15
	4.6 Effects of Thermal Gradients	IV-4-15
5	INPUT TO EQUIPMENT	IV-5-1
6	SUMMARY	IV-6-1

REFERENCES

APPENDIX A

1. INTRODUCTION

A seismic margin evaluation of the Midland Nuclear Power Generating Station has been conducted. The purpose of this assessment was to provide confidence in the safety and structural integrity of critical structures and equipment required to remain operational during an earthquake in order to achieve safe shutdown. This volume presents the results of the seismic analysis conducted for the Service Water Pump Structure (SWPS).

Much of the design and construction of the Midland Plant was completed by 1973. The plant was designed in accordance with criteria and codes in effect at that time (Reference 1). The plant was originally designed to withstand both an Operating Basis Earthquake (OBE) and a Safe Shutdown Earthquake (SSE). The ground response spectra used in the initial design analyses were based on work by Housner (Reference 2) increased by 50 percent in the 0.2 to 0.6 second range.

Recently, the seismic hazard at the Midland site has been reevaluated using current methodology (Reference 3, 4 and 5). Seismic inputs for the site were determined in terms of site specific response spectra at both the original grade and at the top-of-fill locations. These site specific response spectra exceed the original design spectra over a broad frequency range. In order to assure the adequacy of the service water pump structure and Category I equipment at the Midland Plant to withstand the higher postulated seismic excitation, an evaluation of this structure was conducted to determine the seismic margins to current code allowables, and if necessary, the seismic margins to failure. This report presents the results of the service water pump structure seismic analysis. The overall methodology used to develop the seismic models and in-structure response spectra for equipment evaluation are contained in Volume I of this report and will not be presented herein.

1.1 DESCRIPTION OF STRUCTURE

The service water pump structure at the Midland Nuclear Generating Station is a reinforced concrete structure. Plan dimensions of the structure at grade are 86 feet by 106 feet, with a maximum internal height of about 62 feet. The structure houses five service water pumps and associated support equipment. The service water pump structure is embedded in the soil on the north and east sides. On the west side, it is separated from the Class 2 circulating pump structure by an expansion joint. The south side of the structure is in direct contact with the cooling pond. A schematic representation of this structure is presented in Figure IV-1-1.

Under the southern two-thirds of the building, the service water pump structure is supported by a 5-foot thick reinforced concrete mat approximately 74 feet long by 90 feet wide (Figure IV-1-2). The bottom of the concrete mat is founded on glacial till at Elevation 587'. Beneath the northern one-third of this building, remedial underpinning has been designed which transfers all structure loads to the undisturbed glacial till at Elevation 587'. The proposed underpinning is a 4-foot thick, 30-foot high, reinforced concrete wall. This wall is designed to behave as a continuous support member under the perimeter of the structure overhang. The base of the north underpinning wall bells out to a 6 foot thickness. Along the east and west sides of the building the underpinning walls are 4 feet wide for their entire height.

1.2 GROUND MOTION

The service water pump structure including the foundation remedial work is founded on the natural material (glacial till) at the Midland site. The Seismic Margin Earthquake (SME) ground response spectra appropriate for use with structures founded on the original ground was presented in Volume 1 and is shown in Figure IV-1-3 for reference. These spectra were developed based on an envelope of the original ground surface site specific response spectra and the original Housner spectra anchored to 0.12g peak acceleration. Volume I contains the description of the ground response spectra development. These

spectra were used in a response spectrum analysis to develop seismic response loads for the Seismic Margin Review (SMR). The ground response spectra were applied to the soil impedances at the base of the service water pump structure dynamic model. Vertical input was taken as 2/3 of the horizontal spectra.

In-structure (floor) response spectra for the equipment evaluation were developed from time history analyses of the service water pump structure. A site specific artificial earthquake time history consistent with the SME ground response spectra for the original ground surface was developed as described in Volume I to provide the seismic input to the service water pump structure dynamic model. In-structure response spectra for the equipment evaluation were developed by directly integrating the coupled equations of motion for the service water pump structure mathematical model and generating response time histories at all locations of interest for each of the soil cases studied.

1.3 SOIL PROPERTIES

The service water pump structure is founded on glacial till deposits at the Midland site. These deposits consist of very stiff to hard cohesive soils, predominantly grey, silty-clay, which extends to depths ranging from Elevation 587 to 545 at this location. The details of the site geology are discussed in the FSAR (Reference 1). The site characteristics for the Midland plant have been discussed in Volume I of this report.

Figures IV-1-4 and IV-1-5 present the Midland soil profiles for the soft site and stiff site profiles, respectively. In addition, figure IV-1-6 presents an intermediate soil profile. The development of the intermediate profile as well as the low strain shear moduli, strain degradation effects and other engineering characteristics used in the SMR are discussed in Volume I. These profiles were used in conducting layered site analyses to ensure a wide range of soil characteristics to account for uncertainties in the data and provide conservative response results throughout the structure.

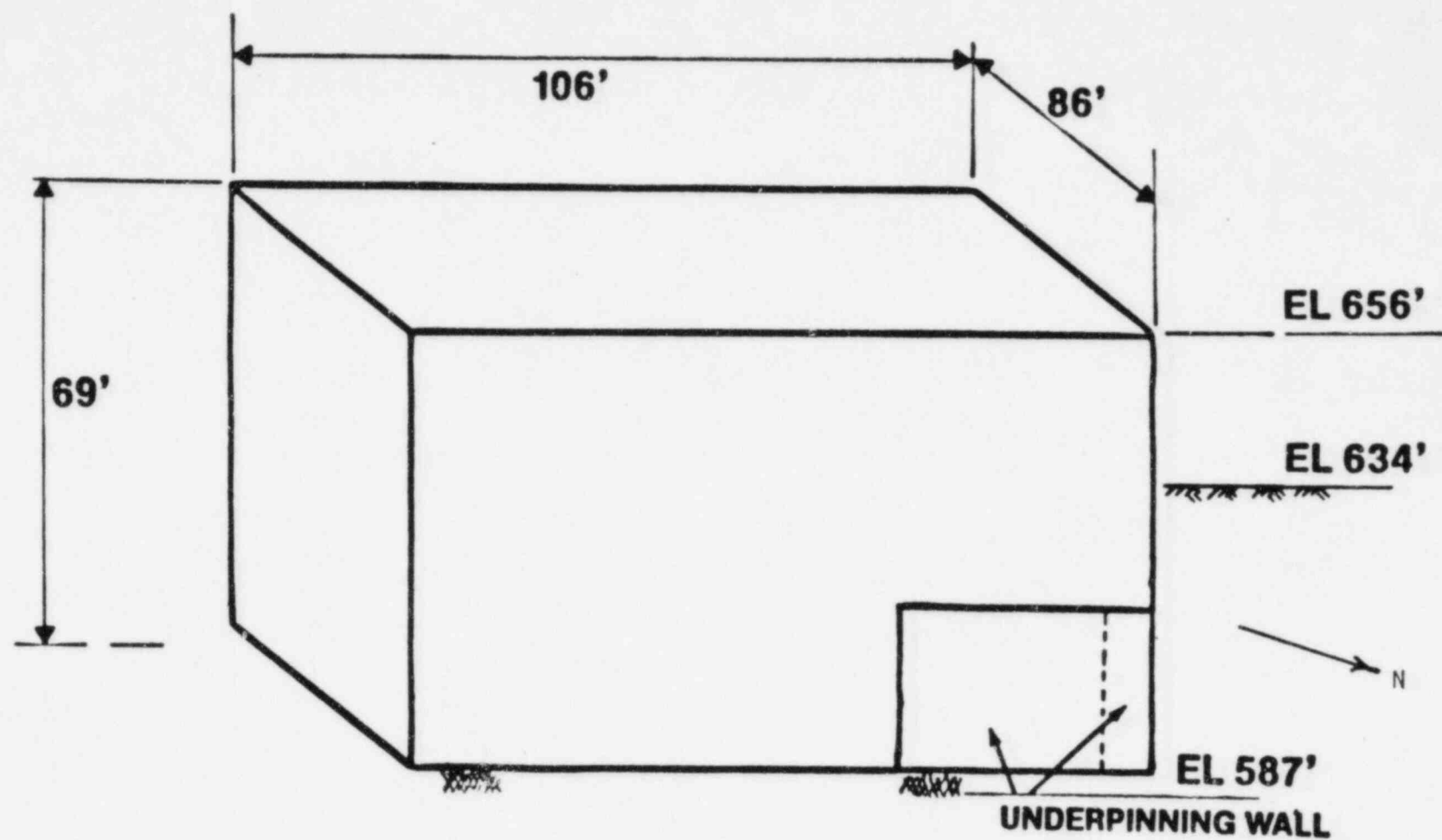


FIGURE IV-1-1. SCHEMATIC REPRESENTATION OF THE SERVICE WATER PUMP STRUCTURE

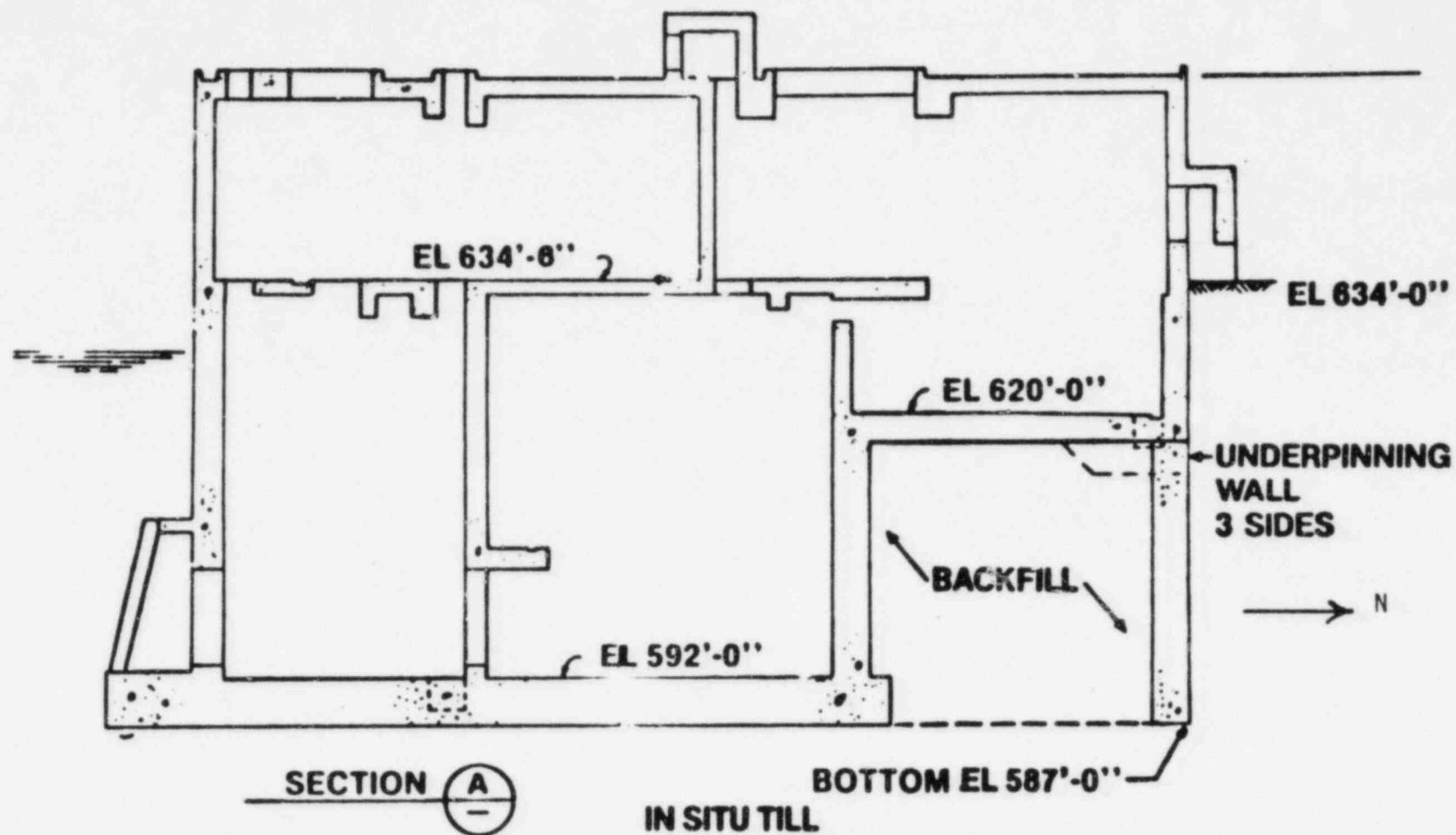


FIGURE IV-1-2. ELEVATION VIEW OF SERVICE WATER PUMP STRUCTURE SHOWING REMEDIAL UNDERPINNING

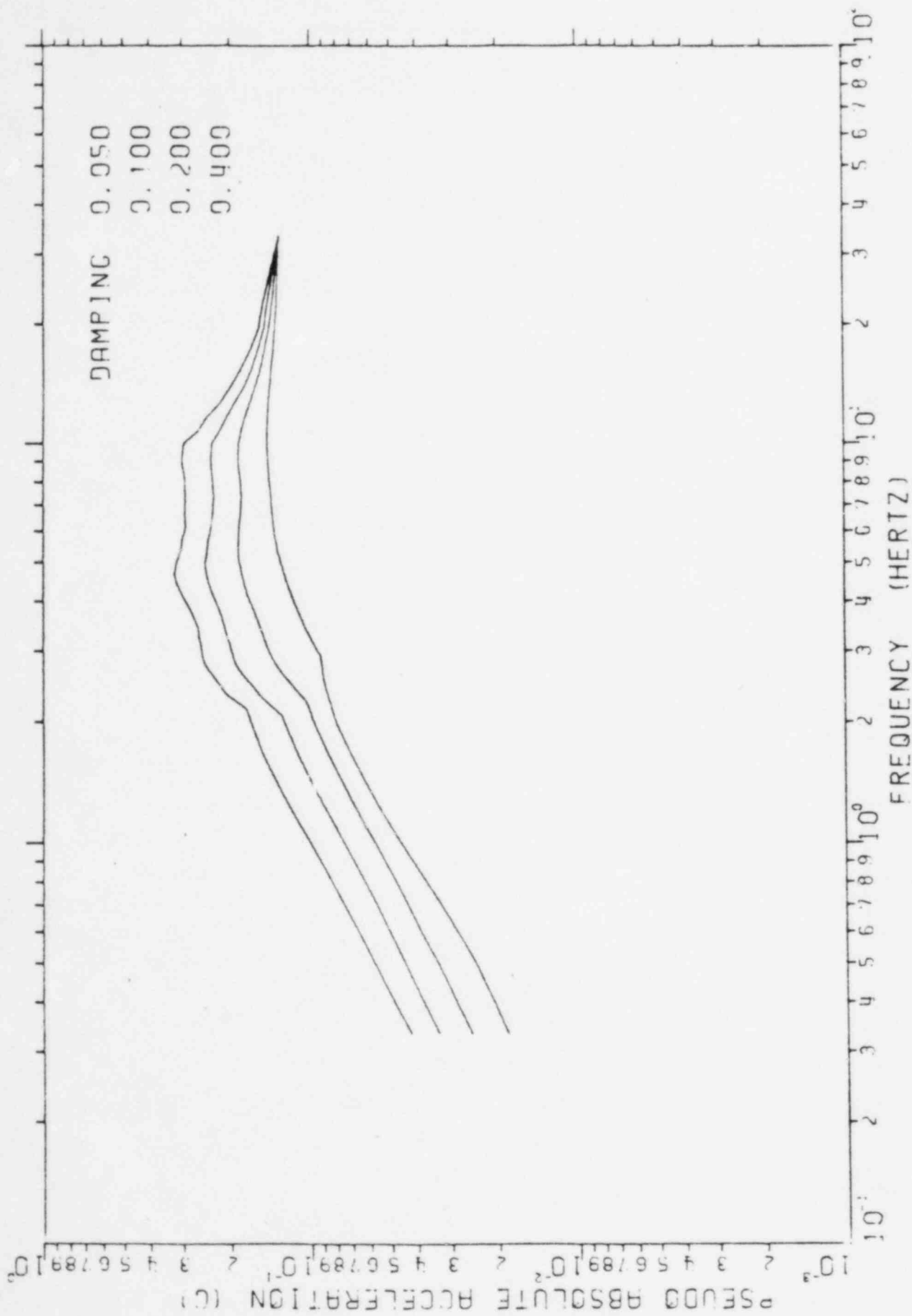


FIGURE IV-1-3. SEISMIC MARGIN EARTHQUAKE ORIGINAL GROUND SURFACE ENVELOPE RESPONSE SPECTRA

Elevation

634	<hr/>				Top of Grade
603	<hr/>				Original Ground
	Glacial Till				
	W_s	= 135 pcf		G_{max}	= $7 \cdot 10^6$ psf
	v	= 0.47		G_{SME}	= $2 \cdot 10^6$ psf
550	V_s	= 1290 fps	<hr/>		
	Glacial Till				
	W_s	= 135 pcf		G_{max}	= $12 \cdot 10^6$ psf
	v	= 0.47		G_{SME}	= $4.2 \cdot 10^6$ psf
	V_s	= 1690 fps			
410	<hr/>				
	Dense Cohesionless Material				
	W_s	= 135 pcf	V_s	= 2540 fps	$\left. \begin{array}{l} G_{max} = 27 \cdot 10^6 \text{ psf} \\ G_{SME} = 17.8 \cdot 10^6 \text{ psf} \end{array} \right\} \text{E}$
	v	= 0.34			
			V_s	= 2970 fps	$\left. \begin{array}{l} G_{max} = 37 \cdot 10^6 \text{ psf} \\ G_{SME} = 25.2 \cdot 10^6 \text{ psf} \end{array} \right\} \text{E}$
260	<hr/>				
	Bedrock				
	W_s	= 150 pcf	V_s	= 5000 fps	
	v	= 0.33			

FIGURE IV-1-4. SOIL LAYERING PROFILE REPRESENTATIVE OF SOFT SITE CONDITIONS

Elevation			
634			Top of Grade
603			Original Ground
Aux. Bldg. - 570	} Glacial Till	$W_s = 120 \text{ pcf}$	$G_{\max} = 7.3 \cdot 10^6 \text{ psf}$
		$\nu = 0.49$	$G_{\text{SME}} = 3.65 \cdot 10^6 \text{ psf}$
		$V_s = 1400 \text{ fps}$	
Reactor Bldg. - 568	} Glacial Till		
SWPS - 585		$W_s = 135 \text{ pcf}$	$G_{\max} = 22.2 \cdot 10^6 \text{ psf}$
		$\nu = 0.42$	$G_{\text{SME}} = 13.3 \cdot 10^6 \text{ psf}$
		$V_s = 2300 \text{ fps}$	
463			
	Glacial Till		
	$W_s = 135 \text{ pcf}$	$G_{\max} = 37.8 \cdot 10^6 \text{ psf}$	
	$\nu = 0.42$	$G_{\text{SME}} = 25.0 \cdot 10^6 \text{ psf}$	
	$V_s = 3000 \text{ fps}$		
363			
	Dense Cohesionless Material		
	$W_s = 135 \text{ pcf}$	$G_{\max} = 37.8 \cdot 10^6 \text{ psf}$	
	$\nu = 0.34$	$G_{\text{SME}} = 31.0 \cdot 10^6 \text{ psf}$	
	$V_s = 3000 \text{ fps}$		
263			
	Bedrock		
	$W_s = 150 \text{ pcf}$	$V_s = 5000 \text{ fps}$	
	$\nu = 0.33$		

FIGURE IV-1-5. SOIL LAYERING PROFILE REPRESENTATIVE OF STIFF SITE CONDITIONS

Elevation

634	<hr/>		Top of Grade
603	<hr/>		Original Ground
	Glacial Till		
	$W_s = 110$ pcf	$G_{max} = 7.7 \cdot 10^6$ psf	
	$\nu = 0.49$	$G_{SME} = 4.08 \cdot 10^6$ psf	
	$V_s = 1500$ fps		
553	<hr/>		
	Glacial Till		
	$W_s = 135$ pcf	$G_{max} = 15 \cdot 10^6$ psf	
	$\nu = 0.42$	$G_{SME} = 7.95 \cdot 10^6$ psf	
	$V_s = 1890$ fps		
463	<hr/>		
	Dense Cohesionless Material		
	$W_s = 135$ pcf	$G_{max} = 25.6 \cdot 10^6$ psf	
	$\nu = 0.34$	$G_{SME} = 13.6 \cdot 10^6$ psf	
	$V_s = 2468$ fps		
263	<hr/>		
	Bedrock		
	$W_s = 145$ pcf	$V_s = 5000$ fps	
	$\nu = 0.33$		

FIGURE IV-1-6. INTERMEDIATE SOIL PROFILE

2. SEISMIC ANALYSIS

2.1 STRUCTURE DYNAMIC MODEL

The service water pump structure is represented by a three-dimensional, lumped-mass, single-stick model which preserves the physical geometry of the various building components. The service water pump structure mathematical model was developed by Bechtel (Reference 7). As part of the SMR evaluation, this model was reviewed to ensure that the overall dynamic characteristics of the structure have been adequately represented. The service water pump structure dynamic model described herein was used to evaluate overall building response to seismic loadings, as well as to generate in-structure response spectra. The overall building dynamic responses developed from this model were also used to develop forces in the individual structural elements.

Figures IV-1-2 and IV-2-1 present a schematic view and plan of the SWPS. Figure IV-2-2 and IV-2-3 present an illustration of the dynamic model superimposed onto the North-South and East-West sections of the SWPS, respectively. Figure IV-2-4 presents an isometric view of the SWPS dynamic model. The mass of the structure is lumped at the major floor elevations. The mass includes concrete, steel, major equipment, water within the building, entrapped soil, and 25% of the floor design live loading. The center of mass was established for each floor level. The horizontal inertial effects of the water mass within the SWPS are lumped at Elevations 589.5, 605, and 620 feet. The vertical water mass inertial effects are lumped at the base (Elevation 589.5 feet) because the water transmits its own dynamic responses down to this level rather than having these effects transmitted through the walls. Similarly, the soil entrapped within the underpinning walls respond horizontally with these walls and the horizontal inertial mass of this entrapped soil is lumped at Elevations 589.5, 605, and 620 feet. The vertical inertial entrapped soil mass effects were not included in the model since this mass is

carried by the soil and does not load the building. Because the vertical and horizontal inertial (mass) effects of the water and entrapped soil are treated differently, the vertical and horizontal centers of mass at which the masses are lumped differ from each other at Elevations 589.5, 605, and 620 feet. These differences are incorporated into the model as shown in Figure IV-2-4.

The beam elements shown in Figure IV-2-4 define the stiffness characteristics of the structural systems between floor levels. These stick elements have been located at the calculated centers of rigidity between each level and are thus horizontally offset from the mass points and from each other. These offsets (eccentricities) are included to properly account for torsional vibrations. Rigid elements are used to connect the center of stiffness and center of mass.

The proposed underpinning design underneath the northern portion of the building has been accounted for in the section properties below Elevation 620 feet. The underpinning wall layout is connected to the existing wall to make up the extension of the beam to Elevation 587 feet.

The soil-structure interaction impedance functions (developed in accordance with the approach discussed in Section 2.2) are attached to the structure portion of the SWPS model at Elevation 590 feet. The design ground motion is input into this structure through these soil-structure interaction impedance functions.

2.2 SOIL-STRUCTURE INTERACTION

2.2.1 Layered Site Analyses

The effects of the layered site characteristics on the service water pump structure seismic response were evaluated by developing equivalent elastic half-space soil impedances based on layered site analyses. These equivalent elastic half-space impedance functions were modified to account for embedment effects and non-standard foundation shapes. The layered site soil profiles presented in the previous section

were used in conducting layered site analyses using the program CLASSI (Reference 8) which calculates the frequency-dependent soil impedances for the structure. The service water pump structure foundation geometry was idealized as a 89' by 106' rectangular foundation as shown in Figure IV-2-5 in all CLASSI analyses. This idealized foundation is founded at Elevation 587 feet.

The results of the CLASSI analyses are presented in Figures IV-2-6 to IV-2-11 for the intermediate soil profile. Soil impedances were developed for all global translational and rotational degrees-of-freedom. Both the real (stiffness) and imaginary (damping) portions of the soil impedance are presented in these figures for a range of soil-structure frequencies varying from 0 to 10 hertz.

CLASSI analyses of the soft site and stiff site layered soil profiles were not run for this structure. Results for the intermediate soil profile demonstrated that soil impedances for these other two soil profiles could be conservatively developed based on the auxiliary building results which are presented in Volume III of this report. The development of the effective elastic half-space shear moduli for the soft site and stiff site layered soil profiles is discussed in Section 2.2.3.

Examination of the stiffness coefficients for the intermediate case soil profile (Figures IV-2-6 to IV-2-11) shows there is a minor frequency dependence and some resonance due to layering effects for horizontal translation degrees-of-freedom. The vertical translation and rocking degrees-of-freedom exhibit much stronger frequency dependence with resonance due to layering effects evident in the 2 to 3 hertz frequency range for the vertical translation stiffness term. The torsional stiffness coefficient and damping coefficients for all degrees-of-freedom are relatively unaffected by layering. It should be noted that because CLASSI incorporates the five percent material damping for the soil in the layered site analysis, the damping coefficient terms are not zero for the static case (0 hertz) as would be expected if only geometric damping was considered in the analysis.

The results of the CLASSI layered site analysis were used to develop effective elastic half-space shear moduli, G_{eff} for all degrees-of-freedom of the structure (horizontal and vertical translation, rocking, and torsion) for the intermediate soil profile. The procedure used to develop effective elastic half-space shear moduli from the CLASSI layered site analysis is presented in Volume I. Appendix A of Volume III presents an illustrative calculation of G_{eff} for the auxiliary building which demonstrates this procedure. The development of G_{eff} for this structure was conducted in a similar manner.

The effective elastic half-space soil shear moduli determined from the CLASSI layered site analysis for the intermediate soil case are as follows:

Structure Degree-of-Freedom	Effective Elastic Half-Space Shear Modulus, G_{eff} (ksf)
Horizontal Translation and Torsion	4,900
Vertical Translation and Rocking	6,200

These effective shear moduli may be compared to the intermediate case soil profile shown in Figure IV-1-6. The G_{eff} value of 4,900 ksf associated with horizontal translation and torsion of the structure primarily reflects the stiffness of the 35 foot layer of glacial till beneath the structure from Elevation 587' to Elevation 553'. Little influence of the stiffer material below Elevation 553' is seen in the effective soil shear modulus for this degree-of-freedom. The vertical and rocking G_{eff} of 6,200 ksf exhibits considerably more influence of the stiffer glacial till material below Elevation 553' which would be expected for degrees-of-freedom primarily associated with vertical motion of the structure.

2.2.2 Energy Entrapment Due to Layering

Two types of damping may be defined for the soil. The first type, known as material or hysteretic damping, is due to energy absorption by the soil due to straining of the material. For the Midland site, this damping has been conservatively estimated to be five percent of critical damping for the SME. Material damping is not significantly affected by layering. The second type of soil damping, known as geometric or radiation damping, involves the wave propagation of energy through the soil away from the structure. For an elastic half-space, these waves will propagate outwards to infinity. Layered soil profiles, however, tend to trap and reflect some of the energy back up towards the structure. One of the principal reasons for conducting a layered site analysis for the SMR was to determine the effect of layering on geometric damping from the structure. In effect, the geometric damping for the layered profile is reduced to some percentage of the damping which would be determined for an equivalent elastic half-space. This decrease in geometric damping may be determined through the use of a factor defined as

$$F_{\text{Layer}} = \frac{C(\text{CLASSI layered site analysis})}{C(\text{theoretical elastic half-space})}$$

where $C(\text{CLASSI layered site analysis})$ is the frequency-dependent damping including layering effects determined by the CLASSI layered site analysis. The term $C(\text{theoretical elastic half-space})$ represents the geometric damping which would be calculated for the structure based on the effective elastic half-space shear moduli presented in the previous section and the idealized foundation shape shown in Figure IV-2-5. This ratio is indicative of the amount of energy entrapped beneath the structure due to layering. The procedure for calculating F_{Layer} is presented in Volume I. Appendix A of Volume III presents a sample calculation of F_{Layer} for the auxiliary building. The calculation of F_{Layer} for this structure is similar.

Layering factors were determined for the intermediate soil profile for the service water pump structure. Layering factors were conservatively limited to a maximum of 75 percent of theoretical elastic half-space geometric damping for all degrees-of-freedom where F_{Layer} was determined to be greater than 0.75. This conservative cutoff on geometric damping was based on results presented in Reference 10. The following layer factors were defined for the service water pump structure:

Structure Degree-of-Freedom	Layering Factor, F_{Layer}
Horizontal Translation and Torsion	0.75
Vertical Translation	0.75
Rocking	0.50

The results for this structure indicated that soil site layering was not significant for horizontal and vertical translations and the torsional degrees-of-freedom. For motions in these directions, the geometric damping of the structure was primarily determined by the glacial till material above Elevation 553' as shown in Figure IV-1-6. The impedance mismatch at Elevation 553' did not significantly reduce geometric damping below theoretical values. For rocking of the structure, layering effects were somewhat more important resulting in a reduction to 50 percent of theoretical elastic half-space damping. Rocking response of low-rise, shear-wall-type structures such as the service water pump structure is relatively unimportant, however, and the lower calculated rocking geometric damping has a negligible effect on overall responses.

2.2.3 Development of Lower Bound and Upper Bound Soil Case Effective Soil Shear Moduli

Table IV-2-1 presents a comparison of the intermediate soil case effective elastic half-space shear moduli and layering factors, F_{Layer} , determined for the service water pump structure and the auxiliary building. Effective soil shear modulus values for the auxiliary building

(bottom of foundation at Elevation 562') reflect properties primarily associated with the deep glacial till layer below Elevation 553'. The layering factor of 0.75 determined for horizontal translation, vertical translation, and torsion implies that soil geometric damping is essentially determined by the soil below Elevation 553'. The 9 foot layer of material between the bottom of foundation base mat at Elevation 562' and the glacial till at Elevation 553' has a negligible influence on the overall damping except for rocking where geometric damping is reduced to 50 percent of theoretical.

The service water pump structure results showed characteristics similar to these determined for the auxiliary building for this soil case. The service water pump structure is founded on glacial till material at Elevation 587'. For horizontal translation and torsional degrees-of-freedom effective soil shear modulus values are primarily due to the glacial till material above Elevation 553'. Vertical translation and rocking soil shear modulus values show some influence of the stiffer material below Elevation 553'. The layering factors developed for the service water pump structure are identical to those determined for the auxiliary building. These high layering factors indicate that the impedance mismatch at Elevation 553' has only a small influence on the soil geometric damping. The layered soil profile beneath the service water pump structure does not entrap enough energy to reduce the soil geometric damping significantly below that determined for a theoretical elastic half-space.

Both the soft site and stiff site soil profiles have layering characteristics (i.e., layer heights and relative impedance mismatch ratios) similar to the intermediate case soil profile. Because of the similar configuration of these profiles, the relative ratio of auxiliary building effective soil shear modulus values to service water pump structure effective soil shear modulus values which would be determined for the soft and stiff site profiles should be in the same proportion as the ratios determined for the intermediate soil case. The layering

factors justified for the intermediate soil case would also be applicable to the other soil profiles. Therefore, because of the similarity of auxiliary building and service water pump structure results for the intermediate soil case and the similar profile characteristics for all three soil profiles, G_{eff} values for the soft and stiff site soil profiles were developed based on auxiliary building results for these other two profiles.

The effective soil shear moduli from the auxiliary building upper bound soil case were used to develop G_{eff} values for the service water pump structure upper bound soil case. Both structures are essentially founded on the deep layer of glacial till extending down to Elevation 463' as shown in Figure IV-1-5. The effective soil shear modulus values determined for the auxiliary building of 18,100 ksf (horizontal translation and torsion) and 19,400 ksf (vertical translation and rocking) show some influence of the material below Elevation 463' but are primarily due to the soil from Elevation 463' to Elevation 562' (bottom of the auxiliary building). Because the service water pump structure has a smaller foundation size (89' x 106' versus 140' x 236') and is founded at a higher elevation (Elevation 587' versus Elevation 562') than the auxiliary building, effective soil shear modulus values for this structure would be expected to be primarily associated with the softer material above Elevation 463' and use of the auxiliary building soil properties is conservative.

Lower bound soil case effective soil shear modulus values for the service water pump structure were determined by ratioing the auxiliary building lower bound soil case results. The principal elevations of the top two glacial till layers shown in Figures IV-1-4 and IV-1-6 for the soft site and intermediate case soil profiles are quite similar (Elevation 550' for the soft site profile versus Elevation 553' for the intermediate soil profile). Intermediate soil case results for both structures demonstrated that these layers were important in determining the effective soil shear modulus. Because of the similarity

of the intermediate and soft site soil profiles, soft site G_{eff} values for these structures would be in approximately the same ratio as the intermediate case results. A ratioing procedure based on the intermediate soil case was used whereby:

$$G_{eff} (SWPS, L.B.) = \frac{G_{eff} (SWPS, I.S.)}{G_{eff} (Aux. Bldg., I.S.)} G_{eff} (Aux. Bldg., L.B.) \quad (2-1)$$

where:

L.B. = Lower bound soil case

I.S. = Intermediate soil case

G_{eff} (structure, soil case) = the effective soil shear modulus for the structure and degree-of-freedom of interest

Table IV-2-2 presents the service water pump structure effective soil shear moduli, G_{eff} , determined for the lower bound, intermediate, and upper bound soil cases. The layer factors presented in Section 2.2.2 for this structure were used for all soil cases.

Effective elastic half-space soil shear moduli for the lower and upper bound soil cases were developed based on auxiliary building results in Volume III. The upper and lower bound soil cases represent a conservative range of soil properties which might be possible at the Midland site. The procedure used to account for variability of such factors as uncertainty in strain degradation effects, uncertainty in modeling soil-structure interaction, and the uncertainty in the knowledge of soil site characteristics is presented in Volume I. The auxiliary building G_{eff} values for the auxiliary building lower and upper bound soil cases already incorporate the uncertainties due to these factors. Thus the G_{eff} values determined for the SWPS represent realistic bounds which account for possible variability in the soil properties.

2.2.4 DEVELOPMENT OF GLOBAL SOIL STIFFNESSES AND DASHPOTS

Soil springs modeling the stiffness of the soil beneath the auxiliary building were developed based on the effective soil shear modulus values presented in Table IV-2-2 and the actual building foundation geometry. Soil stiffnesses were calculated from the frequency-dependent elastic half-space equations shown in Table IV-2-3. These equations and frequency-dependent coefficients are presented in References 11 to 14.

The service water pump structure foundation geometry used in determining the global soil stiffness for the structure is shown in Figure IV-2-5. For horizontal translation and torsional degrees-of-freedom, the entrapped soil beneath the north end of the building was considered to act integrally with the foundation base mat. For vertical translation and rocking degrees-of-freedom, the geometric properties of the foundation were developed based on foundation contact area only.

The use of elastic half-space equations to calculate soil impedances required the development of equivalent rectangles and circles for the service water pump structure based on the actual foundation geometry. The equivalent rectangles developed for the horizontal translation and rocking degrees-of-freedom were developed based on equivalence between the actual foundation geometric properties and the geometric properties of the rectangle. In the vertical direction, an equivalent rectangle was calculated based on area equivalence between the rectangle and the service water pump structure foundation contact area. The equivalent circle used to calculate the torsional soil stiffness was developed based on equivalence of polar moments of inertia between a circle and the actual foundation geometry. The unembedded soil stiffnesses determined for each of the three soil cases studied are shown in Table IV-2-4.

Embedment effects were considered to be applied as a multiplier to the unembedded frequency-dependent elastic half-space soil stiffnesses. Embedment effects considered both the soil in physical contact with the

sides of the structure and stiffening of the soil due to weight of adjacent structures. Volume I presents the procedure used to calculate embedment effects for the SMR. Appendix A of Volume III presents a sample calculation of soil stiffnesses for the auxiliary building including embedment effects, and the calculation of the embedment for the SWPS was conducted in a similar manner.

As shown by Table IV-2-4, embedment effects for the service water pump structure soil stiffnesses are relatively small. Translational degrees-of-freedom are stiffened by about 6 percent while rotational degrees-of-freedom show an increase on the order of 14 to 17 percent. Thus, the corresponding fundamental soil-structure frequencies would be expected to increase in the range of 2 to 8 percent due to embedment effects. The final global soil stiffnesses for the structure, including embedment effects, are presented in Table IV-2-4 for each of the three soil cases studied.

Dashpots modeling soil geometric and material damping were developed using the elastic half-space equations presented in Table IV-2-3. Material damping of 5 percent of critical damping was assumed for the soil. Soil dashpots were calculated accounting for both layering and embedment effects as discussed in Volume I on methodology and criteria. Appendix A of Volume III presents a sample calculation of an embedded dashpot for the auxiliary building which illustrates this procedure.

Table IV-2-5 presents the unembedded dashpots and embedment factors for this structure. Embedment effects for damping increased translational dashpots 9 to 14 percent above their unembedded values. Rotational dashpots were increased by about 30 to 37 percent due to the stiffening effects from the surrounding soil. The embedded dashpots, including 5 percent soil material damping, are presented in Table IV-2-5.

TABLE IV-2-1

COMPARISON OF AUXILIARY BUILDING AND SERVICE
WATER PUMP STRUCTURE EFFECTIVE SOIL SHEAR MODULI AND
LAYERING FACTORS, INTERMEDIATE SOIL CASE

a) Effective Shear Moduli

Structure Degree-of-Freedom	Dynamic Soil Shear Modulus, G_{eff} (KSF)	
	Auxiliary Building	Service Water Pump Structure
Horizontal Translation and Torsion	7,100	4,900
Vertical Translation and Rocking	8,600	6,200

b) Layering Factors

Structure Degree-of-Freedom	Layering Factor, F_{Layer}	
	Auxiliary Building	Service Water Pump Structure
Horizontal Translation and Torsion	0.75	0.75
Vertical Translation	0.75	0.75
Rocking	0.50	0.50

TABLE IV-2-2

SERVICE WATER PUMP STRUCTURE SEISMIC MARGIN EVALUATION
EQUIVALENT ELASTIC HALF-SPACE SHEAR MODULI

Structure Degree-of-Freedom	Dynamic Soil Shear Modulus, G_{eff}		
	Lower Bound Soil Case (KSF)	Intermediate Soil Case (KSF)	Upper Bound Soil Case (KSF)
Horizontal Translation and Torsion	1,300	4,900	18,100
Vertical Translation and Rocking	1,750	6,200	19,400

TABLE IV-2-3

FREQUENCY DEPENDENT ELASTIC HALF-SPACE IMPEDANCE

Direction of Motion	Equivalent Spring Constant For Rectangular Footing	Equivalent Spring Constant For Circular Footing	Equivalent Damping Coefficient
Horizontal	$k_x = k_1 2(1+\nu)G\beta_x \sqrt{BL}$	$k_x = k_1 \frac{32(1-\nu)GR}{7-8\nu}$	$c_x = c_1 k_x (\text{static}) R \sqrt{\rho/G}$
Rocking	$k_\psi = k_2 \frac{G}{1-\nu} \beta_\psi B^2 L$	$k_\psi = k_2 \frac{8GR^3}{3(1-\nu)}$	$c_\psi = c_2 k_\psi (\text{static}) R \sqrt{\rho/G}$
Vertical	$k_z = k_3 \frac{G}{1-\nu} \beta_z \sqrt{BL}$	$k_z = k_3 \frac{4GR}{1-\nu}$	$c_z = c_3 k_z (\text{static}) R \sqrt{\rho/G}$
Torsion	_____	$k_\theta = k_4 \frac{16}{3} GR^3$	$c_t = c_4 k_t (\text{static}) R \sqrt{\rho/G}$

in which:

ν = Poisson's ratio of foundation medium,

G = shear modulus of foundation medium,

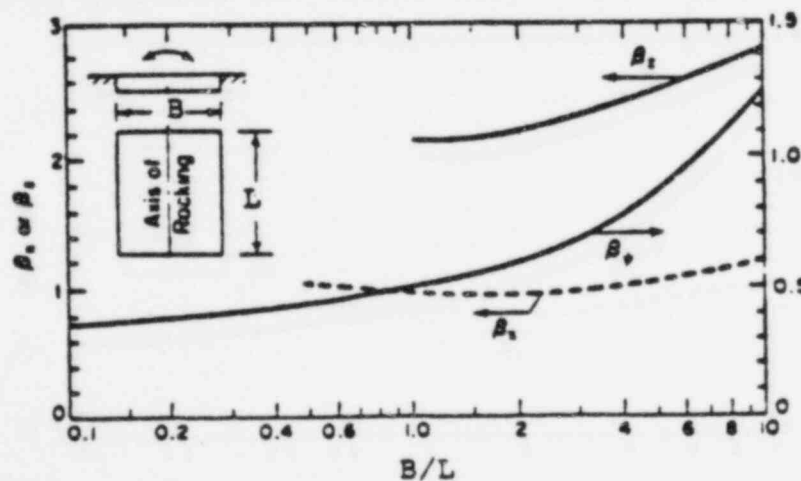
R = radius of the circular base mat,

ρ = density of foundation medium,

B = width of the base mat in the plane of horizontal excitation,

L = length of the base mat perpendicular to the plane of horizontal excitation,

k_1, k_2, k_3, k_4 = frequency dependent coefficients modifying the static stiffness or damping.
 c_1, c_2, c_3, c_4



Constants β_x , β_ψ and β_z for Rectangular Bases

TABLE IV-2-4

SERVICE WATER PUMP STRUCTURE SOIL STIFFNESSES

Motion	Non Embedded Soil Stiffness			Embedment Factor	Embedded Soil Stiffness		
	Lower Bound Soil	Intermediate Soil	Upper Bound Soil		Lower Bound	Intermediate	Upper Bound
Translational							
North-South	$3.48 \cdot 10^5$	$1.26 \cdot 10^6$	$4.66 \cdot 10^6$	1.06	$3.69 \cdot 10^5$	$1.34 \cdot 10^6$	$4.94 \cdot 10^6$
East-West	$3.53 \cdot 10^5$	$1.28 \cdot 10^6$	$4.74 \cdot 10^6$	1.06	$3.74 \cdot 10^5$	$1.36 \cdot 10^6$	$5.02 \cdot 10^6$
Vertical	$3.52 \cdot 10^5$	$1.46 \cdot 10^6$	$4.58 \cdot 10^6$	1.06	$4.79 \cdot 10^5$	$1.55 \cdot 10^6$	$4.85 \cdot 10^6$
Rotational							
North-South	$8.54 \cdot 10^8$	$2.77 \cdot 10^9$	$8.65 \cdot 10^9$	1.14	$9.73 \cdot 10^8$	$3.15 \cdot 10^9$	$9.86 \cdot 10^9$
East-West	$8.55 \cdot 10^8$	$2.78 \cdot 10^9$	$8.63 \cdot 10^9$	1.17	$1.00 \cdot 10^9$	$3.24 \cdot 10^9$	$1.01 \cdot 10^{10}$
Torsional	$8.96 \cdot 10^8$	$3.94 \cdot 10^9$	$1.25 \cdot 10^{10}$	1.16	$1.04 \cdot 10^9$	$3.94 \cdot 10^9$	$1.45 \cdot 10^{10}$

Notes: 1. Units for Translational Soil Springs are K/ft.

2. Units for Rotational Soil Springs are K-ft/rad.

TABLE IV-2-5

SERVICE WATER PUMP STRUCTURE DAMPING CONSTANTS

Motion	Non Embedded Dashpot			Embedment Factor	Embedded Dashpot (3)		
	Lower Bound Soil	Intermediate Soil	Upper Bound Soil		Lower Bound Soil	Intermediate Soil	Upper Bound Soil
Translational							
North-South	$1.57 \cdot 10^4$	$2.94 \cdot 10^4$	$5.65 \cdot 10^4$	1.12	$1.99 \cdot 10^4$	$3.73 \cdot 10^4$	$7.16 \cdot 10^4$
East-West	$1.62 \cdot 10^4$	$3.04 \cdot 10^4$	$5.84 \cdot 10^4$	1.14	$2.09 \cdot 10^4$	$3.91 \cdot 10^4$	$7.51 \cdot 10^4$
Vertical	$2.79 \cdot 10^4$	$4.80 \cdot 10^4$	$8.50 \cdot 10^4$	1.09	$3.29 \cdot 10^4$	$5.66 \cdot 10^4$	$1.00 \cdot 10^5$
Rotational							
North-South	$8.61 \cdot 10^6$	$1.48 \cdot 10^7$	$2.62 \cdot 10^7$	1.30	$1.69 \cdot 10^7$	$2.94 \cdot 10^7$	$5.15 \cdot 10^7$
East-West	$7.74 \cdot 10^6$	$1.33 \cdot 10^7$	$2.35 \cdot 10^7$	1.37	$1.65 \cdot 10^7$	$2.88 \cdot 10^7$	$5.03 \cdot 10^7$
Torsional	$1.24 \cdot 10^7$	$2.41 \cdot 10^7$	$4.63 \cdot 10^7$	1.36	$2.35 \cdot 10^7$	$4.56 \cdot 10^7$	$8.76 \cdot 10^7$

- Notes: 1. Units for Translational Dashpots are K-sec/ft
 2. Units for Rotational Dashpots are K-sec-ft/rad
 3. Includes 5% Soil Hysteretic Damping

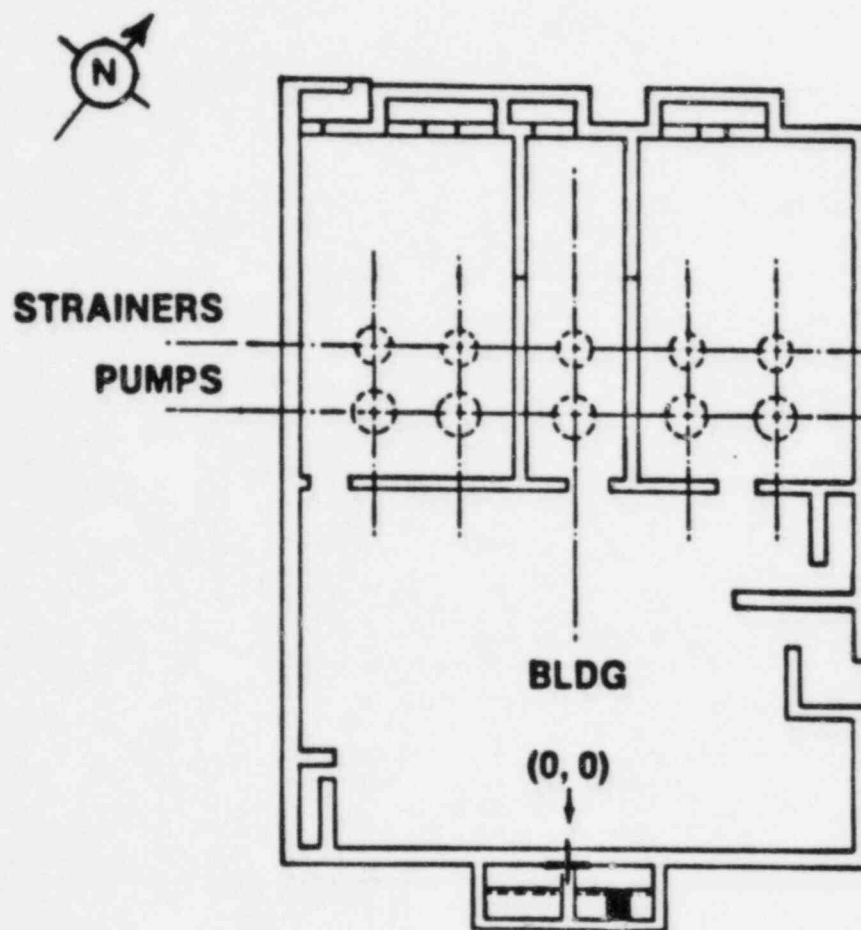


FIGURE IV-2-1. SERVICE WATER PUMP STRUCTURE
PLAN AT ELEVATION 634'-6"

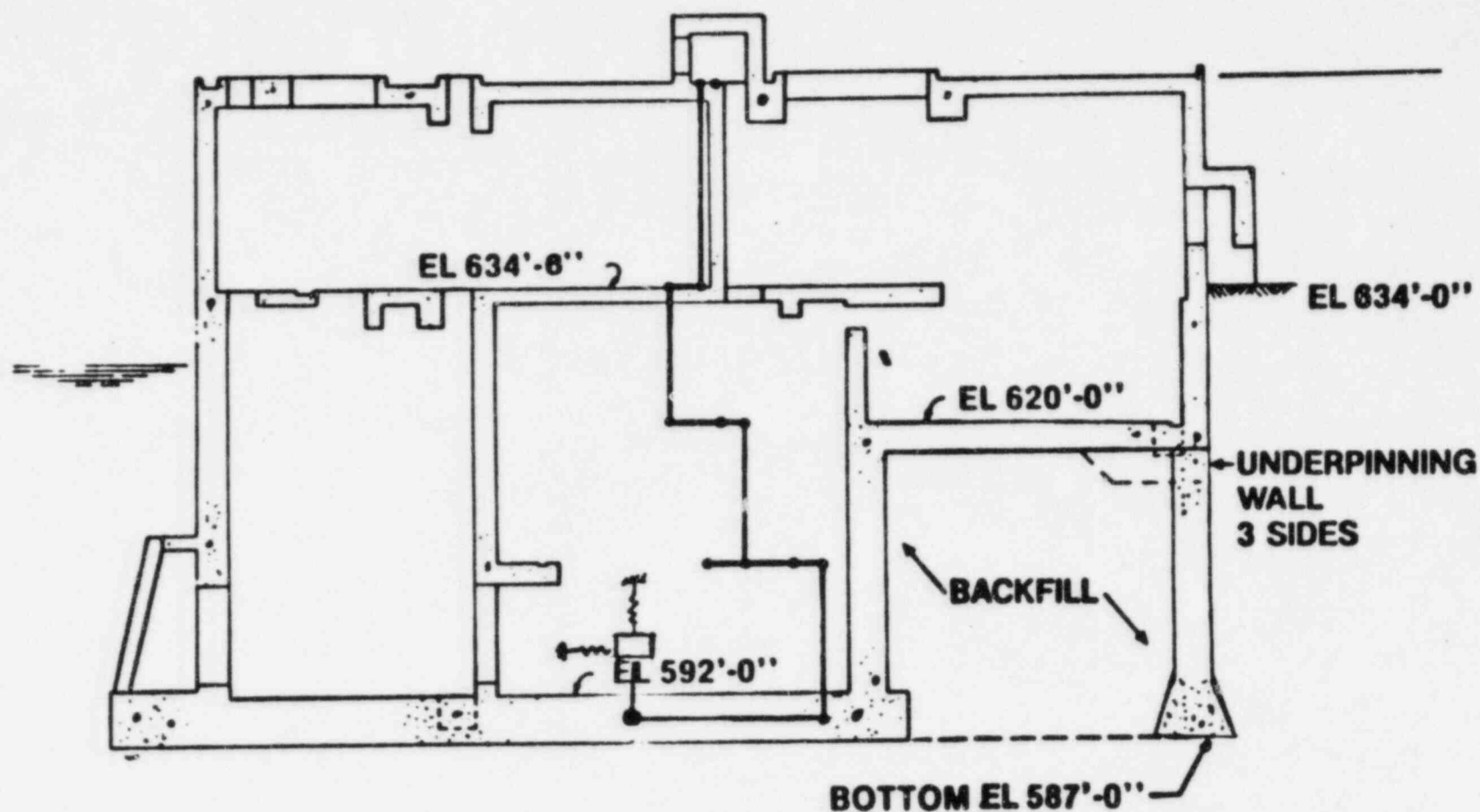


FIGURE IV-2-2. SERVICE WATER PUMP STRUCTURE NORTH-SOUTH SECTION
SHOWING SUPERIMPOSED DYNAMIC MODEL

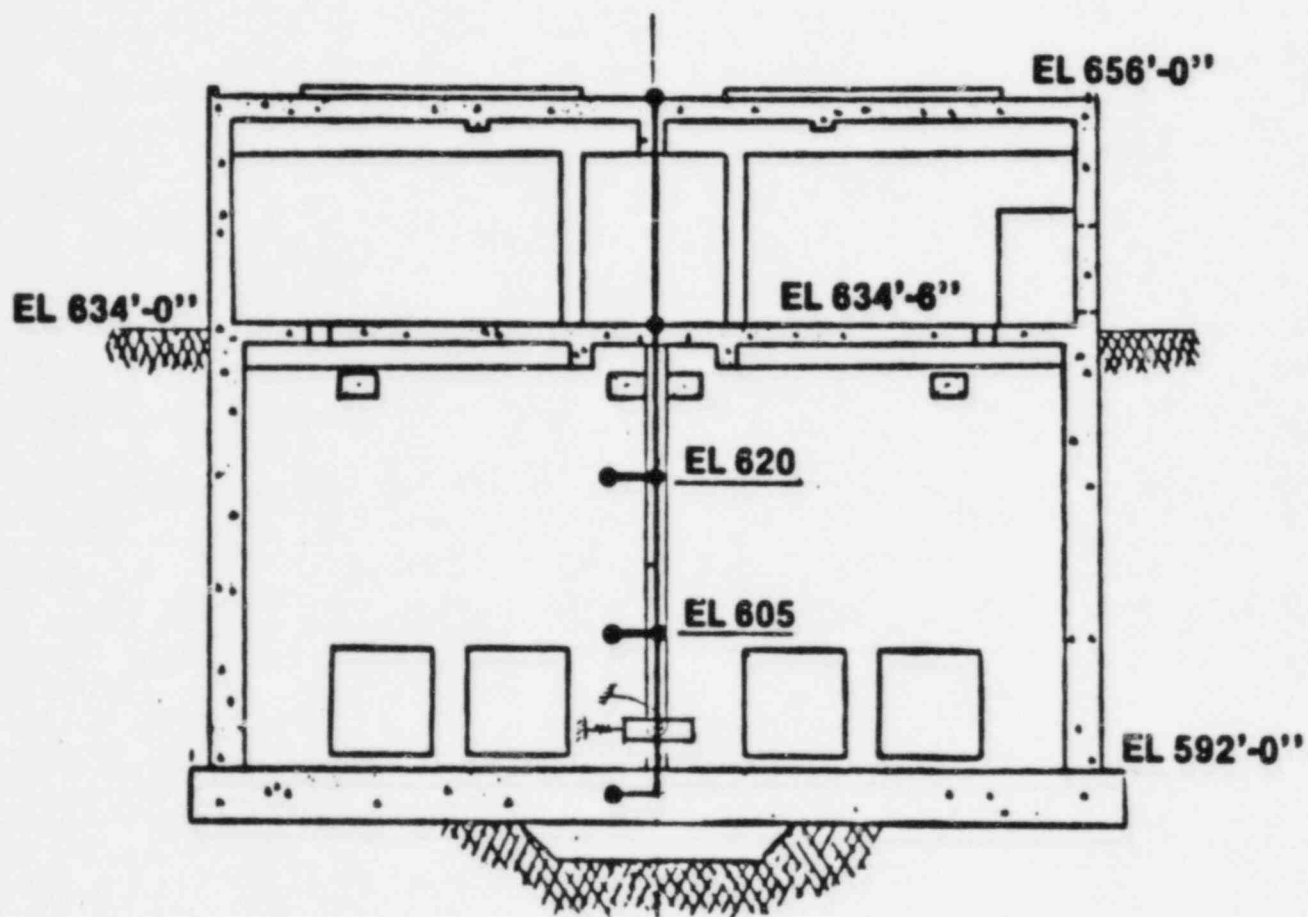



FIGURE IV-2-3. SERVICE WATER PUMP STRUCTURE EAST-WEST SECTION
SHOWING SUPERIMPOSED DYNAMIC MODEL

LEGEND

- Node locations
- Mass for all 3 degrees of freedom
- Mass for two horizontal degrees of freedom
- ▲ Mass for vertical degree of freedom
-  Base location. Damper rotational springs not shown for clarity

NOTES:

1. The mass of the water is lumped at mass points 7, 11, and 15 horizontally and at mass point 16 vertically.
2. The mass of the fill entrapped within the underpinning walls is lumped at mass points 7, 11, and 15 for the two horizontal degrees of freedom only.

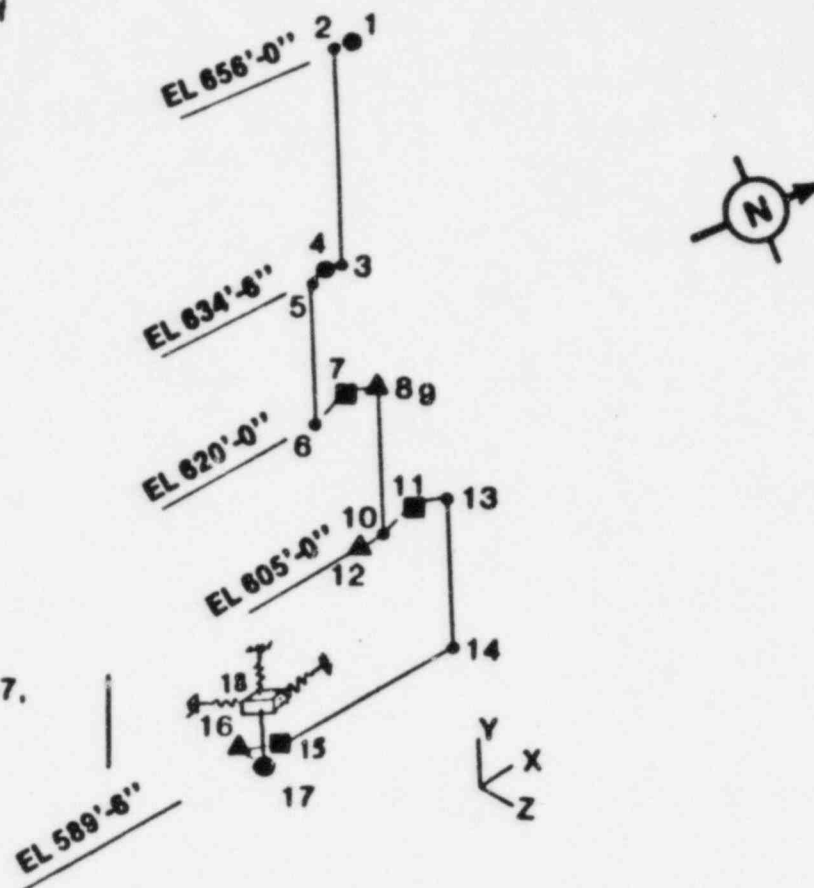


FIGURE IV-2-4. SERVICE WATER PUMP STRUCTURE DYNAMIC MODEL

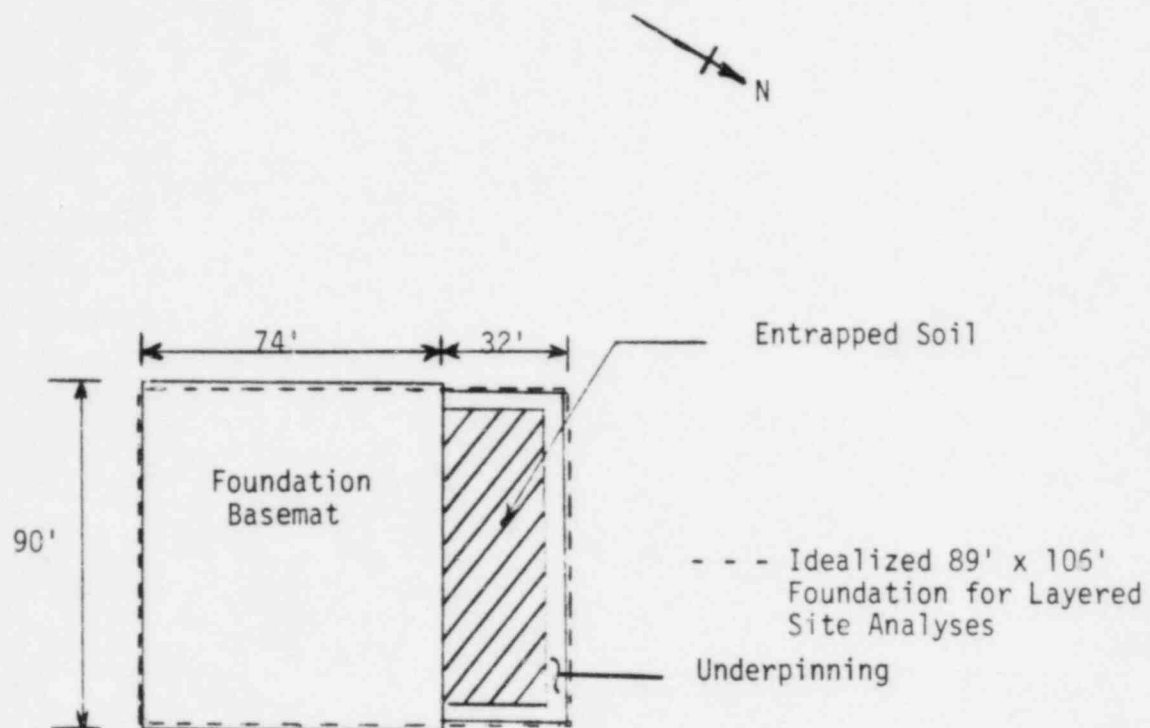


FIGURE IV-2-5. IDEALIZED FOUNDATION GEOMETRY OF SERVICE WATER PUMP STRUCTURE USED IN LAYERED SITE ANALYSES

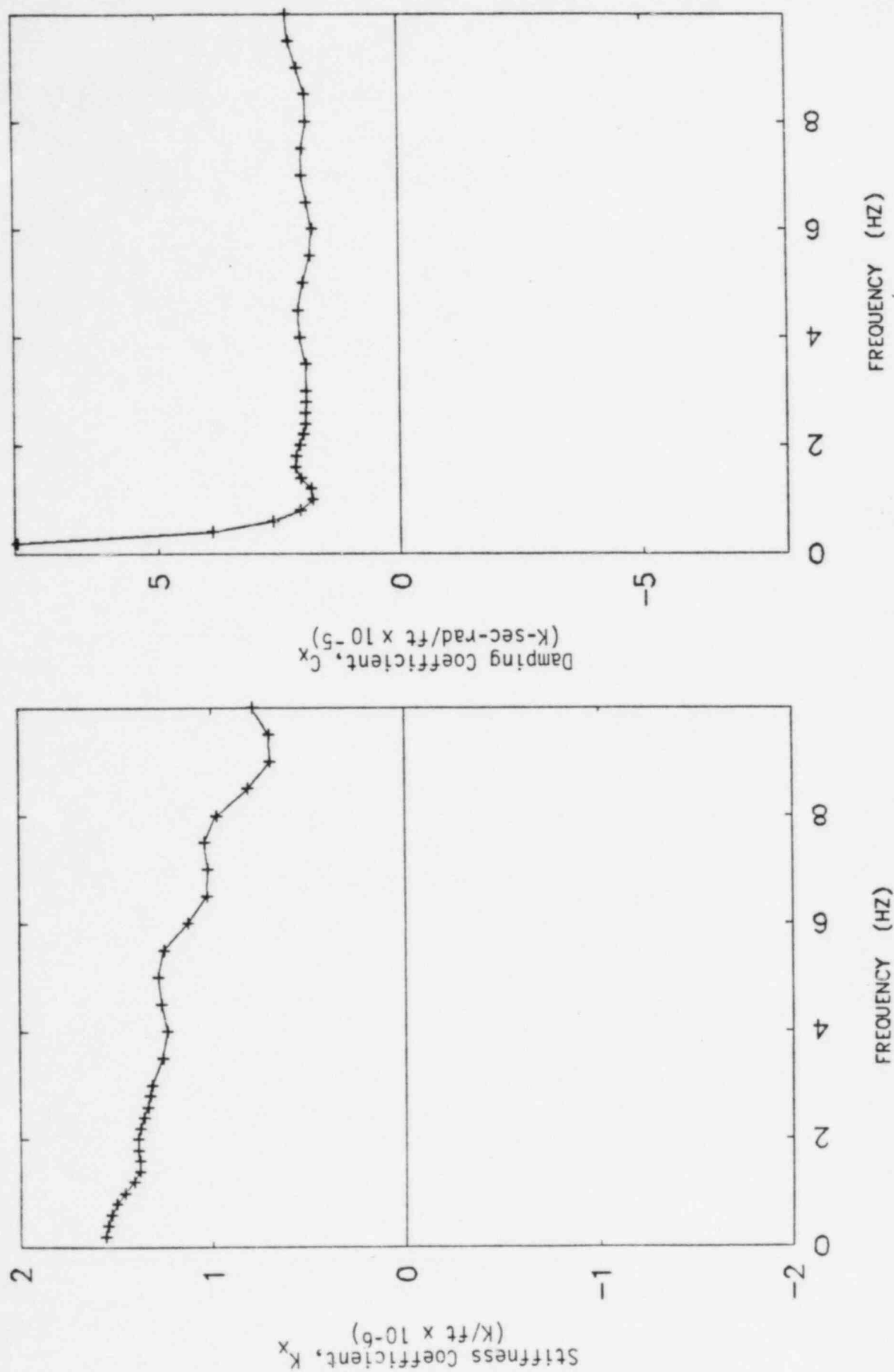
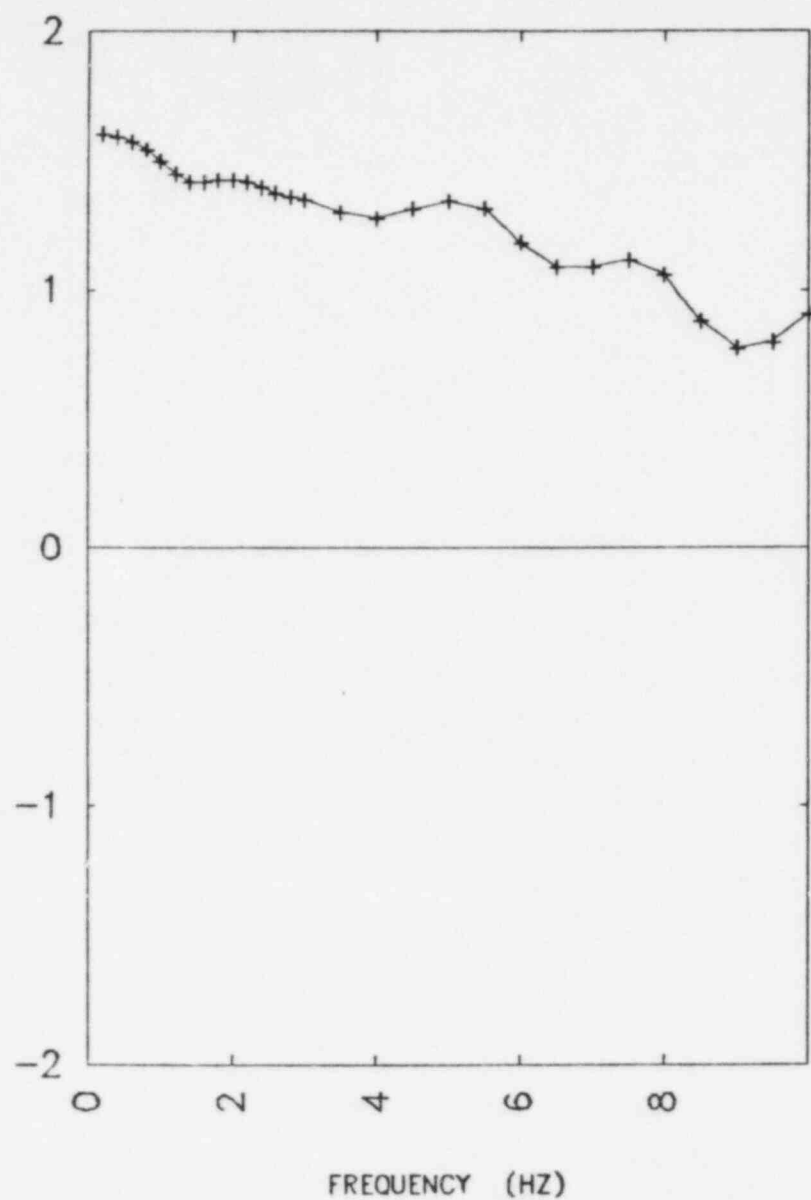


FIGURE IV-2-6. NORTH-SOUTH TRANSLATION SOIL IMPEDANCE
INTERMEDIATE CASE LAYERED SOIL PROFILE

IV-2-23

Stiffness Coefficient, K_x
(k-ft $\times 10^{-6}$)



Damping coefficient, C_x
(K-sec-rad/ft $\times 10^{-5}$)

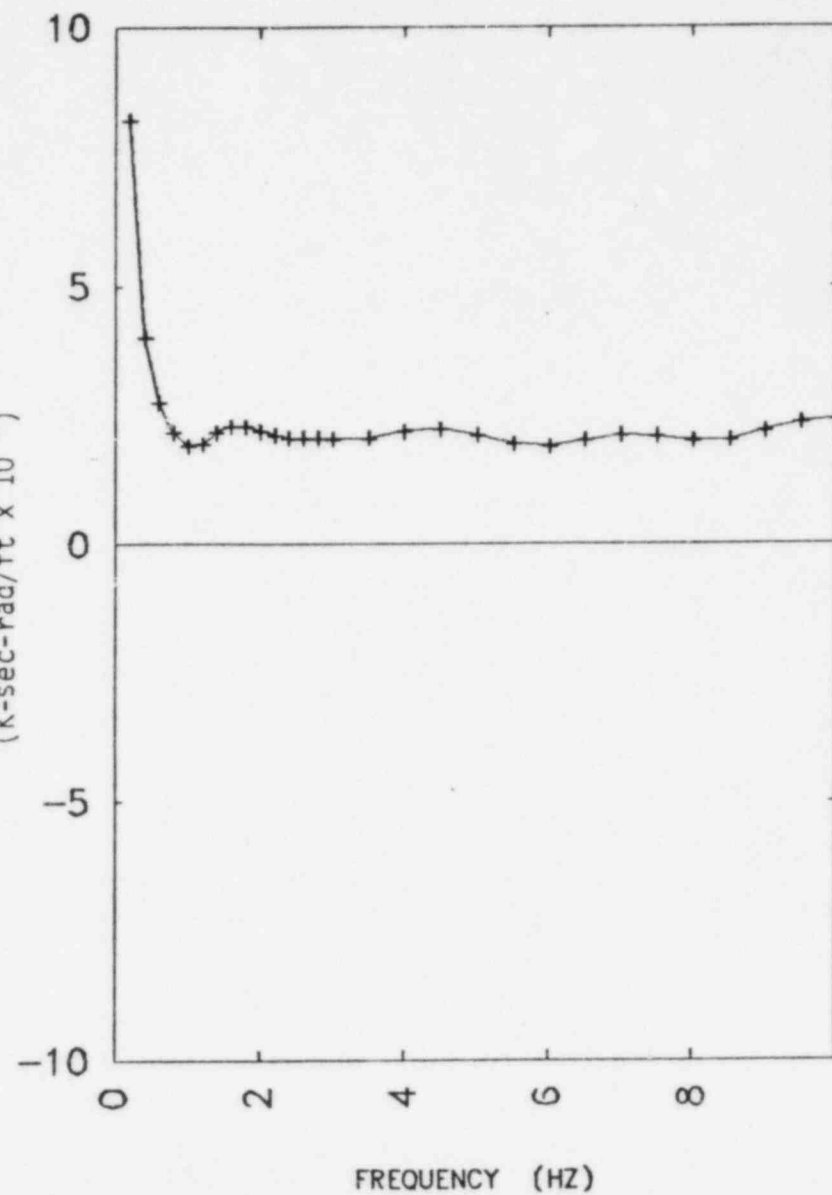


FIGURE IV-2-7. EAST-WEST TRANSLATION SOIL IMPEDANCE
INTERMEDIATE CASE LAYERED SOIL PROFILE

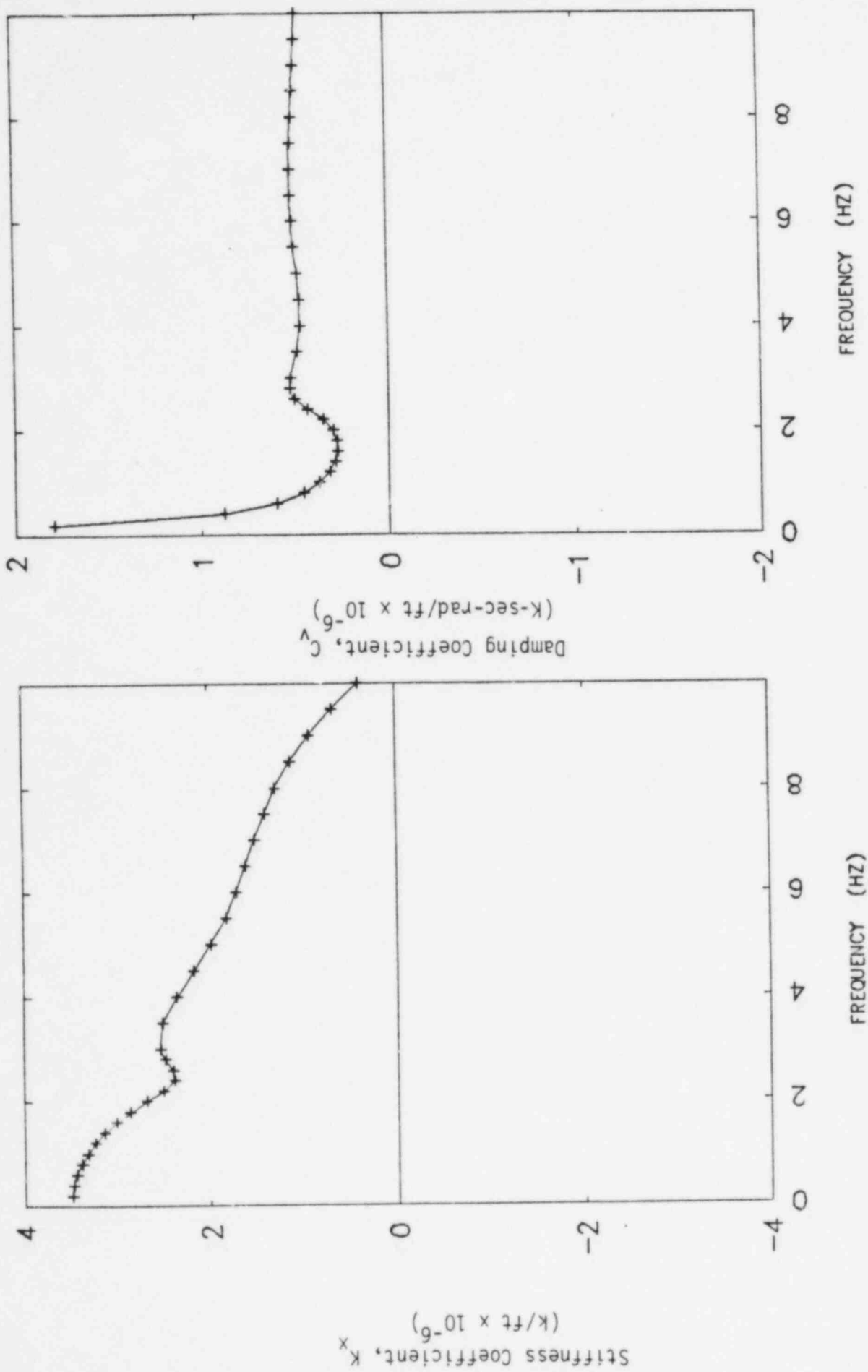


FIGURE IV-2-8. VERTICAL TRANSLATION SOIL IMPEDANCE
INTERMEDIATE CASE LAYERED SOIL PROFILE

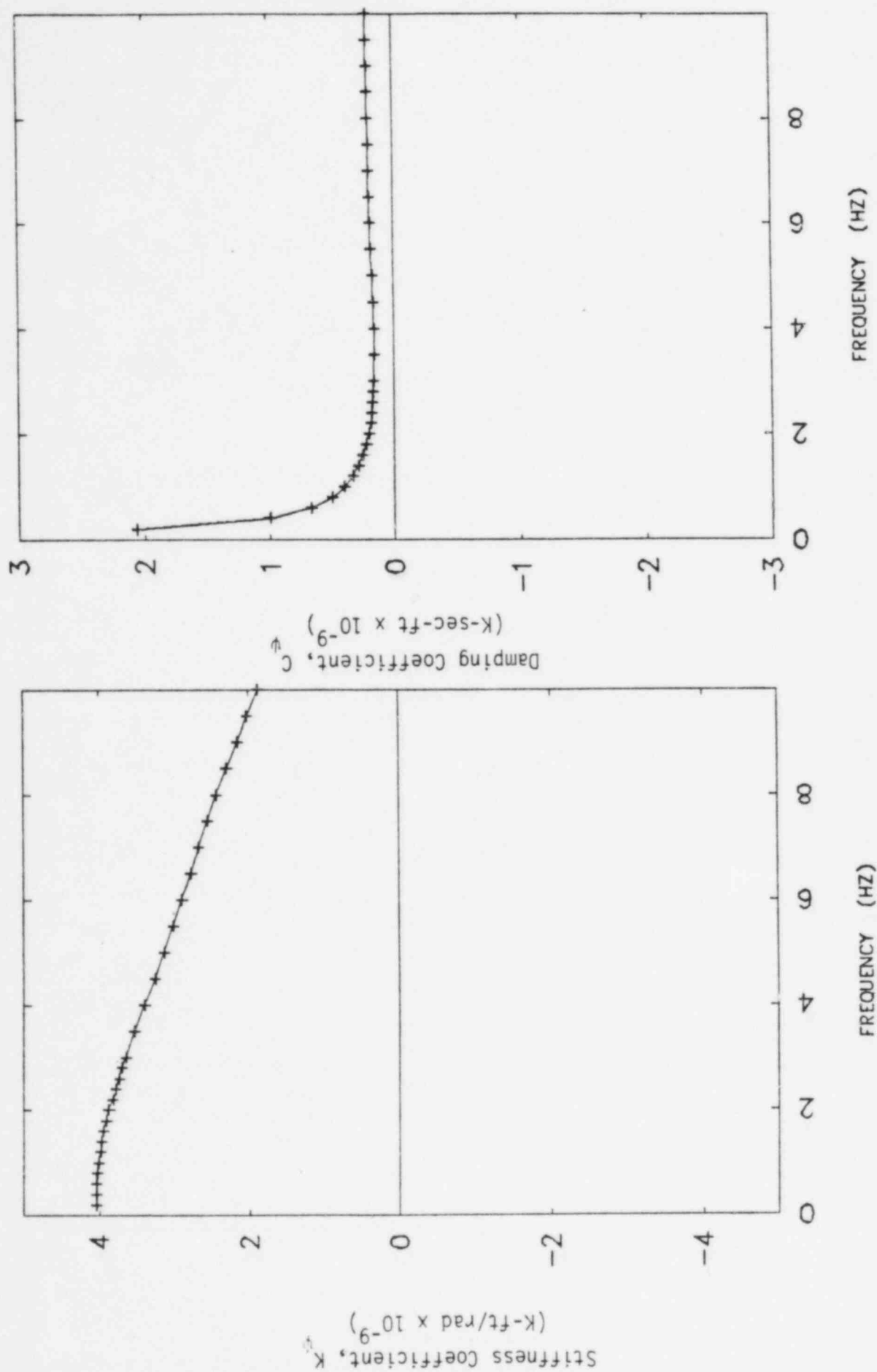


FIGURE IV-2-9. ROCKING ABOUT THE NORTH-SOUTH AXIS SOIL IMPEDANCE
INTERMEDIATE CASE LAYERED SOIL PROFILE

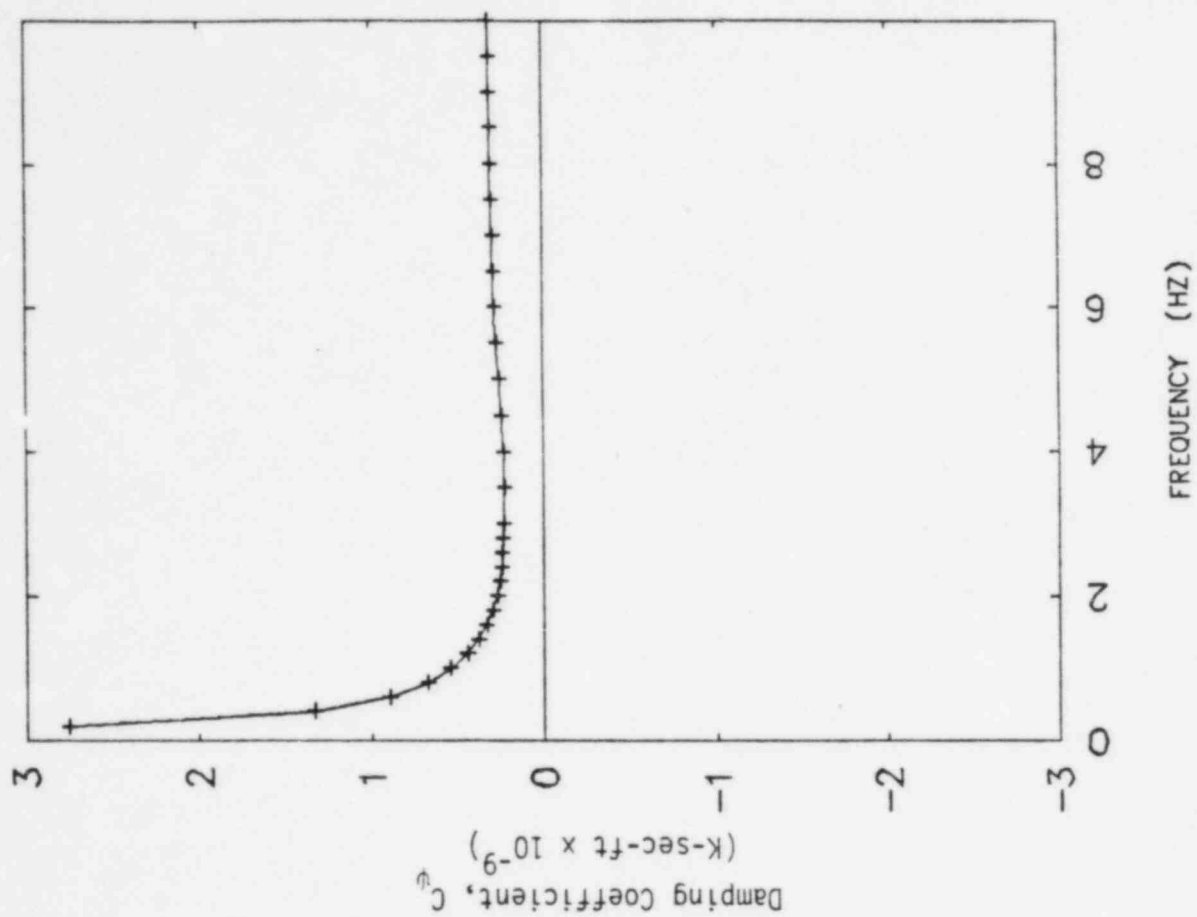
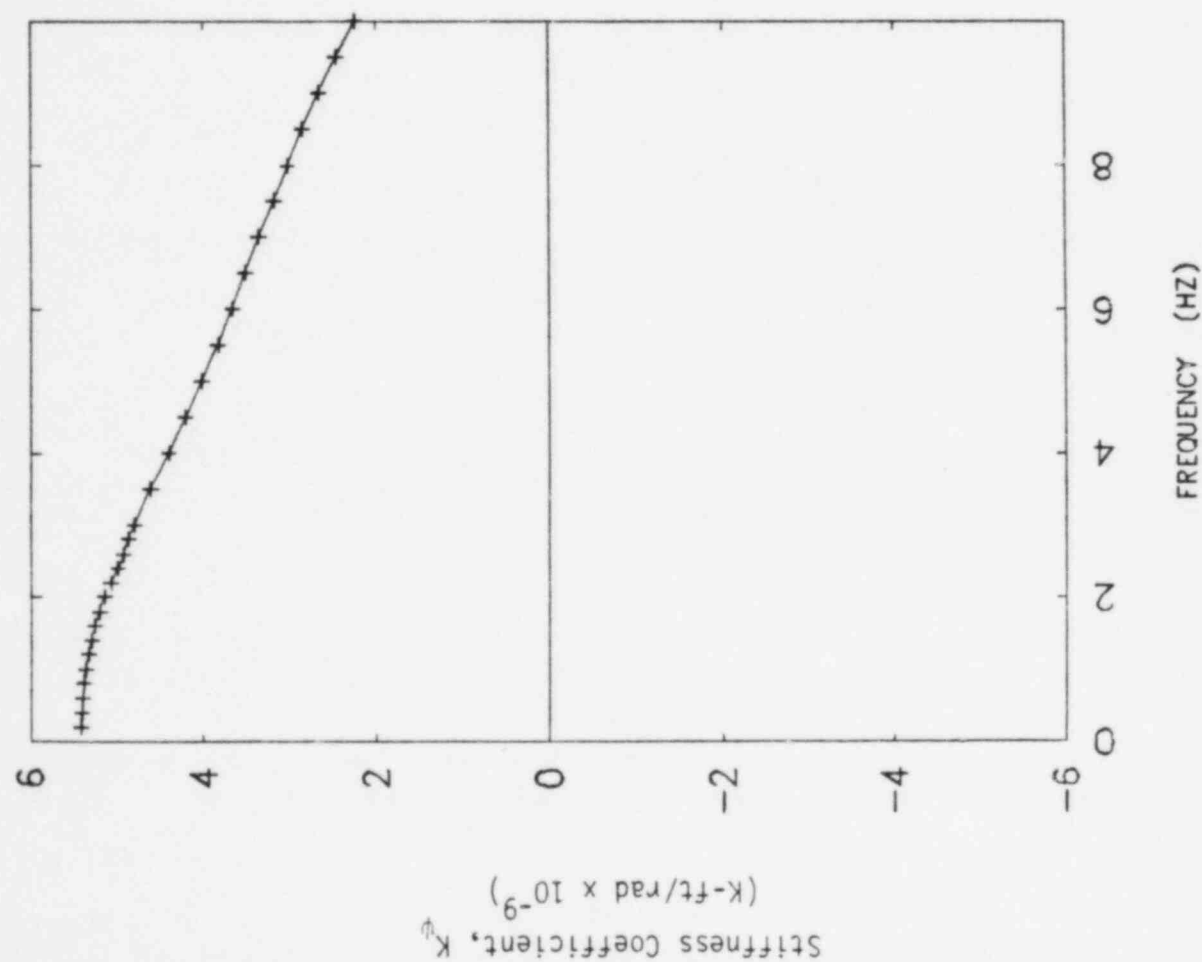


FIGURE IV-2-10. ROCKING ABOUT THE EAST-WEST AXIS SOIL IMPEDANCE
INTERMEDIATE CASE LAYERED SOIL PROFILE

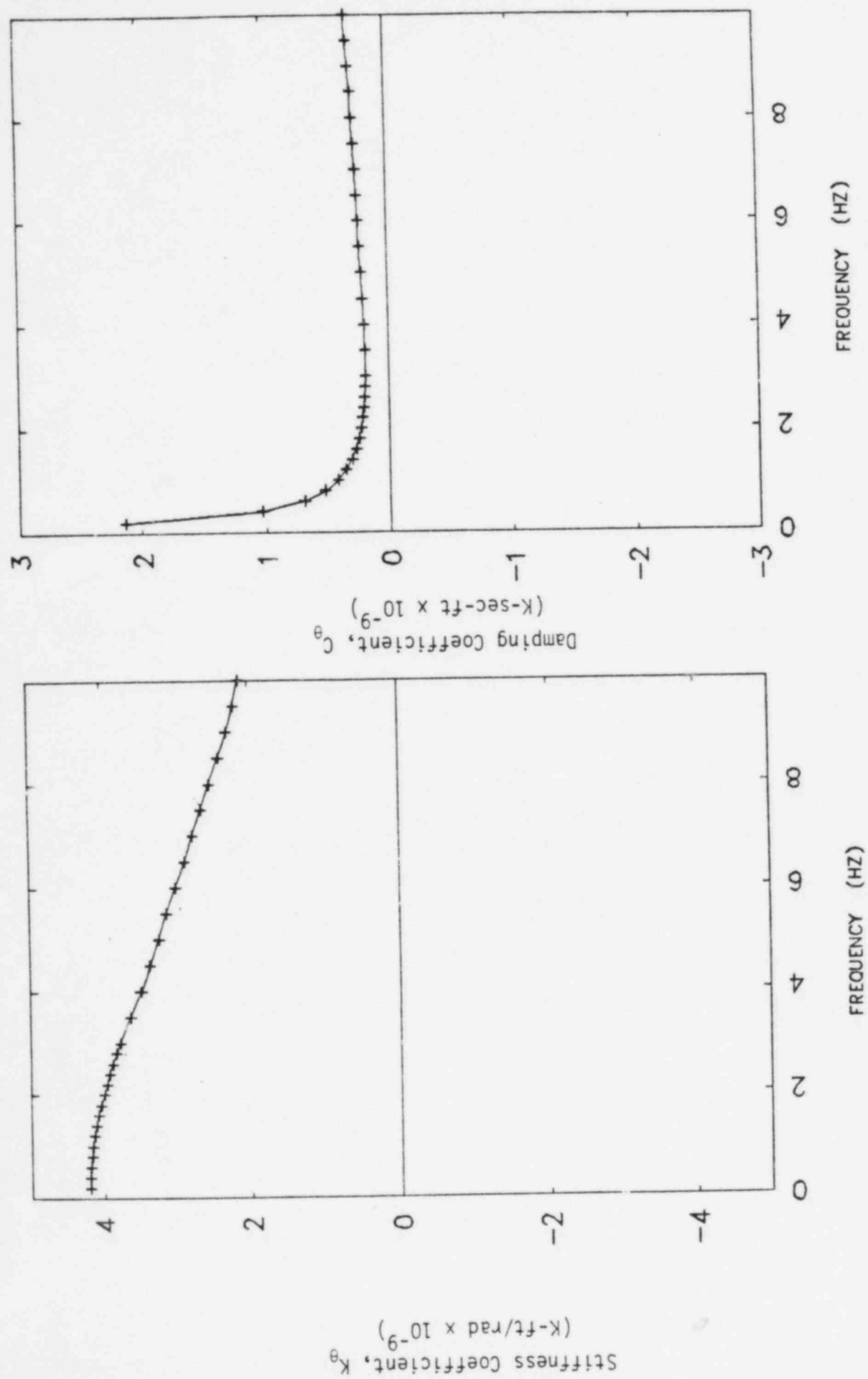


FIGURE IV-2-11. TORSION ABOUT THE VERTICAL AXIS SOIL IMPEDANCE
INTERMEDIATE CASE LAYERED SOIL PROFILE

3. SEISMIC RESPONSE

3.1 MODAL CHARACTERISTICS

The service water pump structure natural frequencies, percentage of total structure mass participating in each mode, and mode description for the three soil cases studied are presented in Tables IV-3-1 through IV-3-3. The fundamental mode for the lower bound soil case is an East-West soil-structure translational mode with a natural frequency of approximately 2.10 hertz. About 77 percent of the structure mass in the East-West direction participates in this mode. Some coupling with the North-South direction occurs at this frequency as shown by the 11 percent of participating structure mass in the North-South direction. The second mode of the structure has a natural frequency of approximately 2.12 hertz with approximately 75 percent of the structure mass in the North-South direction participating. Minor coupling between the North-South and East-West directions also occurs at this frequency. The fundamental vertical natural frequency occurs at about 3.10 hertz. About 96 percent of the vertical structure mass participates in this soil-structure mode. Higher frequency structure modes are primarily associated with out-of-phase soil-structure response. The percentage of structural mass participating in these higher modes is relatively low with at most 11.3 percent of the mass responding in any individual mode. Inclusion of 10 structure modes in the response spectrum analysis for this soil case resulted in at least 99.9 percent of the structure mass being included.

Results for the intermediate soil case are quite similar. The fundamental soil-structure natural frequencies in the North-South and East-West directions occur at 3.84 and 3.86 hertz, respectively. Approximately 75 percent of the structure mass participates in the fundamental North-South mode. The primary East-West translational mode has about 78 percent mass participation. Some coupling occurs between these two directions as evidenced by the 8 percent of structure mass

participation in the orthogonal response directions for these two modes. The fundamental vertical soil-structure mode has a natural frequency of 5.54 hertz and has 96 percent of vertical mass responding in this mode. The higher frequency structure modes are mainly associated with out-of-phase soil-structure response with at most 14 percent of the structure mass participating in any individual mode. Ten structure modes were used in response spectrum analyses for the intermediate soil case which results in at least 99.9 percent of all structure mass being included.

Results for the upper bound soil case are presented in Table IV-3-3. The fundamental soil-structure natural frequencies determined for the North-South and East-West directions occur at 6.52 and 6.58 hertz, respectively. Between 79 and 82 percent of the total structure mass participates in these modes. Little coupling occurs between the East-West and North-South directions for this soil case. In the vertical direction, the fundamental soil-structure frequency occurs at 9.62 hertz. Ninety-seven percent of the total structure mass participates in this mode. Out-of-phase soil-structure translational modes are slightly more important for this soil case with between 16 and 17 percent of the structure mass responding in the higher modes. Use of fifteen structure modes in the response spectrum analysis for this soil case resulted in 99.9 percent of the total structure mass being included in the results.

3.2 COMPOSITE MODAL DAMPING

Response spectrum analysis techniques assume the structure has classical normal modes. In other words, the equations of motion are assumed to uncouple and the response of the structure can be calculated as the superimposed response of a series of single-degree-of-freedom systems. For multi-degree-of-freedom structures with more than approximately 20 percent critical damping, the structure does not normally possess classical normal modes. Structural response can be rigorously computed only by a step-by-step technique such as direct integration time history analysis. However, when modal damping values are appropriately selected, normal mode techniques such as response spectrum

analysis can be used to calculate accurate seismic response loads. The use of response spectrum analysis techniques to compute the structure seismic loads allows a more accurate representation of the SME input characteristics without the peaks and valleys associated with an artificial time history input.

Service water pump structure seismic response loads were determined from response spectrum analysis using composite modal damping techniques to define modal damping for the combined soil-structure modes. Typically, composite modal damping for the structure is defined by an empirical technique such as stiffness proportional damping. This technique works well for determining structural modal damping for buildings comprised of structural systems which have different element damping ratios associated with each load-carrying subsystem. However, experience with these techniques has shown that when a structure with relatively low overall damping (approximately 4 to 7 percent of critical damping) is coupled to a soil model with large radiation and material damping (approximately 15 to 20 percent of critical damping), resulting composite modal damping values may lead to underprediction of structural response for locations high in the structure. The procedure presented in Volume I of this report was used to define composite modal damping for the coupled soil-structure model of the service water pump structure, and avoids this difficulty. This method is based on matching the response computed from the coupled equations of motion with the modal response at selected locations. Soil impedances are considered to act at the centroid of the overall foundation in determining structure dynamic characteristics. Structure response transfer functions are then developed at a number of locations in the structure for both the rigorous and normal mode solutions. Modal damping values for the normal mode solution are iterated upon until the transfer functions for the two solutions essentially match. By choosing locations which are sensitive to damping, composite modal damping values are determined which generally predict conservative response at all locations.

Composite modal damping values were determined using the program SOILST (Reference 15). The embedded stiffnesses and dashpots presented in Tables IV-2-4 and IV-2-5 defined the soil impedances beneath the structure in this analysis. Structural damping of 7 percent of critical damping was used for the reinforced concrete service water pump structure. The fixed base structure modes and corresponding structural modal damping were input to program SOILST to determine composite modal damping which accounted for both structural damping and soil geometric and material damping.

Composite modal damping values were determined for a number of locations in the structure. Typical floors were chosen in the building that were relatively high in the structure and were judged to have dynamic responses sensitive to modal damping. Composite modal damping values for all important modes were chosen based on a conservative fit of the data for all locations studied.

Composite modal damping values were determined using the methodology described above for all modes contributing to more than about 10 percent of the total degree-of-freedom response at the structure location studied. Local modes associated with structure response only were damped at the building structural damping value of 7 percent of critical. High frequency structure modes were conservatively damped at 3-1/2 percent of critical damping. The rationale for lightly damping higher frequency modes was based on a parametric study of auxiliary building response as discussed in Volume III.

The composite modal damping values used to determine seismic response loads in the service water pump structure are presented in Tables IV-3-1 to IV-3-3. Damping for the fundamental horizontal translational soil-structure modes ranges from 14 percent of critical damping for the upper bound soil case to 22 percent of critical damping for the lower bound soil case. Composite modal damping values used for the fundamental vertical mode range from 49 to 60 percent of critical damping. Higher frequency modes typically are highly damped. Because of high partici-

pating mass percentages in the fundamental modes, overall seismic response loads in the structure are primarily determined by the damping associated with the fundamental modes in each direction.

To ensure that composite modal damping values were conservatively chosen for all structure modes, comparisons of structural response predicted by direct integration time history analysis using concentrated dashpots to model the soil damping were made with the seismic response determined by modal superposition using composite modal damping. Response accelerations at typical locations in the structure were determined from direct integration of the coupled equations of motion. At these same locations response accelerations were then developed from a modal superposition time history analysis of the flexible base structure model using the modal damping values defined for each soil case by Tables IV-3-1 to IV-3-3. The same input time history was used in both time history analyses. Response accelerations from the two analyses were compared to ensure the accelerations based on the composite modal damping values approximately met or exceeded those determined from the direct integration time history analyses. Table IV-3-4 presents comparisons of zero period accelerations in the structure obtained by these two procedures for the upper bound soil case. The results for the upper bound soil case are presented since seismic response loads throughout the structure are generally controlled by this soil case. Results for the other soil cases were similar.

3.3 STRUCTURE SEISMIC RESPONSE

Seismic loads throughout the structure were determined from the dynamic model of the service water pump structure for each of the three soil cases studied. The overall seismic loads computed for the building were distributed to the individual structural elements as described in Section 3.3.3 of this volume.

The seismic loads in the structure were determined using response spectrum modal analysis techniques. Earthquake excitation was specified as the SME ground response spectra for the original ground surface. The development of these spectra is described in Section 2.2 of

Volume I of this report. The vertical input was assumed to be 2/3 of the horizontal spectra. Soil-structure interaction effects were considered for the upper, intermediate, and lower bound soil cases. The effects of embedment on the soil-structure interaction parameters were discussed in Section 2 of this volume.

The overall seismic loads were developed from the SRSS of the modal responses including consideration of closely spaced modes as discussed in Section 6.4 of Volume I. The structural response loads were determined for each of the three earthquake direction components acting independently and were then combined by SRSS. For the SMR evaluation, the highest load computed for the structural element from any of the three soil cases was used to determine its code margin.

3.3.1 Effects of Soil Conditions on Seismic Loads

Plots of SRSS horizontal seismic shear and overturning moments are shown in Figure IV-3-1 through IV-3-4 for the three soil cases studied. Seismic response loads in the structure were generally controlled by either the intermediate or the upper bound soil case. Seismic shear loads above Elevation 620' are maximized by the upper bound soil case. At lower elevations in the structure, the intermediate soil case shear loads either control or are approximately the same as the upper bound soil case results. Overturning moments in the structure determined from both the intermediate and upper bound soil case results are virtually identical at all locations in the structure.

Figures IV-3-5 and IV-3-6 presents plots of SRSS axial force and SRSS torsional moment in the structure. Axial loads in the structure were maximized at all elevations by the upper bound soil case. Torsional moments in the structure were maximized by the intermediate soil case above Elevation 620'. Below this elevation, the lower bound soil case resulted in the maximum seismic torsional loads. The seismic code margin evaluation was based on the worst case soil condition which resulted in the maximum load in the element considered, even though the worst case soil condition cannot occur simultaneously for a number of different elements.

3.3.2 Comparison of SMR and FSAR Design Loads

One basis for selecting various elements for code margin evaluation for the SMR was the ratio of SME seismic load to the FSAR seismic load. In order to determine the relative magnitudes of the SMR loads to the corresponding FSAR loads, comparisons of the lateral shear forces, overturning moments, vertical axial forces, and torsional response throughout the structure are shown in Figures IV-3-7 through IV-3-12.

Figures IV-3-7 through IV-3-10 show comparisons of the lateral seismic shear forces and corresponding overturning moments throughout the service water pump structure. Below Elevation 620', the FSAR shears and moments exceed the SMR loads by about 5 to 10 percent. At locations higher in the structure, FSAR seismic shear forces and moments either approximately equal SMR values or exceed them by about 5 percent. The underpinning structure is being designed to 1.5 times the FSAR.

A comparison of FSAR and SMR vertical axial forces is shown in Figure IV-3-11. In the vertical direction, the axial forces calculated for the SMR exceed the FSAR values by about 10 percent. This slight increase in vertical loads has only a small effect on the code margins determined for the structure. As shown by Figure IV-3-12, seismic torsional moments determined for the SMR exceed the FSAR values at all elevations. SMR torsional response loads are about 25 to 35 percent higher than FSAR values for locations high in the structure. At lower elevations, the SMR torsional moments are as large as FSAR values at certain locations. These high torsional loads develop because of coupling which occurs for the lower bound and intermediate soil cases, and results in increased lateral loads in the peripheral shear walls of the structure.

3.3.3 Element Loads

The dynamic model used for the seismic analysis of the service water pump structure consisted primarily of interconnected vertical beam elements representing the stiffness properties of the structure. Each vertical element typically modelled the combined stiffness of the

structural members of the load-resisting system at that story. Overall seismic loads acting on the structure were developed for these elements from the response spectrum analyses. Distribution of the overall loads to the individual structural members was performed using techniques appropriate for the load-resisting system evaluated.

The service water pump structure is composed primarily of concrete shear walls interconnected by concrete floor slabs. For this type of structural system, the floor slabs act as diaphragms transmitting the seismic inertial forces to the load-resisting shear walls. If the diaphragms have sufficient stiffness, the walls spanning a story are constrained to displace together in the lateral directions. The overall seismic lateral loads can then be distributed to the individual walls in proportion to their relative rigidities. This technique is commonly used to develop load distributions for the design of concrete shear wall/floor slab systems.

The rigid diaphragm approximation was judged to be adequate for the determination of lateral seismic loads acting on the shear walls of the service water pump structure. Load distributions to the individual structural elements were developed as described in Section 6.7 of Volume I. Structural elements included in these load distributions were typically those considered to be seismic load-resisting in calculations performed to determine the stiffness properties of the dynamic model. In general, all exterior and interior concrete walls capable of resisting seismic loads were included. The walls receiving seismic forces were identified by individual elements having rectangular dimensions in plan. Some walls were modeled by a series of continuous elements. Major wall openings were treated as complete discontinuities in the element layout with the openings effectively spanning the full story height.

Story stiffnesses for elements identified as being seismic load-resisting were calculated by Bechtel as part of the development of stiffness properties of the dynamic model. These story stiffnesses were determined as described in Section 6.7 of Volume I. Out-of-plane wall

stiffnesses were not included so that conservative in-plane loads would be produced. In-plane wall story stiffnesses considered the effects of both shear and flexural deformations. As an approximation, the flexural wall story stiffnesses were based on a condition of rotational fixity imposed at the top and bottom of the stories. The influence of flexural deformations diminishes for walls whose lengths are greater than their story heights and the lateral deflections of these walls are due primarily to shear deformations. The distribution of lateral seismic load, therefore, is not expected to be sensitive to the treatment of wall rotational boundary conditions.

Seismic in-plane shears and overturning moments for the walls of the service water pump structure were calculated following the methodology for shear wall/floor slab systems described in Section 6.7 of Volume I. Wall element relative rigidities associated with the rigid diaphragm approximation were based on the wall story stiffnesses. Individual wall shears due to overall structure shears and torsional moments were then calculated using equations presented in Reference 16. Load input to these equations consisted of shears and torsional moments predicted by the structure response spectrum analyses. For conservatism, the possibility of a reduction in structure seismic load due to embedment effects was neglected. Seismic loads acting on the existing wall elements evaluated in the SMR are listed in Tables IV-4-1 and IV-4-2. Seismic loads acting on the underpinning wall and connectors evaluated are listed in Table IV-4-4.

Overall axial loads due to seismic response were available from the results of the response spectrum analyses. These axial loads were distributed to the walls in proportion to their cross-sectional areas. These axial loads have some effect on the capacities of the walls against shear and overturning moment. However, capacities of the walls are not particularly sensitive to small changes in the axial loads due to seismic response. Axial loads determined in this manner were included in the shear and overturning moment capacity calculations.

The concrete floor slab at a given elevation serves as a diaphragm distributing floor inertial forces to the load-resisting shear walls. The slab also redistributes seismic shears from the walls of the story above to the walls of the story below when there is an alteration in the relative wall stiffness distribution from story-to-story. The diaphragm can be idealized as a beam subjected to load comprised of the seismic floor inertial force and shears from the walls of the story above. Support reactions for the idealized beam consist of the shears for the walls of the story below. Diaphragm in-plane shears and moments at the critical sections were determined based on these applied loads and reactions. For slabs framing into an exterior wall, the diaphragm shear at the wall is equal to the difference in wall shears between the story above and the story below. This treatment accounts for diaphragm loads due to both floor inertial forces and redistribution of lateral seismic loads due to changes in the stiffness distribution of the vertical load-resisting elements. It is conservative since the diaphragm load calculated in this manner includes the inertial load associated with the wall itself which is not actually transmitted through the diaphragm. Applied seismic loads acting on the diaphragms selected for evaluation in the SMR are listed in Table IV-4-3.

The load combination used in the structures capacities evaluation is discussed in Section 7.1 of Volume I. The dead and live load cases account for loads occurring at normal operating conditions. Forces and stresses in the reinforced concrete structural members of the service water pump structure due to loads occurring at normal operating conditions were taken from the results of the static analyses supplied by Bechtel (Reference 17). Two sets of analytical results corresponding to the use of different soil springs representing different differential settlement conditions were available. Five load cases for each set of results were supplied. One load case combined the stresses due to all loads occurring at normal operating conditions, including applied dead, live, lateral earth pressure, surcharge, settlement, hydrostatic

pressure, and jacking preloads. The other four load cases report stresses due to Bechtel's dynamic soil decrements. In Bechtel's static analysis of the service water pump structure, the backfill soil is assumed to displace more than the structure under seismic ground motion. Under this assumption, the soil pulls away from the structure. To represent the soil's inability to transmit tension across the structure interface, Bechtel's dynamic soil decrement load cases cancel out the imposed lateral earth pressures occurring at normal operating conditions. The four load cases correspond to different combinations of backfill soil displacement relative to the structure. The code margins for the structural elements were based on the following load combination.

$$U = D + L + P_L + T + DSD + SME$$

where:

- D = Dead Loads
- L = Live Loads
- P_L = Jacking Preload effects
- T = Differential settlement
- DSD = Dynamic Soil Decrement
- SME = Seismic Margin Earthquake loads

In this load combination, the loads from the worst case differential settlement condition were used. Also, the dynamic soil decrement load case yielding the worst case loading when combined with the normal operating condition loads was included. The effects of thermal gradients through the walls and slabs are discussed in Section 4-6.

The three-dimensional finite element model used for these static analyses generally consisted of plate elements representing the walls and slabs and beam elements representing the columns and the beams. Results from the static analyses for the plate elements modeling the concrete walls and slabs consisted of membrane normal and shear forces per unit length and out-of-plane bending and twisting moments per unit length. For the walls and slabs, net in-plane axial forces, shears, and moments were calculated by integrating the reported plate element membrane stresses along the cross-sections being evaluated. In-plane shears and moments obtained from Bechtel static finite element analysis results for the walls and diaphragms evaluated in this study are also listed in Tables IV-4-1 through IV-4-4. Out-of-plane moments predicted by the plate elements were taken directly from the analytical results.

TABLE IV-3-1

SERVICE WATER PUMP STRUCTURE NATURAL FREQUENCIES, MODAL MASS, AND MODAL DAMPING

LOWER BOUND SOIL

Mode Number	Modal Frequency (Hz)	Percentage of Total Structure Mass Participating in Each Mode			Modal Damping (% Critical)	Mode Description
		North-South Response	East-West Response	Vertical Response		
1	2.10	11.2	76.7	---	22	East-West (E/W) Soil-Structure Translation
2	2.12	75.3	11.4	0.9	22	North-South (N/S) Soil-Structure Translation
3	3.10	2.2	---	95.9	60	Vertical Soil-Structure Translation
4	3.23	---	2.3	---	7	E/W Response of Upper Floors
5	4.16	11.3	---	3.0	34	Out-of-Phase N/S Soil-Structure Mode
6	4.56	---	9.4	0.1	34	Out-of-Phase E/W Soil-Structure Mode
7					3.5	
.					.	
10					3.5	

Participating mass percentages less than 0.1 percent are not shown.

TABLE IV-3-2

SERVICE WATER PUMP STRUCTURE NATURAL FREQUENCIES, MODAL MASS, AND MODAL DAMPING

INTERMEDIATE SOIL

Mode Number	Modal Frequency (Hz)	Percentage of Total Structure Mass Participating in Each Mode			Modal Damping (% Critical)	Mode Description
		North-South Response	East-West Response	Vertical Response		
1	3.84	75.5	8.4	0.8	15	North-South (N/S) Soil-Structure Translation
2	3.86	8.0	78.3	0.2	15	East-West (E/W) Soil-Structure Translation
3	5.54	2.3	0.1	96.4	60	Vertical Soil-Structure Translation
4	6.01	---	1.0	---	7	E/W Response of Upper Floors
5	7.61	14.0	---	2.5	41	Out-of-Phase N/S Soil-Structure Mode
6	8.30	---	12.0	---	38	Out-of-Phase E/W Soil-Structure Mode
7					3.5	
•					•	
10					3.5	

Participating mass percentages less than 0.1 percent are not shown.

TABLE IV-3-3

SERVICE WATER PUMP STRUCTURE NATURAL FREQUENCIES, MODAL MASS, AND MODAL DAMPING

UPPER BOUND SOIL

Mode Number	Modal Frequency (Hz)	Percentage of Total Structure Mass Participating in Each Mode			Modal Damping (% Critical)	Mode Description
		North-South Response	East-West Response	Vertical Response		
1	6.52	79.0	0.4	0.7	14	North-South (N/S) Soil-Structure Translation
2	6.58	0.4	82.0	---	14	East-West (E/W) Soil-Structure Translation
3	9.62	1.8	---	96.9	49	Vertical Soil-Structure Translation
4	10.07	---	0.1	---	7	E/W Response of Upper Floors
5	13.69	17.4	---	1.8	19	Out-of-Phase N/S Soil-Structure Mode
6	14.68	---	16.2	---	19	Out-of-Phase E/W Soil-Structure Mode
.					.	
.					.	
15					3.5	

Participating mass percentages less than 0.1 percent are not shown.

TABLE IV-3-4
COMPARISON OF IN-STRUCTURE ZERO PERIOD ACCELERATION DETERMINED
BY DIRECT INTEGRATION AND MODAL SUPERPOSITION

UPPER BOUND SOIL CASE

Location	North-South Response Due to North-South Excitation		East-West Response Due to East-West Excitation		Vertical Response Due to Vertical Excitation	
	Direct Integration	Modal Superposition	Direct Integration	Modal Superposition	Direct Integration	Modal Superposition
Elevation 634'-6"	0.212	0.223	0.211	0.224	0.105	0.099
Elevation 620'-0"	0.185	0.194	0.182	0.197	0.099	0.099
Elevation 589'-6"	0.151	0.164	0.150	0.160	0.093	0.097

All accelerations are in G units

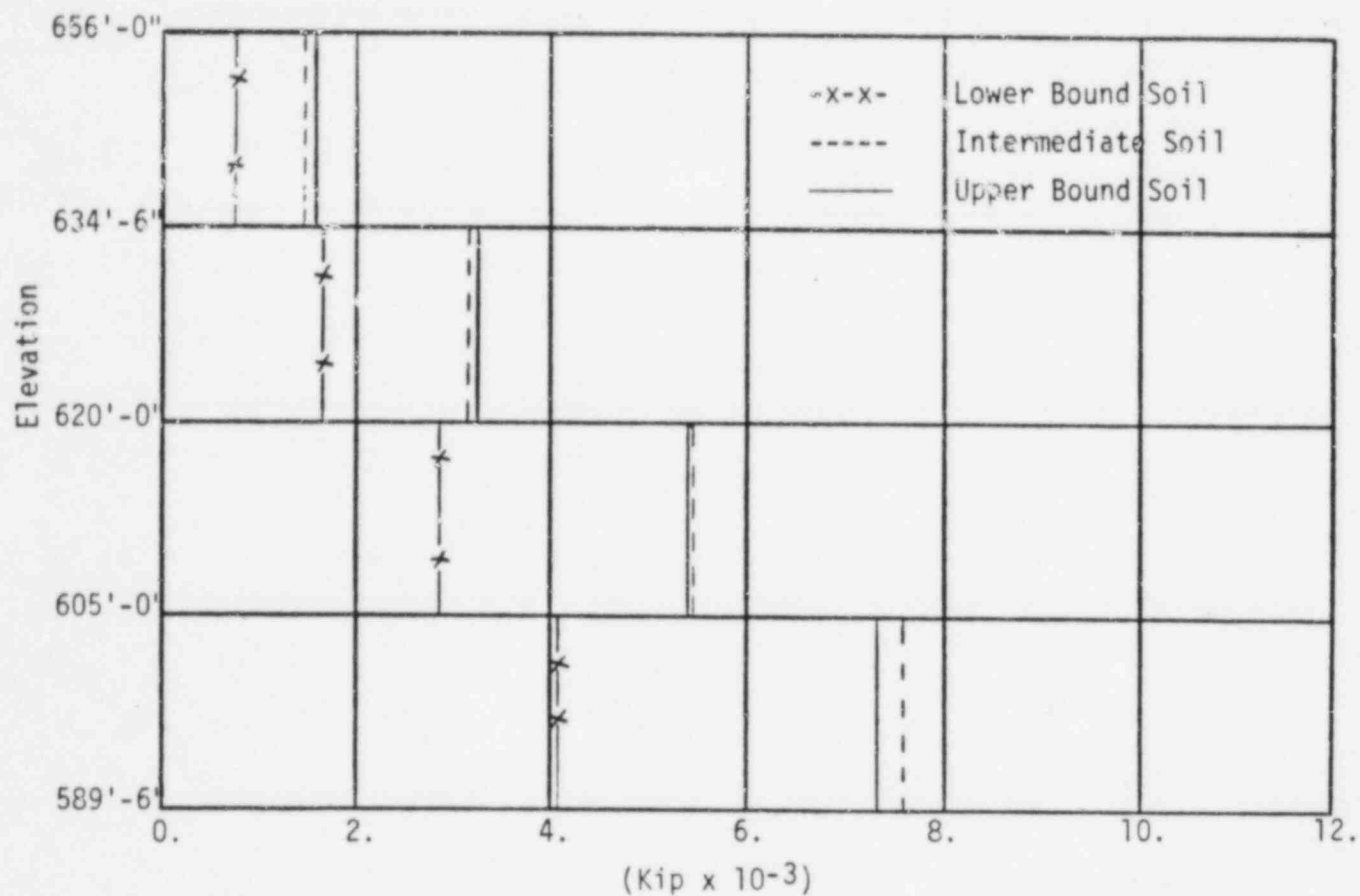


FIGURE IV-3-1. SERVICE WATER PUMP STRUCTURE N-S SRSS SHEAR

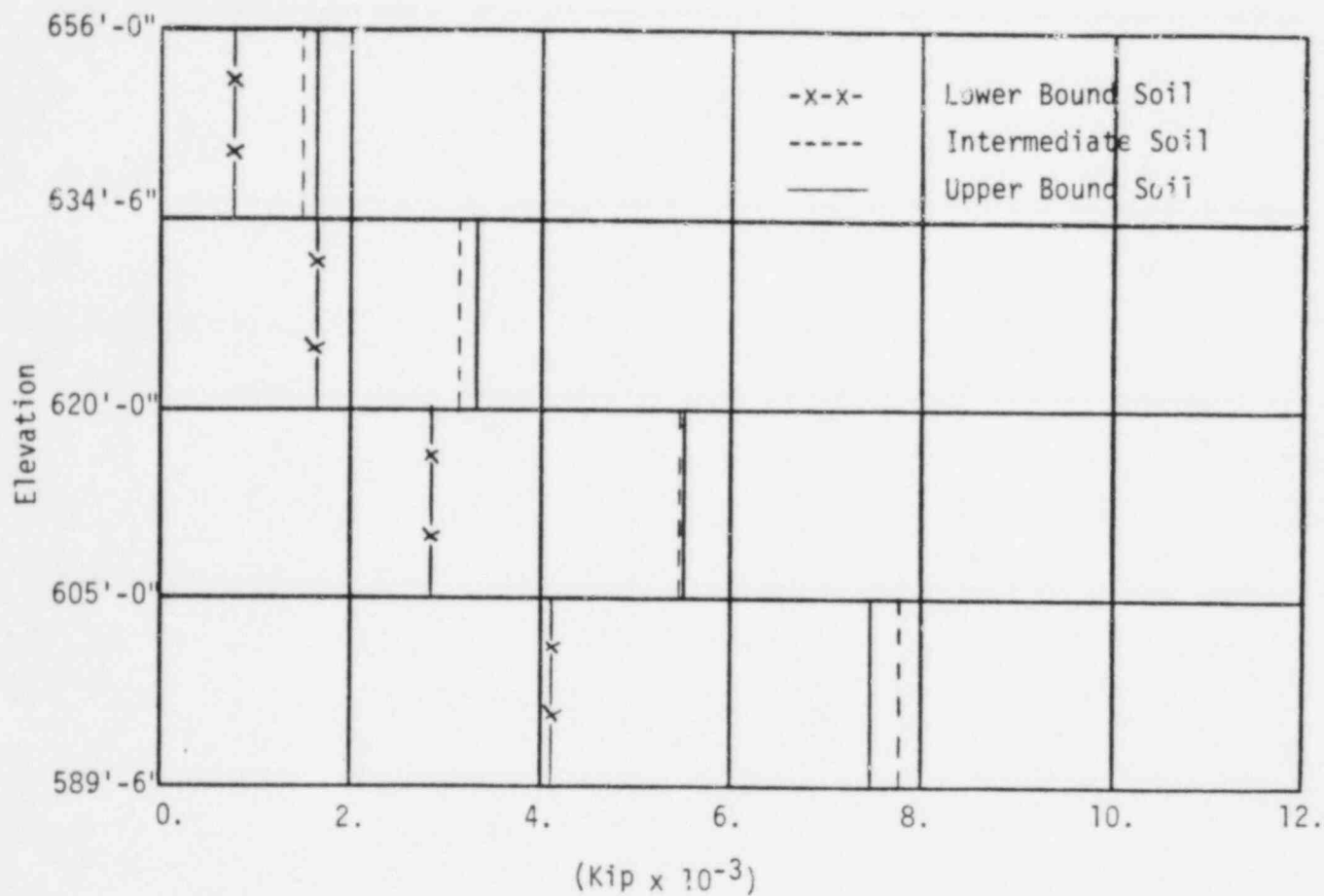


FIGURE IV-3-2. SERVICE WATER PUMP STRUCTURE E-W SRSS SHEAR

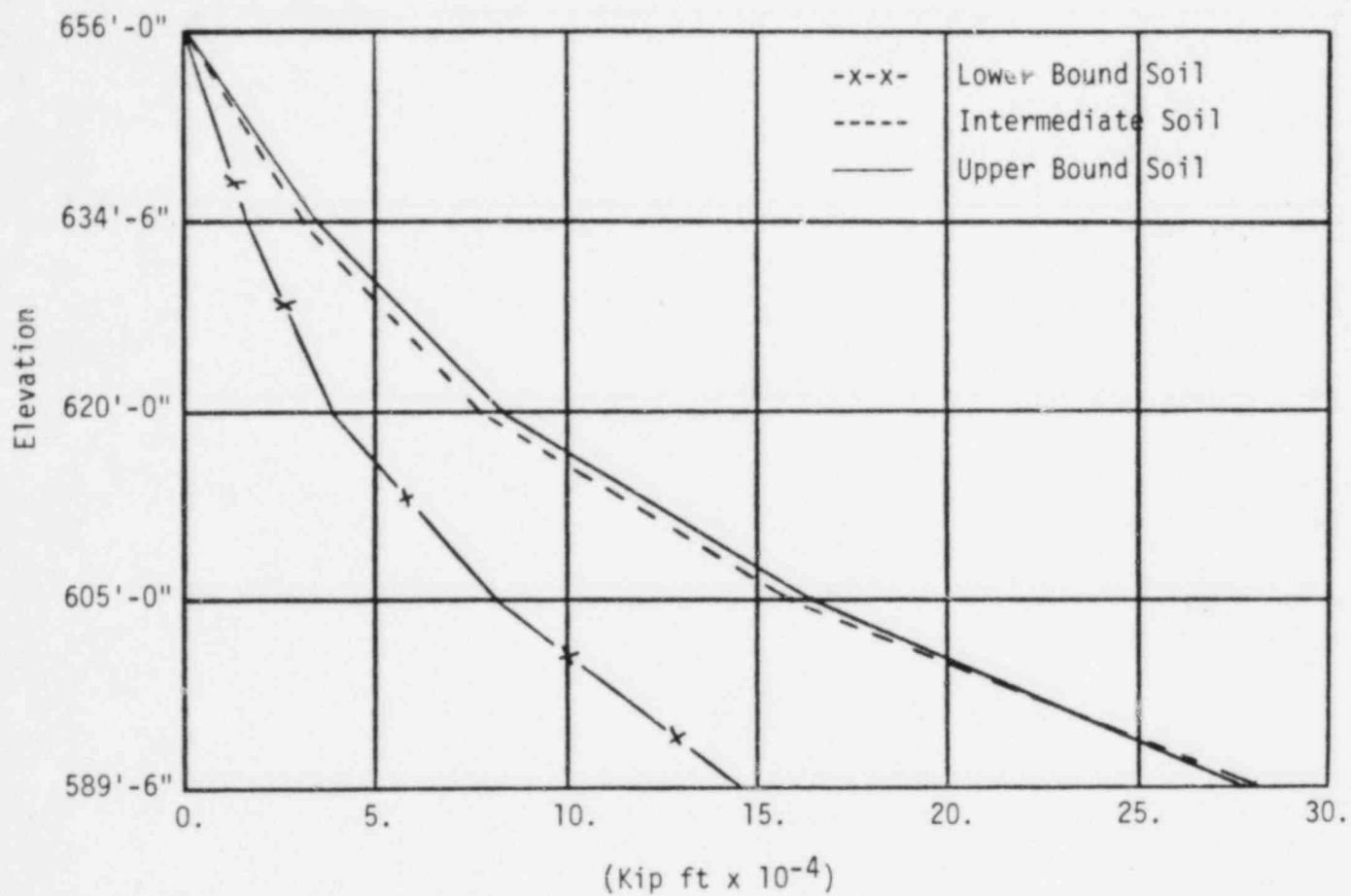


FIGURE IV-3-3. SERVICE WATER PUMP STRUCTURE SRSS MOMENT ABOUT N-S AXIS

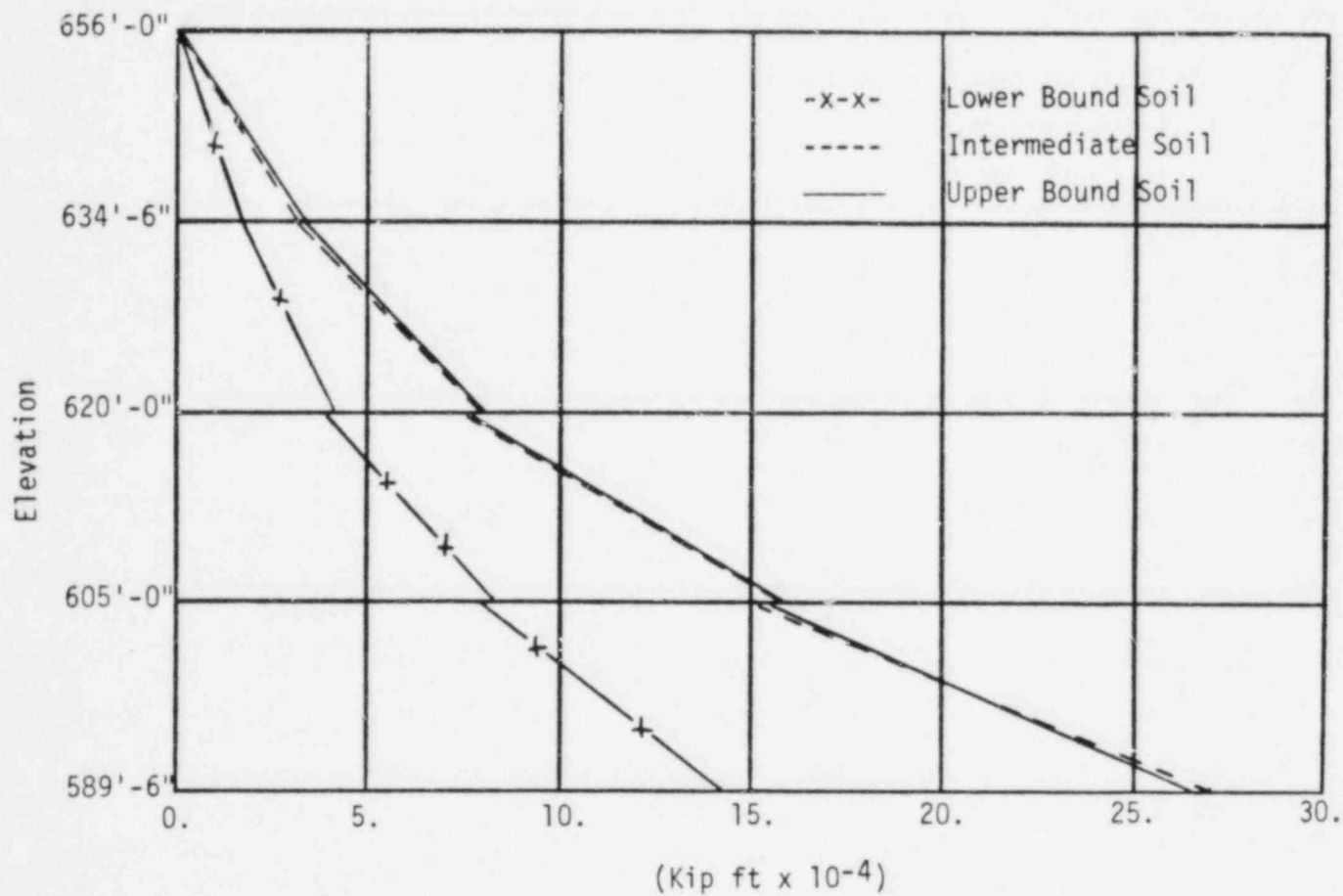


FIGURE IV-3-4. SERVICE WATER PUMP STRUCTURE SRSS MOMENT ABOUT E-W AXIS

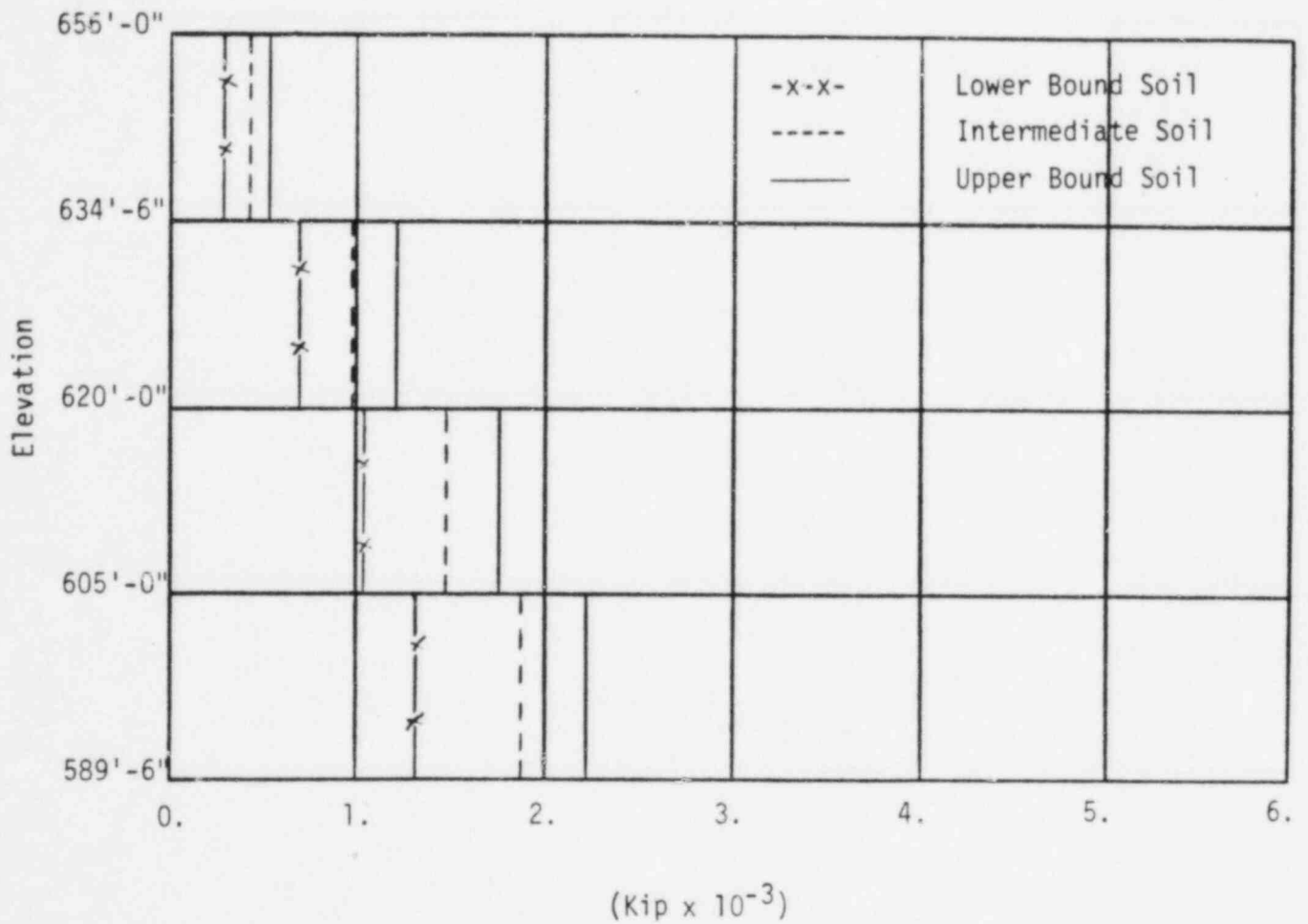


FIGURE IV-3-5. SERVICE WATER PUMP STRUCTURE SRSS AXIAL FORCE

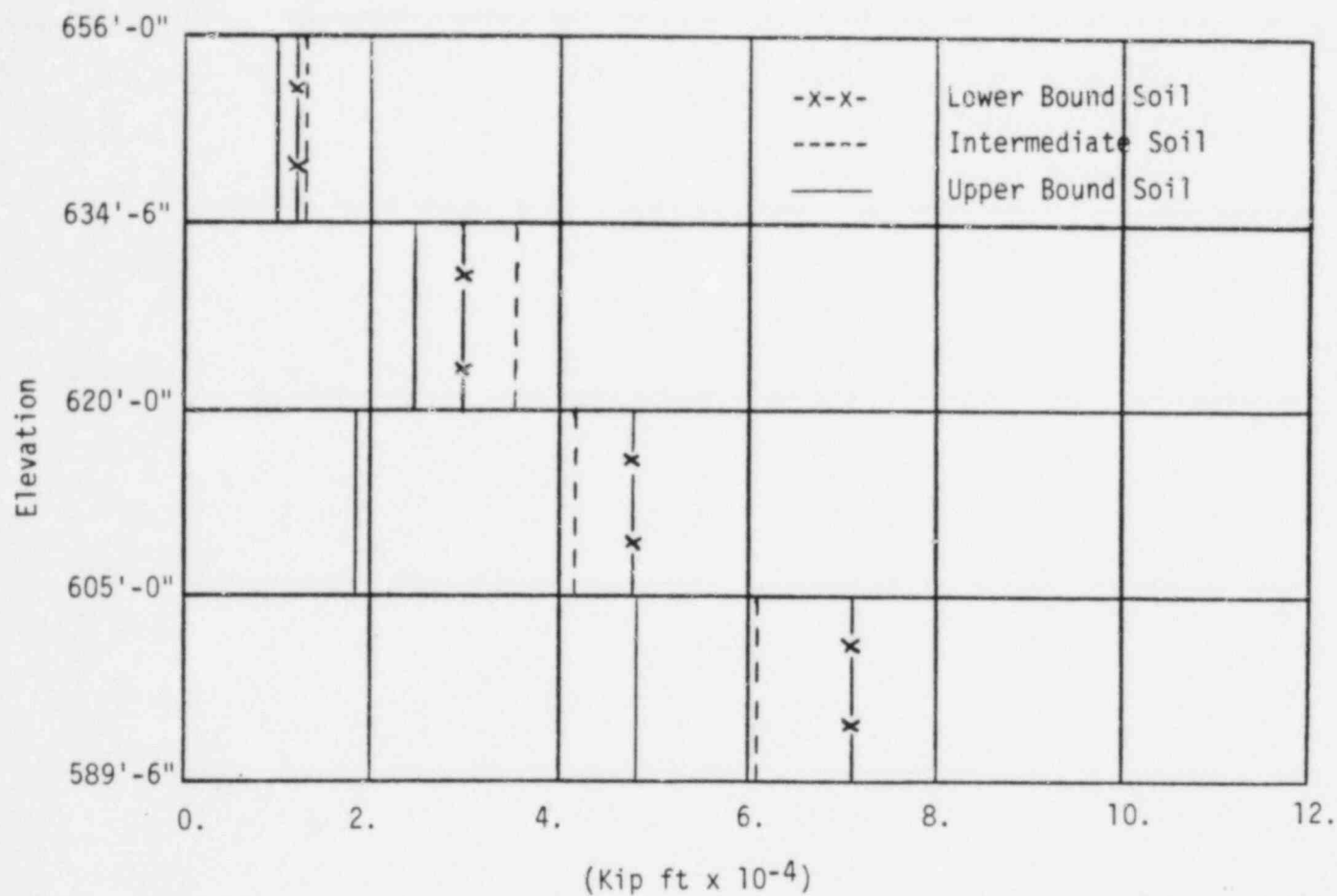


FIGURE IV-3-6. SERVICE WATER PUMP STRUCTURE SRSS TORSION

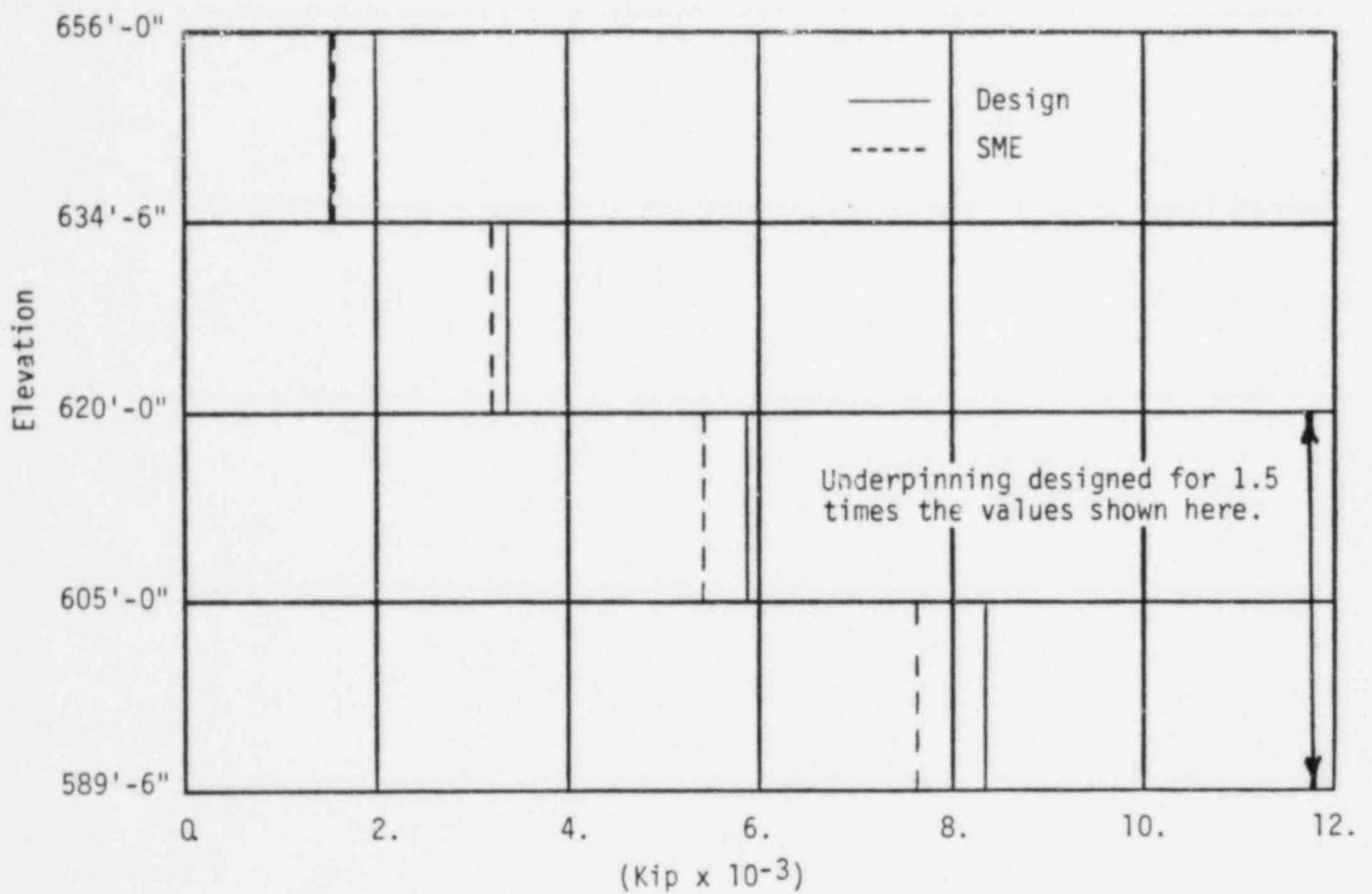


FIGURE IV-3-7. SERVICE WATER PUMP STRUCTURE N-S SHEAR COMPARISON

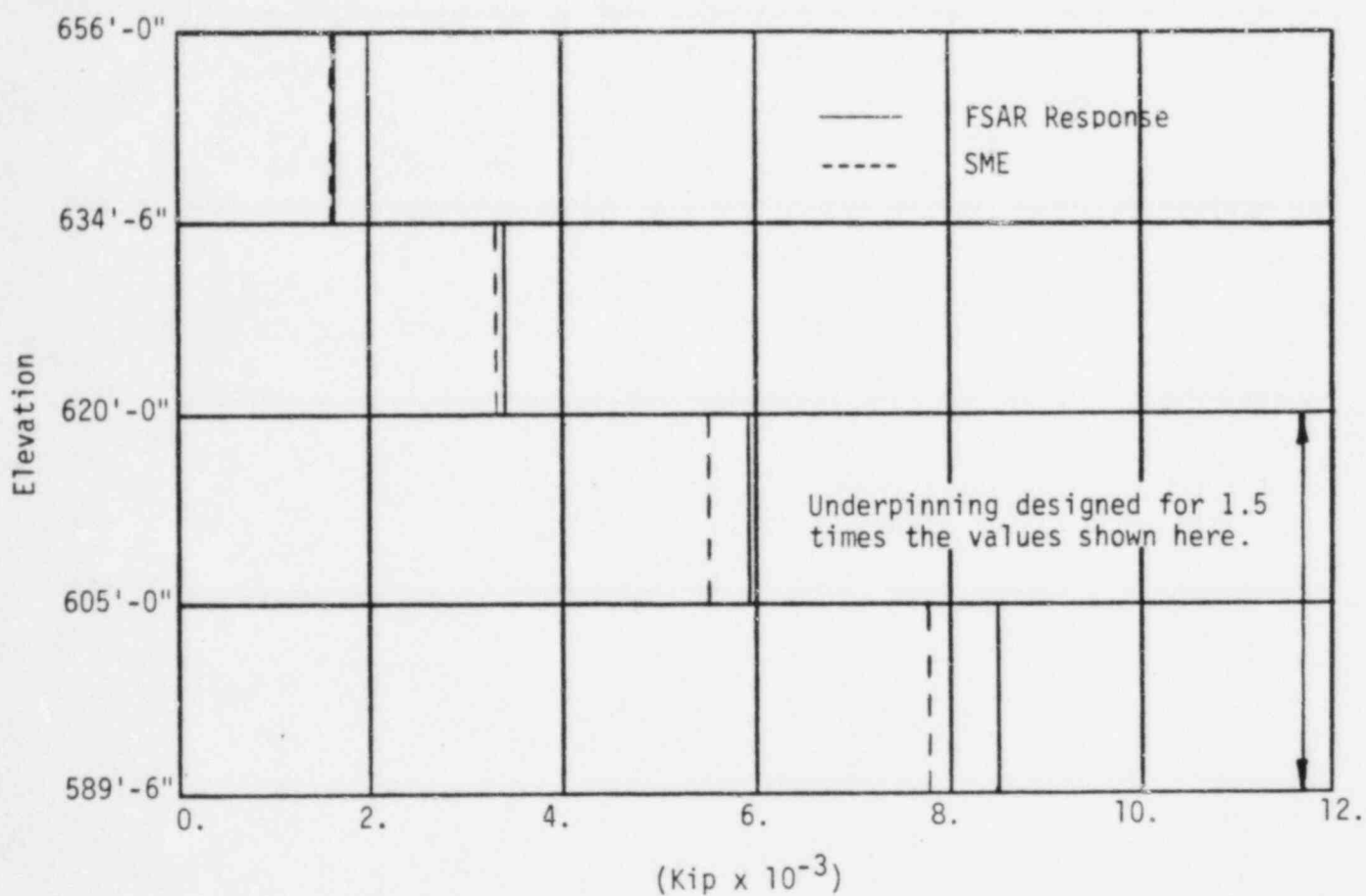


FIGURE IV-3-8. SERVICE WATER PUMP STRUCTURE E-W SHEAR COMPARISON

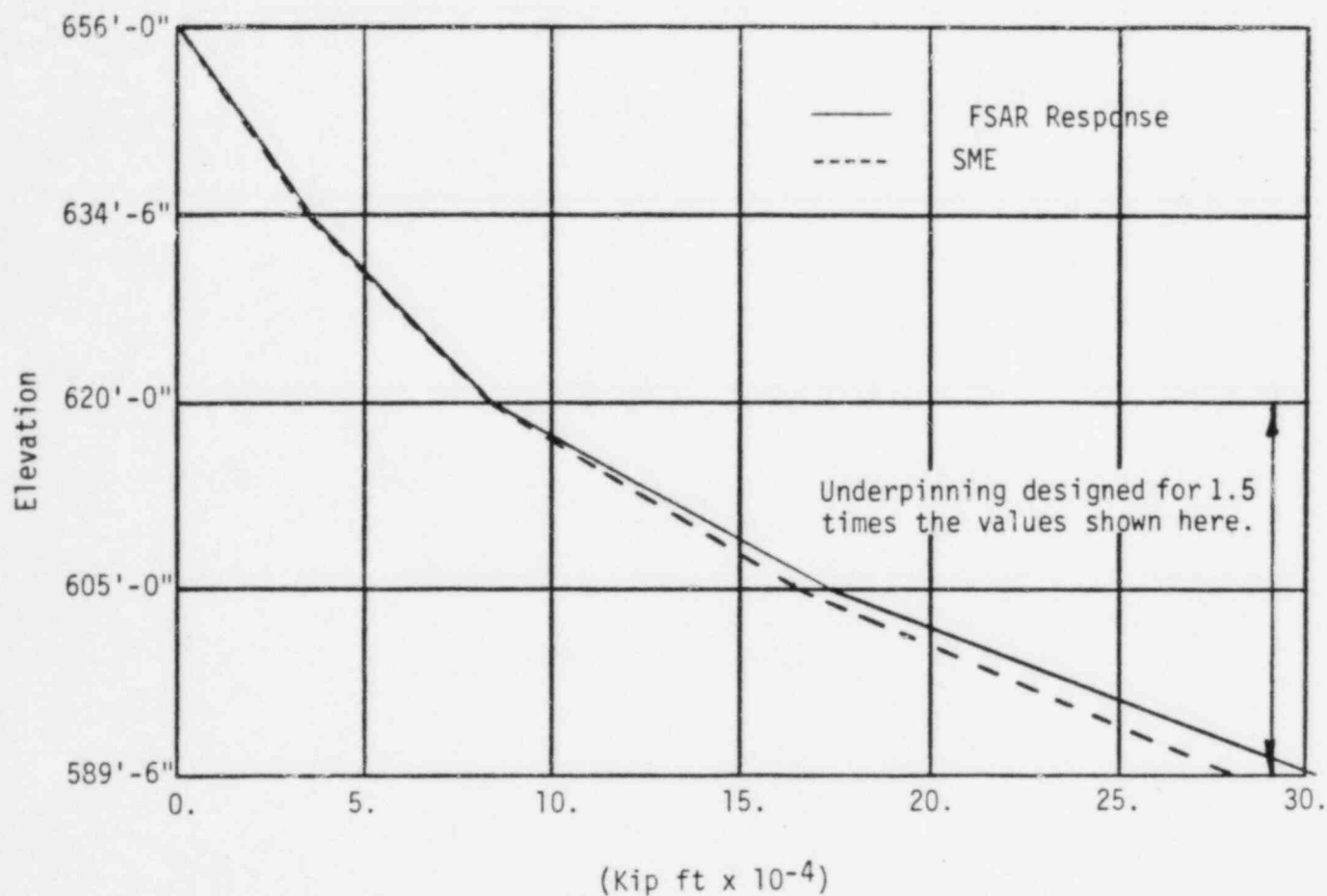


FIGURE IV-3-9. SERVICE WATER PUMP STRUCTURE MOMENT ABOUT N-S AXIS COMPARISON

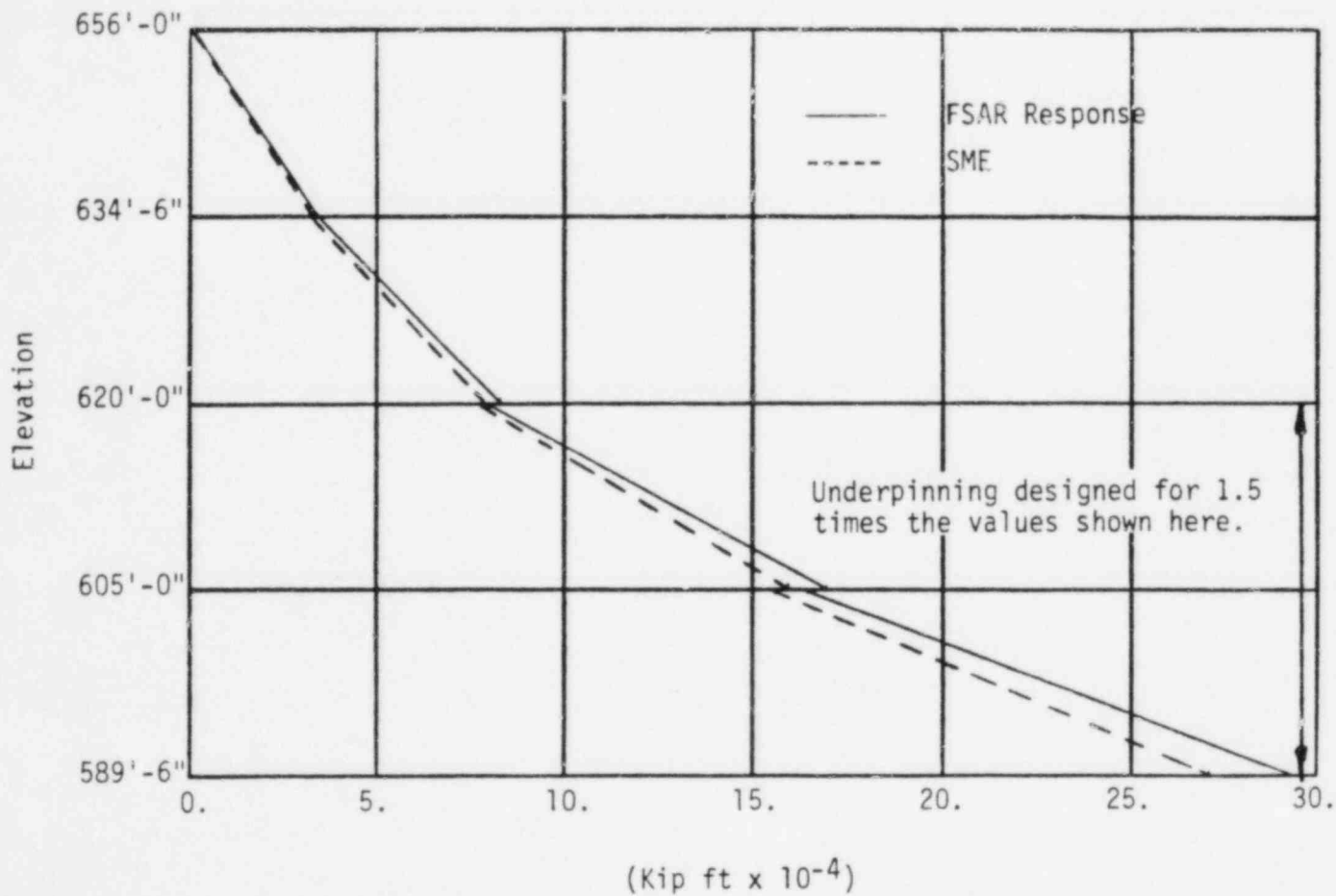


FIGURE IV-3-10. SERVICE WATER PUMP STRUCTURE MOMENT ABOUT E-W AXIS COMPARISON

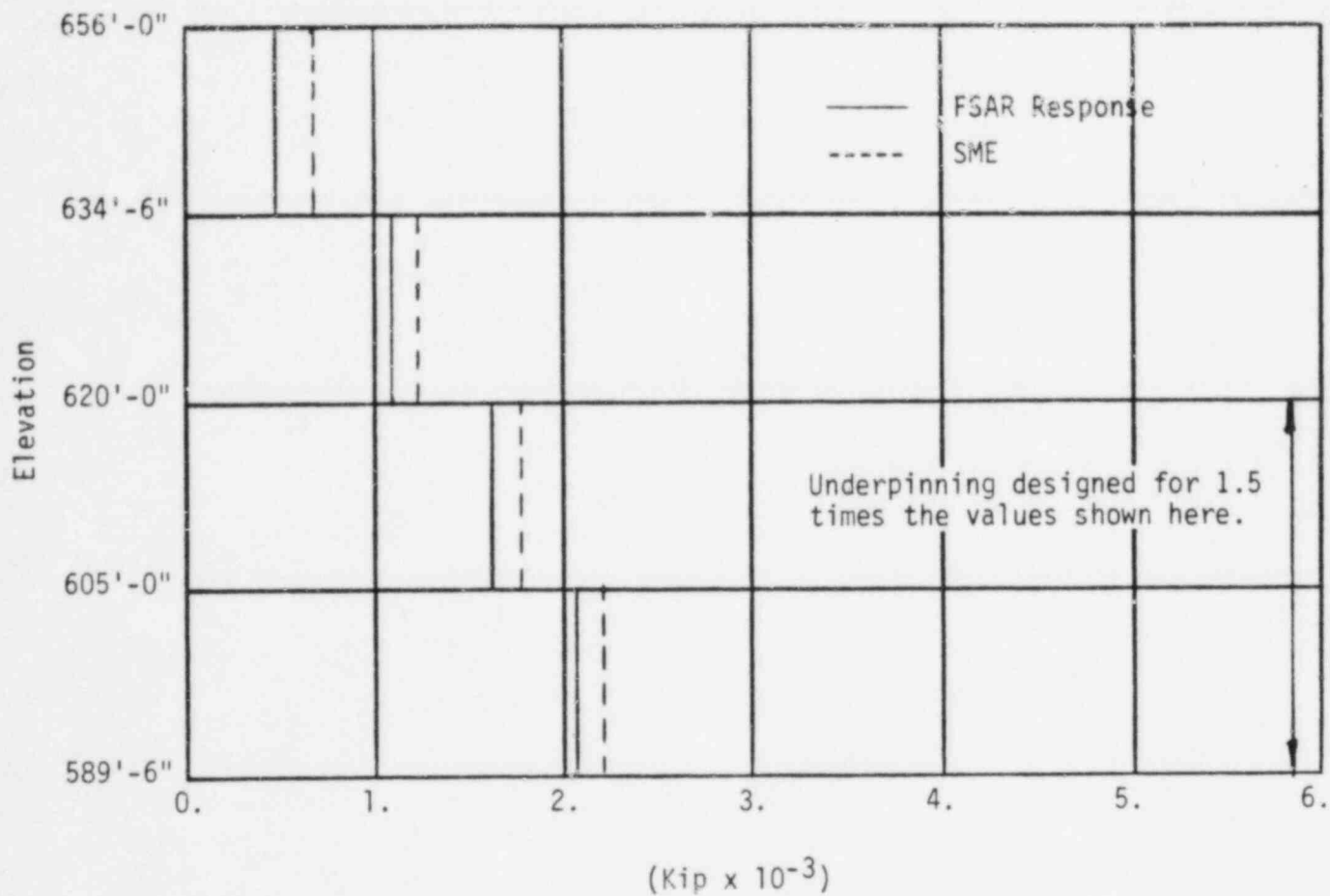


FIGURE IV-3-11. SERVICE WATER PUMP STRUCTURE AXIAL FORCE COMPARISON

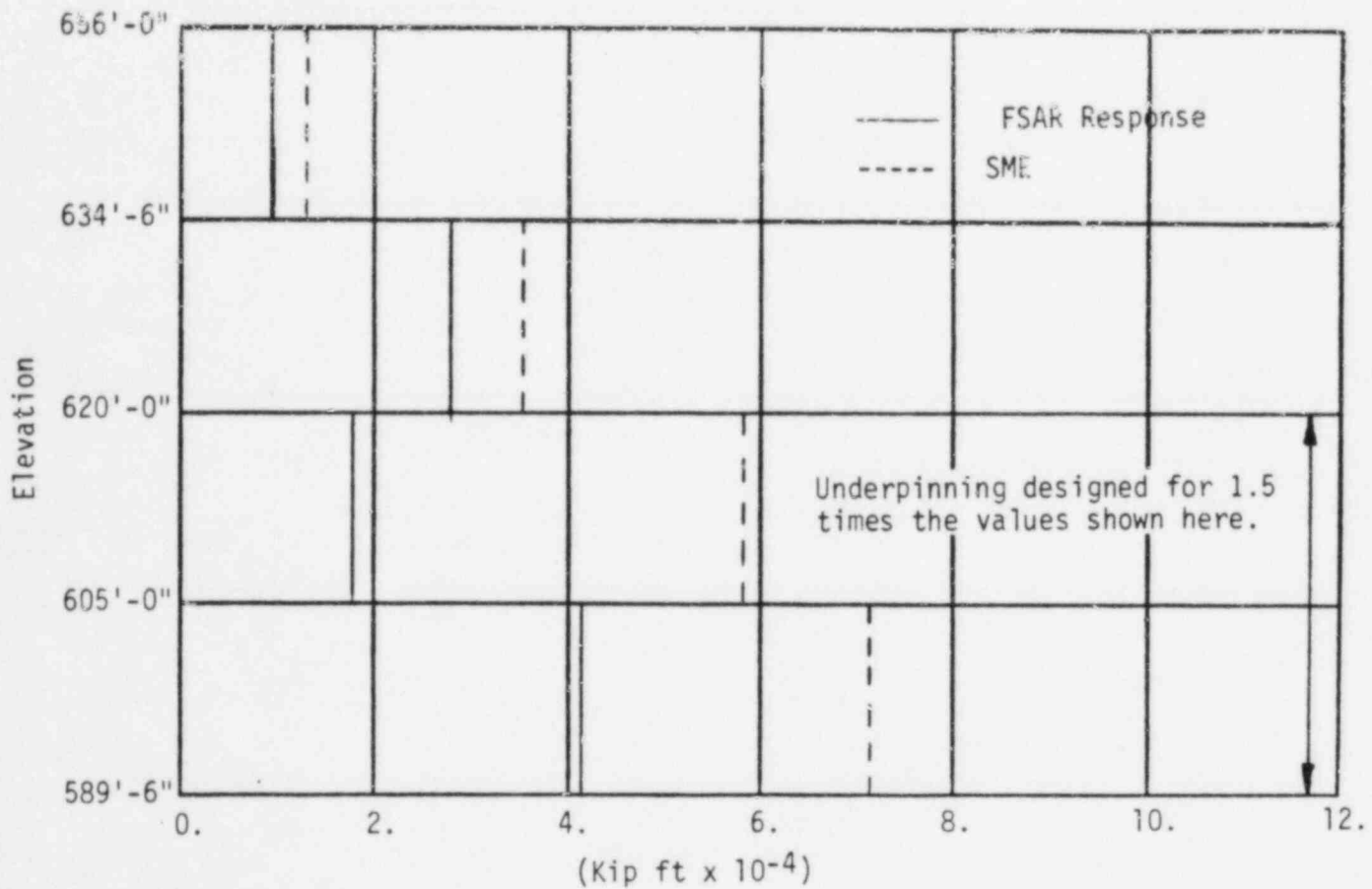


FIGURE IV-3-12. SERVICE WATER PUMP STRUCTURE TORSIONAL MOMENT COMPARISON

4. CODE MARGINS

For the service water pump structure code margins evaluation, a number of structural elements were selected from locations throughout the structure to compare their capacities as prescribed by the acceptance criteria against their loads due to the SME combined with those due to normal operating conditions and dynamic soil decrements. The selected existing shear walls, floor diaphragms, and underpinning wall are listed in Tables IV-4-1 through IV-4-4. Each shear wall and underpinning wall is identified in Figure IV-4-1. Each floor diaphragm is assigned an identification number in Table IV-4-3. The location of the selected diaphragms is then referenced by their identification numbers in Figures IV-4-2 and IV-4-3.

The structural elements selected for evaluation in this study are those expected to be more highly stressed due to seismic loads relative to other elements within the service water pump structure. General criteria used to identify structural elements to be included in the SMR structures capacities evaluation involved several considerations. The layout of the shear walls was reviewed to determine the distribution of walls throughout the structure and the availability of resistance to lateral load. The load distributions were compared to identify walls required to resist a significant portion of the seismic load at each story. To provide an approximate assessment of the relative wall capacities, wall thicknesses, reinforcement patterns, and the presence of openings which would tend to reduce the amount of material available for load resistance were reviewed. Particular attention was given to the major walls since their relative rigidities are typically greater than smaller walls and consequently receive greater loads.

Diaphragm elements were selected for detailed evaluation on a basis similar to that for the shear walls. Review of the shear wall layout through the structure also provided insight into the manner in which the floor slabs function as diaphragms in providing load paths to the walls. From the load distributions, locations of possible significant diaphragm stress were identified. Slab thicknesses, reinforcement patterns, and the presence of openings were reviewed to provide an approximate assessment of the relative diaphragm capacities.

Capacities for the structural elements selected for review were developed in accordance with the structural acceptance criteria described in Section 7.2 of Volume I. For the reinforced concrete portions of the service water pump structure, the ultimate strength design provisions of ACI 349-80, "Code Requirements for Nuclear Safety Related Concrete Structures" (Reference 18), were followed. The ultimate strengths were conservatively based on minimum specified concrete crushing strengths. The concrete used in the construction of the existing service water pump structure was typically specified to have a minimum compressive strength of 4,000 psi. Concrete for the underpinning walls was specified to have a minimum compressive strength of 6000 psi at 60 days. Reinforcing steel used was required to conform to ASTM Designation A615, Grade 60 and has a specified minimum yield stress of 60,000 psi.

4.1 SHEAR WALL CAPACITY OF EXISTING STRUCTURE

The shear strength provisions for concrete walls are contained in Section 11.10 of ACI 349-80. The total ultimate strength capacity is composed of separate contributions from the concrete and the steel reinforcement. ACI 349-80 provides alternative formulations with different levels of detail required for determining the concrete in-plane shear strength. Section 11.10.5 specifies the concrete shear strength as the value corresponding to an average shear stress of $2 \sqrt{f'_c}$ (psi) acting on the effective area for walls in compression.

$$V_c = 2 \sqrt{f'_c} h d \quad \text{for walls in compression} \quad (4-1)$$

- V_c = Nominal concrete shear strength, lb
 f'_c = Concrete compressive strength, psi
 h = Wall thickness, in
 d = Effective wall depth, in

This strength is subjected to a reduction specified in Sections 11.3.2.3 and 11.10.5 of ACI 349-80 if the wall is loaded in tension. This definition of the concrete shear strength was typically used to determine the wall capacities. Alternative formulations for the concrete in-plane shear strength are permitted by Section 11.10.6 of ACI 349-80. Use of these formulations for low-rise shear walls such as the walls of the service water pump structure typically leads to concrete in-plane shear strengths greater than those predicted by Equation 4-1. Because wall shear strengths were determined using Equation 4-1 rather than the alternative formulations of Section 11.10.6 of ACI 349-80, resulting code margins for shear walls governed by shear are conservative. The wall in-plane shear strength contributed by the steel reinforcement was determined following the provisions of Section 11.10.9 of ACI 349-80. The steel shear strength was based on the horizontal reinforcement provided in each wall. The effective wall depth, d , was taken as 0.8 times the wall length as permitted by Section 11.10.4 of ACI 349-80. The wall ultimate shear strength was taken as the sum of the concrete and reinforcing steel shear strengths reduced by a strength reduction factor of 0.85. Some of the walls must also transmit out-of-plane shears due to lateral forces. Because the in-plane concrete shear strength was determined in accordance with Sections 11.10.2 to 11.10.8 of ACI 349-80, Section 11.10.1 eliminates the need to consider interaction between in-plane and out-of-plane shear. For walls separated into a series of piers by significant openings, shear capacities were developed for the individual piers. The total seismic shear acting on the wall was distributed to the piers in proportion to their relative rigidities using equations presented in Reference 16. Shears due to loads from normal

operating conditions and the dynamic soil decrement acting on the individual piers were determined as noted in Section 3.3.3 using stresses occurring in the plate elements modeling these piers.

Shear wall resistance to overturning moment is provided by the internal couple consisting of the vertical wall reinforcement stressed in tension and the concrete stressed vertically in compression. An efficient means of developing overturning resistance is by concentrating the necessary vertical reinforcement at the ends of the wall so that the moment arm will be a maximum. In general, however, vertical reinforcement of the service water pump structure walls was uniformly distributed along the lengths of the walls.

As noted in Reference 19, experimental results indicate that the flexural strengths of rectangular shear walls with height-to-length ratios equal to or greater than 1.0 and containing uniformly distributed vertical reinforcement are adequately predicted by the design provisions for reinforcement concrete beams loaded axially and in bending. These provisions are contained in Section 10.2 of ACI 349-80. The flexural strength calculated using these provisions can be expressed by the following equation presented in Reference 19.

$$M'_u = A_s f_y L \left[\left(1 + \frac{N_u}{A_s f_y} \right) \left(\frac{1}{2} - \frac{B_1 C}{2L} \right) - \frac{C^2}{L^2} \left(1 + \frac{B^2}{3} - B_1 \right) \right] \quad (4-2)$$

where:

$$\frac{c}{L} = \frac{q + \alpha}{2q + 0.35\beta_1}$$

$$c = \frac{A_s f_y}{L h f'_c}$$

$$\alpha = \frac{N_u}{L h f'_c} \text{ and } \beta = \frac{f_y}{87,000}$$

- M'_u = Design resisting moment at section, in.-lb.
- A_s = Total area of vertical reinforcement at section, sq. in.
- f_y = Specified yield strength of vertical reinforcement, psi
- L = Horizontal length of shear wall, in.
- c = Distance from extreme compression fiber to neutral axis, in.
- d = Distance from extreme compression fiber to resultant of tension force, in.
- h = Thickness of shear wall, in.
- N_u = Design axial load, positive if compression, lb.
- f'_c = Specified compressive strength of concrete, psi
- β_1 = 0.85 for strength f'_c up to 4000 psi and reduced continuously at a rate of 0.05 for each 1000 psi of strength in excess of 4000 psi

Reference 19 presented the following approximation to this equation:

$$M'_U = 0.5A_s f_y L \left(1 + \frac{N_U}{A_s f_y} \right) \left(1 - \frac{B_1 C}{L} \right) \quad (4-3)$$

Upon inspection of Equation 4-3, it is apparent that this approximation is equivalent to obtaining the flexural strength of an underreinforced beam with the uniformly distributed reinforcement lumped at midlength of the wall.

Based on the findings of Reference 19, the design provisions in Section 10.2 of ACI 349-80 were used to determine the resistances to overturning moment for the walls of the service water pump structure. In accordance with Section 9.3.2 of ACI 349-80, the calculated overturning moment resistances, M'_U , were modified by the appropriate strength reduction factor ϕ .

$$M_U = \phi M'_U$$

where ϕ = strength reduction factor per Section 9.3.2 of ACI 349-80.

Most of the major walls of the service water pump structure are intersected at their ends by other walls oriented transversely. Due to deformational compatibility at the intersections, these transverse walls will behave similar to flanges of a wide-flanged beam. However, only the resistance to overturning moment provided by the web of the wall loaded in-plane was accounted for. This is conservative since the additional overturning resistance provided by the flanges may be significant due to their greater internal moment arms.

Some of the walls evaluated in this study contain small openings for doorways, pipe penetrations, etc. Typical details call for additional vertical reinforcement to be provided at the faces of the openings to make up for the reinforcement interrupted by these openings. The flexural strength of a wall containing small openings was calculated for the wall as a single element rather than as a series of individual piers since the openings are generally small compared to the wall itself and are usually isolated as opposed to occurring in a regular pattern through the wall height. Failure is expected to occur due to gross, overall behavior. The additional reinforcement around the openings is normally sufficient to resist any stress concentrations.

Some of the walls of the service water pump structure are subjected to out-of-plane forces imparted by adjacent soil or water. The presence of out-of-plane moments about a horizontal axis through the wall is expected to influence the capacity of the wall to resist the in-plane overturning moment due to horizontal seismic response of the building. The procedure used to account for the effects of out-of-plane moments on the wall overturning moment capacities is described in Appendix C of Volume III.

The out-of-plane moments used included contributions from normal operating condition loads, the dynamic soil decrements, and dynamic response of the water contained in the structure, wall inertia, and the soil entrapped by the underpinning walls. Out-of-plane moments due to normal operating conditions and the dynamic soil decrements were available from the results of Bechtel's static analyses performed on their finite element model. The calculation of the impulsive and convective hydrodynamic pressures was generally based on Housner's equations contained in Reference 2 with modifications included to more appropriately represent the behavior of the structure as a flexible tank. These modifications included use of accelerations from the structure response spectrum analyses to predict the fluid impulsive forces and distribution of the impulsive hydrodynamic pressures by the

approximation noted in Reference 24. This approach is similar to that described in Volume VI for the evaluation of the borated water storage tank. Wall inertial forces were based on structure accelerations from the response spectrum analyses. Lateral pressures from the entrapped soil were determined using structure accelerations and estimated effective entrapped soil masses.

Capacities for the selected shear walls determined in accordance with ACI 349-80 are presented in Tables IV-4-1 and IV-4-2. The possibility of failure due to in-plane shear or overturning was considered for these walls. Shear capacities for the walls whose code margins are governed by shear are listed in Table IV-4-1 while overturning capacities for the walls whose code margins are governed by overturning are listed in Table IV-4-2. Applied in-plane shear and overturning loads due to seismic, normal operating condition, and dynamic soil decrement loads are also listed in these tables. These loads were calculated as described in Section 3.3.3.

The code margins for the selected shear walls were developed from the calculated loads and capacities and are listed in Tables IV-4-1 and IV-4-2. The code margin, CM, is defined as the ratio of the code capacity to the applied load. The applied load is specified by the load combination given in Section 3.3.3 and is taken as the sum of the applied loads due to the seismic, normal operating condition, and dynamic soil decrement load cases.

$$CM = \text{Code Margin} = \frac{C}{P}$$

$$C = \text{Element code capacity}$$

$$P = \text{Applied load due to the combined normal operating condition, dynamic soil decrement, and seismic load cases} = P_{NOL} + P_{DSD} + P_{SME}$$

$$P_{NOL} = \text{Applied load due to normal operating condition load}$$

$$P_{DSD} = \text{Applied load due to the dynamic soil decrement}$$

$$P_{SME} = \text{Applied load due to the SME}$$

In general, the walls are subjected to axial loads occurring simultaneously with the shears and overturning moments. The magnitudes of the axial load can have an influence on the shear and overturning capacities. Code margins were determined based on the capacities and loads under consideration (shear or overturning) with the effect of the axial load included in the capacities.

For each of the selected shear walls, a factor F_{SME} is also listed in Tables IV-4-1 and IV-4-2. This term is the factor by which the SME ground motion would have to be multiplied to cause loads equal to the code capacities:

$$F_{SME} = \frac{C - (P_{NOL} + P_{DSD})}{P_{SME}}$$

When the effect of axial load was included in the capacity, this equation was modified to account for the influence of the axial load due to seismic response. F_{SME} factors less than the code margins occur when the seismic axial load tends to reduce the capacity against shear or overturning moment. As an example, derivation of the F_{SME} factor for the south wall from Elevation 589'-6" to Elevation 605'-0" is as follows:

$$\begin{aligned} M_{SME} &= \text{Overturning moment due to the SME factored by } F_{SME} \\ &= 70,600 F_{SME} \text{ k-ft} \end{aligned}$$

$$\begin{aligned} M_{NOL} + M_{DSD} &= \text{Overturning moment due to normal operating conditions and dynamic soil decrement} \\ &= 6,800 \text{ k-ft} \end{aligned}$$

$$\begin{aligned} M_{NET} &= M_{SME} + (M_{NOL} + M_{DSD}) \\ &= 70,600 F_{SME} + 6,800 \end{aligned}$$

$$\begin{aligned}
 M_U &= \text{Overturning moment capacity per Equation 4-3 including} \\
 &\quad \text{the effects of the axial load due to the SME factored} \\
 &\quad \text{by } F_{SME} \\
 &= -9.26F_{SME}^2 - 6,520F_{SME} + 148,000 \text{ k-ft}
 \end{aligned}$$

$$\begin{aligned}
 M_U &= M_{NET} \\
 -9.26F_{SME}^2 - 6,520F_{SME} + 148,000 &= 70,600F_{SME} + 6,800 \\
 -9.26F_{SME}^2 - 77,100F_{SME} + 141,000 &= 0
 \end{aligned}$$

$$F_{SME} = 1.8$$

4.2 DIAPHRAGM CAPACITY OF EXISTING STRUCTURE

Capacities of diaphragms for in-plane shear and moment are not directly addressed by ACI 349-80. However, it is common to design concrete diaphragms by the same provisions as those used for shear walls because of similarities in geometry and loading. Section 11.8 of Reference 20 specifies the same limiting shear stress for shear walls and diaphragms. Consequently, in-plane shear and flexural capacities of the diaphragms selected for evaluation were calculated in the same manner as the corresponding capacities of the shear walls. The slabs must also transmit out-of-plane shears due to vertical forces. Because the in-plane concrete shear strength was determined in accordance with Sections 11.10.2 to 11.10.8 of ACI 349-80, Section 11.10.1 eliminates the need to consider interaction between in-plane and out-of-plane shear.

The diaphragms of the service water pump structure selected for evaluation correspond to locations where slab openings reduce the amount of material available to resist the applied loads. The diaphragm sections evaluated are also on the load paths to the east-west direction exterior walls. These walls, in addition to being among the major lateral load-resisting walls, resist larger portions of the torsional moments due to their greater distance from the story centers of rigidity. The diaphragm sections selected for evaluation are those expected to be the most highly stressed. Figures IV-4-2 and IV-4-3 identify the selected critical diaphragm sections at the roof (Elevation 656'-0") and the floor at Elevation 634'-6".

The diaphragms selected for evaluation were found to be governed by shear rather than in-plane moment. As noted in Section 3.3.3, the shears acting on diaphragms adjacent to exterior walls were calculated conservatively. The slab openings separate the diaphragms into piers similar to the piers of a shear wall. Code capacities and applied loads were determined for these piers as individual structural elements. Loads due to the SME, normal operating conditions, and dynamic soil decrement, code capacities, code margins, CM_s , and F_{SME} factors are listed in Table IV-4-3. The code margins and F_{SME} factors were determined in the same manner as for the shear walls.

4.3 EFFECTS OF REINFORCEMENT BAR CUTTING

The shear wall and diaphragm capacities were based on information available from the structural drawings for the selected elements. The presence of small and large openings indicated on the structural drawings was accounted for in the development of these capacities. Available non-conformance reports noting deviations from the construction specifications were reviewed to verify that there were no gross deviations that would significantly influence the capacity of the selected structural elements. The calculated wall capacities do not include the effect of any minor deviations. The capacities reported in Tables IV-4-1 through IV-4-3 also do not address the reduction in strength due to reinforcement cutting permitted by Reference 21 since the exact location and number of reinforcement bars cut within this allowance was unavailable. Per Section 2.1 of Appendix E of Reference 21, one bar could be cut each way, each face, with the radial distance to the next cut bar on the same face, in the same direction, no less than five feet. Per Section 2.2 of Appendix E of Reference 21, two bars could be cut each way, each face, with the radial distance to the next cut bar on the same face, in the same direction, no less than 10 feet. Additional limitations are noted in Section 7.2 of Volume I.

To determine the effect of the reinforcement cutting allowance and non-conformances on the shear capacity of the walls, the wall with the lowest code margin against shear, which is the original below grade north wall from Elevation 589'-6" to Elevation 605'-0", was recalculated. The effect of reinforcement cutting is expected to be dependent on the crack pattern that leads to failure of the wall. If a crack crosses a horizontal bar where it has been cut or where it does not have sufficient development length from the cut to develop its yield strength, then the effectiveness of that bar may be significantly reduced. As an approximation, a crack was assumed to form at a 45 degree angle from horizontal through the story height of the wall noted above. This angle is approximately consistent with the crack angle assumed in the derivation of the shear strength provided by web reinforcement of concrete beams. For the worst case of horizontal bars cut at both faces every five feet along the assumed crack, the reinforcement area effective in resisting shear was modified and the total wall shear strength recalculated. No non-conformances were reported for the wall at this story. Using the revised shear strength, a code margin of 2.8 was determined for this wall compared to 3.5 as originally calculated.

To determine the effects of the reinforcement cutting allowance and the non-conformances on the overturning moment capacity of the walls, the wall with the lowest code margin against overturning, which is the south exterior wall from Elevation 589'-6" to Elevation 605'-0", was recalculated. It was assumed that vertical bars at each face were cut every five feet along a horizontal plane. No non-conformances were reported for the wall at this story. Using the effective reinforcement area, the overturning moment was recalculated. A code margin of 1.6 corresponds to this revised capacity compared to 1.9 as originally calculated.

To determine the effect of the reinforcement cutting allowance and non-conformances on the capacities of the diaphragms, the diaphragm with the lowest code margin, which is noted by diaphragm identification number 1, was recalculated. Because this diaphragm is governed by shear, the effect of reinforcement cutting on the shear capacity was considered using the same approach developed for the shear walls. Using the revised shear strength, a code margin of 2.7 was determined for this diaphragm compared to 3.2 as originally calculated.

The code margins for the walls and the diaphragms were still found to be greater than unity when the reinforcement cutting allowance and non-conformances were considered for the selected examples. It can be concluded that the cutting allowance and the non-conformances do not adversely affect the results of this study for the walls and diaphragms of the service water pump structure.

4.4 UNDERPINNING WALL CAPACITIES

Evaluation of the underpinning walls of service water pump structure was conducted on the basis of the drawings showing the preliminary design configuration. The north underpinning wall was selected for study. The code margin of this wall was determined using the same methodology and criteria developed for shear walls described in Section 4.1. This wall was found to be governed by shear. Applied loads, code capacity, code margin, and F_{SME} factor are listed in Table IV-4-4 for shear on the north underpinning wall.

The connectors providing load transfer between the north underpinning wall and the base mat of the existing structure above were also evaluated. The connectors to be used at the top faces of the service water pump structure underpinning walls are 2.25-inch diameter anchor bolts fabricated from ASTM A540 Grade 23 Class 4 steel with a minimum specified yield strength of 120 ksi. A total of 27 connectors are provided for the north underpinning wall. One end of each connector is anchored into the concrete at the top of the underpinning wall while the other end is anchored by a steel plate bearing against the top face

of the existing base mat. The eccentricity between the connector location and the underpinning wall centerline was considered in the evaluation of the connectors. The capacities of the underpinning connectors at the interface between the north underpinning wall and the existing base mat above were determined using the strength provisions of ACI 349-80. The connectors were found to be governed by shear. The connectors' shear capacity was evaluated based on the shear friction provisions contained in ACI 349-80. The shear capacity at the interface was calculated by the following equation:

$$V_u = \phi \mu (A_{vf} f_y), \text{ lb} \quad (4-4)$$

where:

- A_{vf} = Connector tensile stress area, in²
- f_y = Connector yield stress, psi
- ϕ = Strength reduction factor
- μ = 1.0 for concrete-to-concrete interfaces

Additional steel area must be provided to resist any direct tension acting across an interface transmitting shear by shear-friction. As noted in Reference 23, the presence of axial compression across an interface will increase the shear-friction capacity available.

Applied shear loads considered in the evaluation of the connectors between the north underpinning wall and the existing base mat above included in-plane and out-of-plane shears due to the SME, normal operating conditions, and dynamic soil decrements. Because the principal effect of the SME is to cause in-plane shear on the wall, the code margin for the connectors was based upon a comparison of the available in-plane shear capacity and the applied in-plane shear load. The effect of the applied out-of-plane shear was conservatively accounted for by deducting vectorially the maximum out-of-plane shear per unit wall length from the net shear capacity per unit length calculated by Equation 4-4. The available connector in-plane shear capacity was found by factoring this capacity

per unit length by the total wall length. The in-plane shear applied load and code capacity, code margin, and F_{SME} factor for the connectors evaluated are listed in Table IV-4-4.

4.5 SOIL BEARING AND STRUCTURE STABILITY CAPACITY

Factors of safety for soil bearing pressures for net dead, live, and seismic loads reported in the FSAR (Reference 1) range from 3.8 for the lower mat based on an ultimate soil bearing capacity of 50,000 lb/ft² to 5.9 under the underpinning walls based on an ultimate soil bearing capacity of 52,000 lb/ft². SME shears, overturning moments, and axial loads for the service water pump structure are nearly equal or less than the corresponding FSAR loads at the building foundation locations so that factors of safety much less than those reported in the FSAR would not be expected for SME loads. Since the SME overall overturning moments and base shears are less than the corresponding FSAR loads, factors of safety for structure stability against sliding and overturning are greater than the corresponding FSAR values.

4.6 EFFECTS OF THERMAL GRADIENTS

Some of the exterior walls and diaphragms whose code margins were evaluated as part of the SMR are subjected to thermal gradients at normal operating conditions. These thermal gradients can introduce additional moments on the structural members due to restraint imposed by their supports against the thermal curvature. Design thermal gradients for the walls and slabs evaluated in the SMR were transmitted as a part of Reference 17. These values were based on the most severe combination of interior operating temperature and the worst effective winter exterior temperature.

An approach to account for thermal gradients was included in a study described in Appendix C of Volume III to determine the effect of out-of-plane moments on in-plane wall and diaphragm capacities. Based upon the results of this study, it was determined that the effect of out-of-plane moments and thermal gradients on the in-plane moment capacities could be adequately represented by the simplified method described in Appendix C of Volume III.

Table IV-4-1

CODE MARGINS AND F_{SME} FACTORS FOR SHEAR WALLS GOVERNED BY SHEAR

Wall ⁽¹⁾	V_{SME} (kips)	$V_{NOL} + V_{DSD}$ (kips)	V_{NET} (kips)	V_U (kips)	CM	F_{SME}
Original belowgrade north wall, El. 589'-6" to El. 605'	3020	950	3970	13800	3.5	4.3
North end wall, El. 620' to El. 634'-6", northeast pier ⁽²⁾	192	12	204	1120	5.5	5.8

NOTE: (1) See Figure IV-4-1 for locations of walls.

(2) This wall consists of a series of piers. Load and capacity are reported for the controlling pier only.

 V_{SME} = Shear due to SME $V_{NOL} + V_{DSD}$ = Shear due to normal operating load and dynamic soil decrement $V_{NET} = V_{SME} + (V_{NOL} + V_{DSD})$ V_U = Code ultimate shear capacity

CM = Code margin

Table IV-4-2

CODE MARGINS AND F_{SME} FACTORS FOR SHEAR WALLS GOVERNED BY OVERTURNING MOMENT

WALL (1)	M_{SME} (k-ft)	$M_{NOL} + M_{DSD}$ (k-ft)	M_{NET} (k-ft)	M_U (k-ft)	CM	F_{SME}
South wall, El. 589'-6" to El. 605'	70600	6800	77400	147000	1.9	1.8
West wall, El. 589'-6" to El. 605'	101000	28000	129000	360000	2.8	2.7

NOTE: (1) See Figure IV-4-1 for locations of walls.

M_{SME} = Overturning moment due to SME

$M_{NOL} + M_{DSD}$ = Overturning moment due to normal operating loads and dynamic soil decrement

$M_{NET} = M_{SME} + (M_{NOL} + M_{DSD})$

M_U = Code ultimate overturning moment capacity

CM = Code margin

Table IV-4-3

CODE MARGINS AND F_{SME} FACTORS FOR DIAPHRAGMS

Diaphragm	Diaphragm ID No. (1)	V_{SME} (kips)	$V_{NOL} + V_{DSD}$ (kips)	V_{NET} (kips)	V_U (kips)	CM	F_{SME}
Roof at Elevation 656'-0", between 18-inch interior wall and north wall.	1	78	82	160	519	3.2	5.6
Roof at Elevation 656'-0", adjacent to the south wall.	2	363	49	412	1590	3.9	4.2
Floor slab at Elevation 634'-6", adjacent to the south wall.	3	248	256	504	2390	4.7	8.6

NOTES: (1) See Figures IV-4-2 and IV-4-3 for locations of diaphragms corresponding to diaphragm identification numbers.

(2) Each diaphragm consists of a series of sections separated by openings. Load and capacity are reported for the controlling section only.

V_{SME} = Shear due to SME

$V_{NOL} + V_{DSD}$ = Shear due to normal operating loads and dynamic soil decrement

$V_{NET} = V_{SME} + (V_{NOL} + V_{DSD})$

V_U = Code ultimate shear strength capacity

CM = Code margin

Table IV-4-4

NORTH UNDERPINNING WALL AND IN-PHASE CONNECTOR CODE MARGINS AND F_{SME} FACTORS

	V_{SME} (k)	$V_{NOL} + V_{DSD}$ (k)	V_{NET} (k)	V_U (k)	CM	F_{SME}
North underpinning wall	3260	610	3870	14200	3.7	4.2
Connectors between north underpinning wall and existing base mat above	1880	470	2350	8820	3.8	4.2

Notes: V_{SME} = Shear due to SME

$V_{NOL} + V_{DSD}$ = Shear due to normal operating loads and dynamic soil decrement

V_{NET} = Net Shear

$$= V_{SME} + (V_{NOL} + V_{DSD})$$

V_U = Code ultimate strength shear capacity

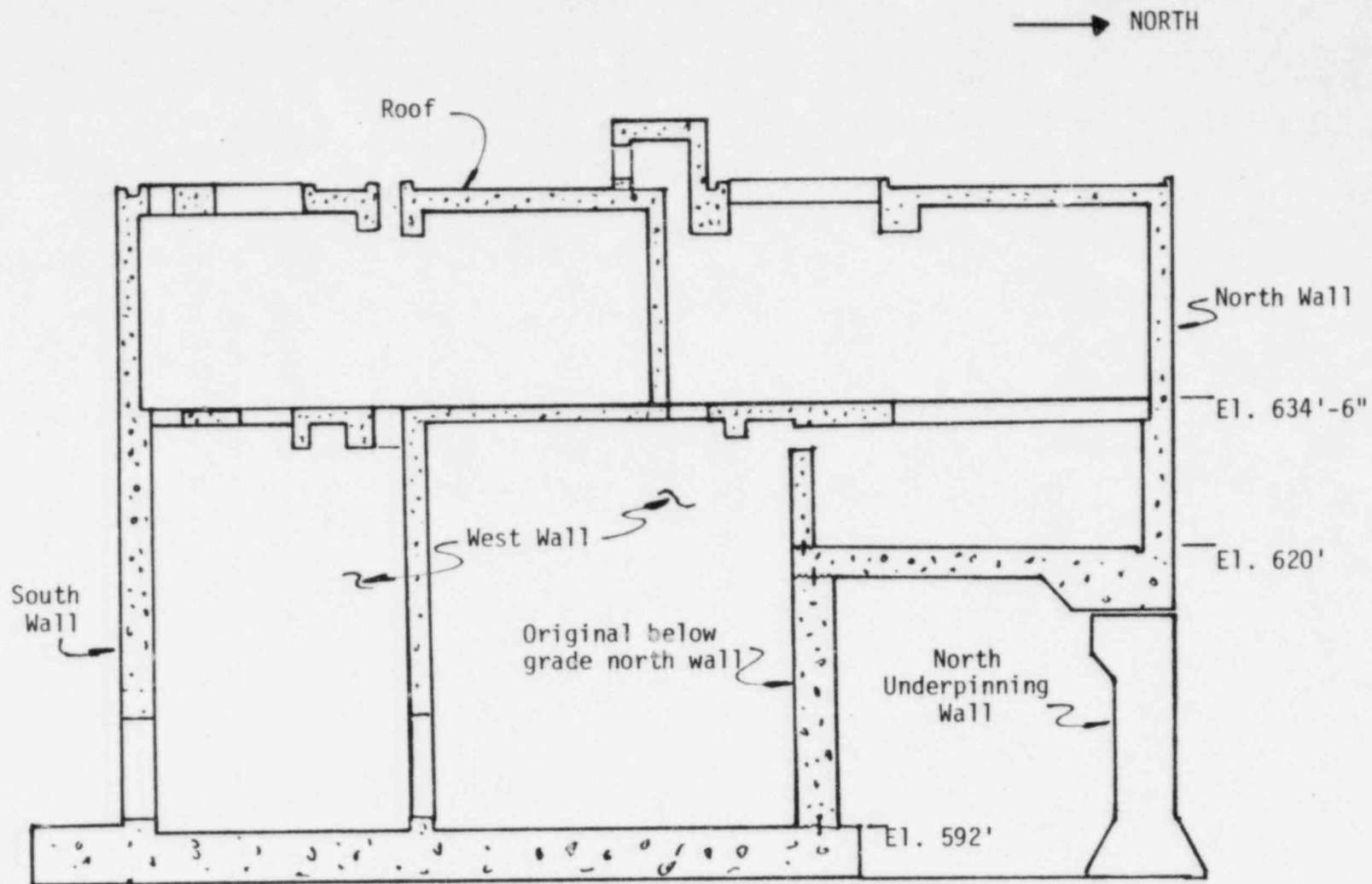


FIGURE IV-4-1. CROSS SECTION OF SERVICE WATER PUMP STRUCTURE LOOKING WEST

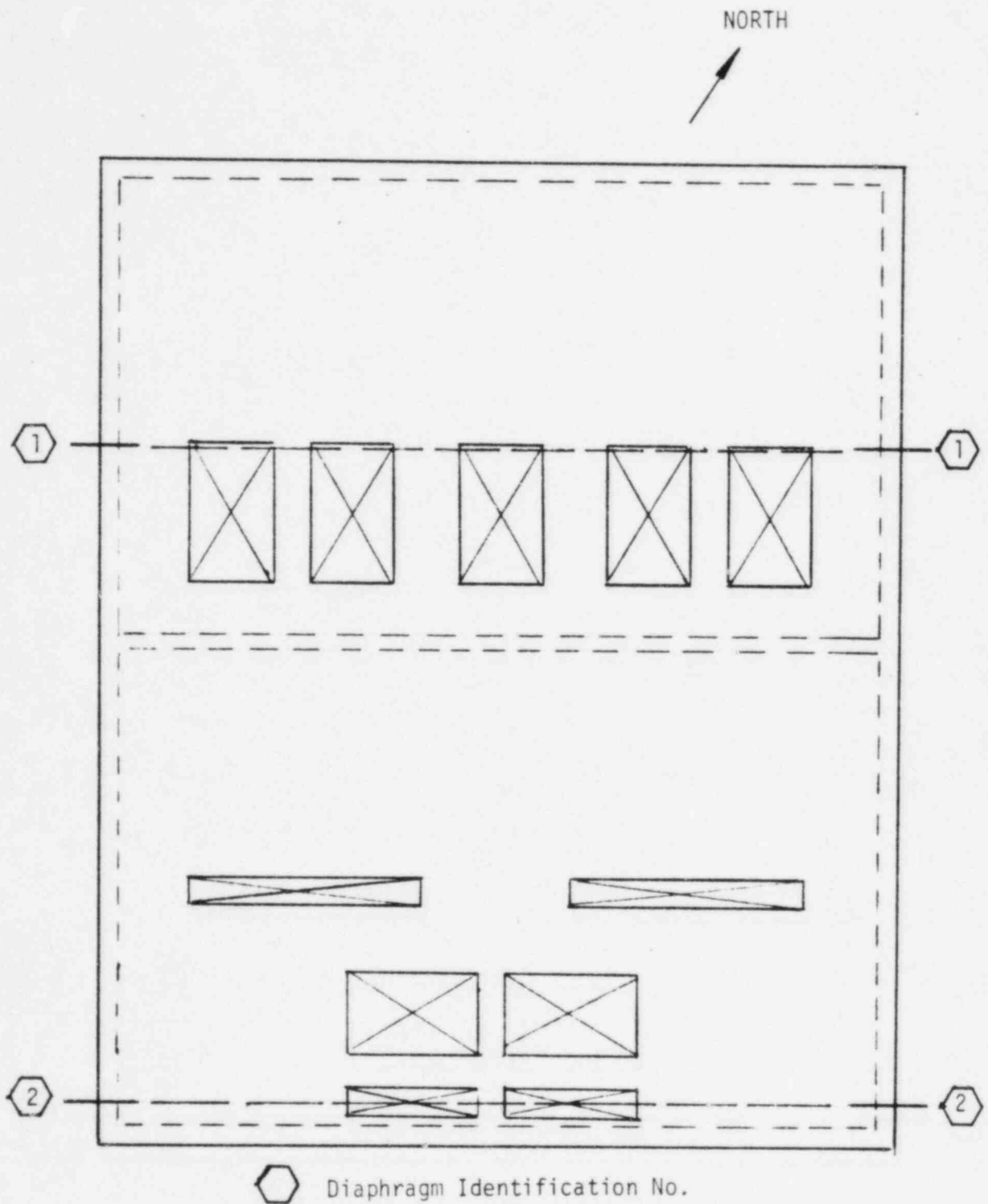


FIGURE IV-4-2. SERVICE WATER PUMP STRUCTURE ROOF
PLAN AT ELEVATION 656'-0"

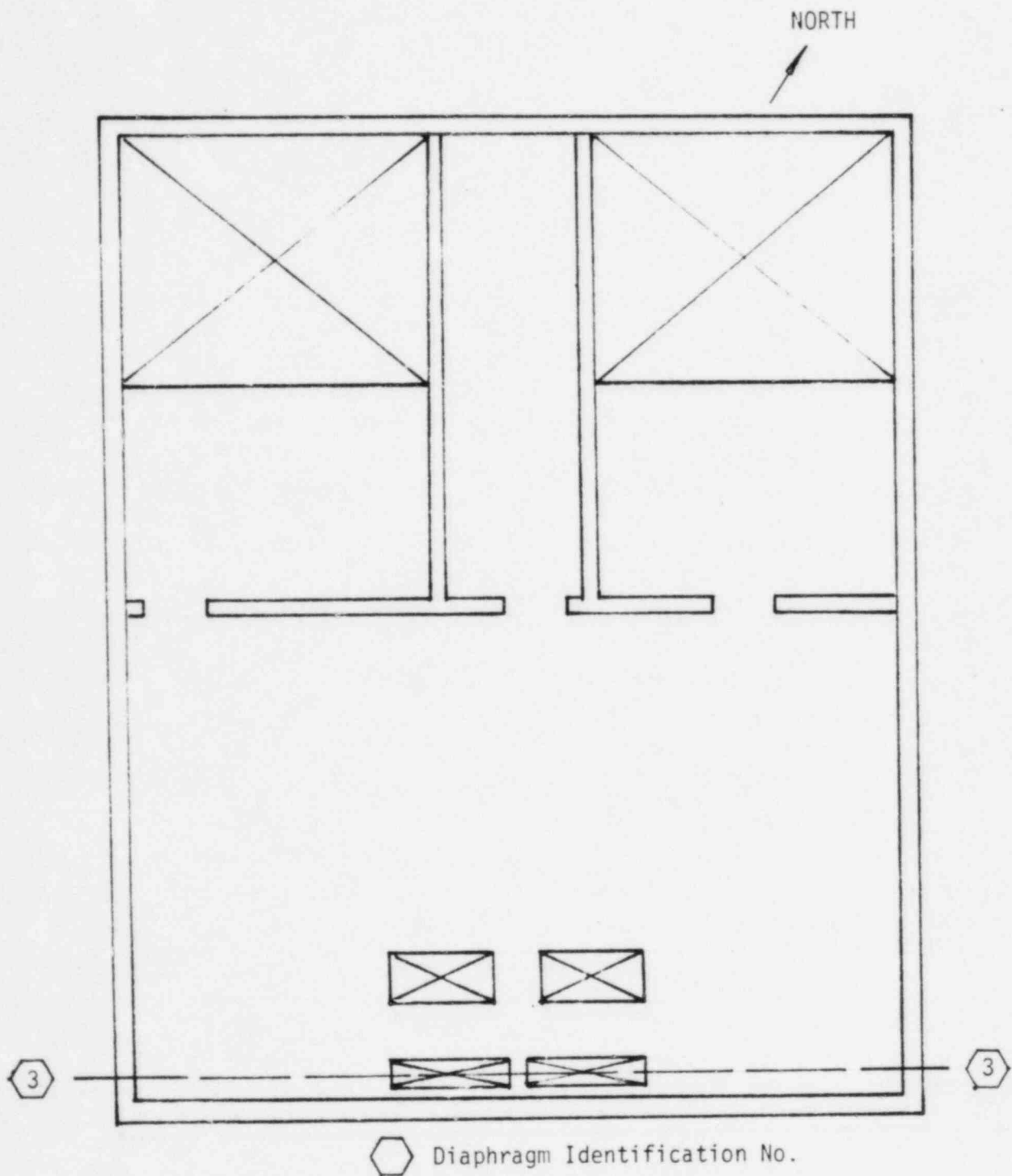


FIGURE IV-4-3. SERVICE WATER PUMP STRUCTURE FLOOR SLAB
AT ELEVATION 634'-6"

5. INPUT TO EQUIPMENT

Seismic input to equipment for the SMR was specified by in-structure response spectra. These spectra were generated by time history analysis using the coupled equations of motion of the structure as discussed in Section 8 of Volume I of this report. The time history input used was an artificial earthquake whose response spectra essentially envelop the SME ground response spectra at the original ground location. The development of the artificial earthquake is discussed in Section 2 of Volume I. The spectra developed for the service water pump structure considered the effects of multidirection excitation, the range of soil characteristics previously discussed, and the torsional response of the structure.

In-structure response spectra were developed for all locations of critical equipment within the service water pump structure. Spectra were generated for the lower bound, intermediate, and upper bound soil conditions. These spectra were smoothed and the peaks broadened ± 10 percent as discussed in Section 8 of Volume I. Final spectra were developed from an envelope of the three soil conditions. The in-structure response spectra developed for the service water pump structure include the effects of the torsional response of the structure. The method of accounting for the torsional components is described in Section 8.1 of Volume I. Enveloped in-structure response spectra for the North-South (N-S), East-West (E-W), and vertical directions for equipment damping ratios of 2, 3, 4, and 7 percent of critical are shown in Figures IV-A-1 through IV-A-12.

The vertical spectra as shown are applicable for piping and equipment located adjacent to major walls or on rigid slabs. For flexible floor slabs within the service water pump structure, vertical

input to equipment for the SME was determined by means of Vertical Amplification Factors (VAFs). These factors were developed from analyses of selected flexible floor slabs throughout the structure as described in Appendix A of Volume I. Damping ratios of 2 through 7 percent of critical are considered appropriate for the response of piping and equipment for the SME.

6. SUMMARY

As part of the Seismic Margin Review (SMR) conducted for Midland, the ability of the service water pump structure to withstand seismic excitation was investigated. The evaluation was conducted using new seismic response loads developed for the Seismic Margin Earthquake (SME) together with design dead, live settlement, and dynamic soil decrement loads (including jacking loads). The seismic loads were developed using a site specific earthquake for Midland as well as new soil-structure interaction parameters which reflect the site layering characteristics. Margins against code allowable values were calculated for selected elements throughout the structure.

The seismic excitation of the structure was specified in terms of site specific response spectra developed for the original ground location. These spectra have a peak ground acceleration of approximately 0.13g. The vertical component was specified as 2/3 of horizontal.

Soil properties used in the evaluation were based on soil profiles developed from geotechnical investigations conducted for the site. In addition, an intermediate profile based on approximately mid-range properties was used in the analysis. Layered site analyses for the intermediate soil profile were used to develop the soil impedance functions for the structure using an equivalent rectangular foundation plan. Effective shear moduli (G_{eff}) were calculated based on elastic half-space formulae by maintaining the same stiffness values as those obtained for the layered site analyses for the intermediate soil profile. Intermediate soil case results demonstrated that upper and lower bound G_{eff} values for this structure could be conservatively developed from auxiliary building results. The G_{eff} values were then used to develop global stiffnesses and dashpots for these soil cases. These parameters were then adjusted to account for embedment. Damping

values were conservatively limited to 75 percent of theoretical elastic half-space values for all degrees-of-freedom except rocking which was limited to 50 percent of theoretical.

The vertical beam lumped-mass dynamic model of the structure used for the SMR evaluation was the same model used for the seismic design. As part of the SMR evaluation, the model was reviewed for the general methodology used in its development and for adequacy to characterize the seismic response of the structure. The detailed calculations used in the model development were not checked as part of the SMR program.

Composite modal damping ratios were computed for the combined soil-structure model by matching structure response determined by directly integrating the coupled equations of motion to the dynamic response calculated by modal analysis techniques at several locations in the structure. Structural damping based on seven percent of critical was used throughout the structure.

Structural loads were determined using response spectrum modal analysis. Modal responses were combined on an SRSS basis except for closely spaced modes which were combined by the absolute sum. The responses to three directions of input motion were calculated independently and combined by the SRSS method.

In general, the upper bound soil condition resulted in maximum structural loads. Depending on the location within the structure, the intermediate or lower bound soil case could control in certain instances. The code margin evaluation was based on the maximum load condition in all instances. When compared with seismic design loads, the maximum SME loads were generally found to be lower with the exception of vertical axial loads and torsional response. Overall seismic loads determined by the structure response spectrum analyses were distributed to the resisting structural elements by methods appropriate to the load-resisting system being evaluated.

Overall seismic loads determined by the response spectrum analyses were distributed to the resisting structural elements by the rigid diaphragm approximation. This method is appropriate for the concrete shear wall and diaphragm system of the service water pump structure. Seismic shears and overturning moments were distributed to the individual walls in proportion to their relative rigidities. Seismic loads acting on the diaphragms were determined using information available from the load distributions to the individual walls. The shear walls and diaphragms were evaluated for seismic loads combined with loads due to normal operating conditions and dynamic soil decrements predicted by Bechtel's static analyses.

Capacities for the shear walls were developed in accordance with the ultimate strength design provisions contained in ACI 349-80. Shear walls were checked for their ability to resist in-plane shears and overturning moments. Code margins and F_{SME} factors were determined for the selected walls based on comparisons of the loads due to seismic, normal operating conditions, and dynamic soil decrements and the code ultimate strength capacities. The lowest code margins calculated were found to be 3.5 for walls governed by shear and 1.9 for walls governed by overturning. The SME would have to be increased by at least a factor of 1.8 before the code margin for any wall would be exceeded. To account for the effects of the reinforcement cutting allowance and available non-conformance reports indicating deviations from the construction specifications, the governing walls were reevaluated assuming the worst case possible due to these field conditions. Code margins of 2.8 and 1.6 were calculated for the walls governed by shear and overturning, respectively.

Diaphragm capacities were determined using ACI 349-80 criteria developed for shear walls. The diaphragms evaluated were found to be governed by shear. The lowest code margin for the diaphragms was found to be 3.2. For any diaphragm to reach code capacity, the SME would have to be increased by a factor of 4.2. Accounting for the worst case effects of the reinforcement cutting allowance led to a code margin of 2.7 for the governing diaphragm.

Capacities of both the north underpinning wall and their connectors to the existing structure were determined. The wall was evaluated using the same acceptance criteria developed for the shear walls. A code margin of 3.7 was found for this wall. Shear strength of the connectors between the north underpinning wall and the existing base mat above was calculated using the shear-friction provisions of ACI 349-80. The connectors were found to have a code margin of 3.8. The SME would have to be increased by a factor of 4.2 before the code capacity of the selected underpinning wall would be exceeded.

Code margins for the selected structural elements were all conservatively based on minimum specified material strengths and maximum seismic load cases. Reductions in loads to account for inelastic energy dissipation were not used for the service water pump structure. All code margins were determined to be greater than unity. Before the code capacity is reached for any service water pump structure element investigated, the SME would have to be increased by a factor of 1.8. It can, therefore, be concluded that the service water pump structure has more than sufficient structural capacity to resist the SME based on code criteria and significantly higher capacity before failure is expected.

In-structure response spectra were generated for the service water pump structure SMR by time-history analyses using the coupled equations of motion. Envelopes of spectra for the three soil cases and upper and lower bound relative soil stiffness conditions were generated for the two horizontal and the vertical directions. Horizontal in-structure response spectra were increased five percent at all frequencies to account for accidental torsion. Vertical amplification factors to account for the vertical response of flexible floor slabs were developed for use in the evaluation of piping and equipment located near the centers of the flexible slabs. The effects of out-of-plane moments and thermal gradients on in-plane wall and diaphragm capacities were considered.

REFERENCES

1. Final Safety Analysis Report (FSAR) Midland Plant - Units 1 and 2, Consumers Power Company.
2. TID-7024, Nuclear Reactors and Earthquakes, Lockheed Aircraft Corporation and Holmes and Narver, Inc., August, 1963.
3. Site-Specific Response Spectra, Midland Plant - Units 1 and 2, Part I, Response Spectra - Safe Shutdown Earthquake, Original Ground Surface, Weston Geophysical Corporation, prepared for Consumers Power Company, February, 1981.
4. Site-Specific Response Spectra, Midland Plant - Units 1 and 2, Part II, Response Spectra - applicable for the Top-of-Fill Material at the Plant Site, Weston Geophysical Corporation, prepared for Consumers Power Company, April, 1981.
5. Draft, Site-Specific Response Spectra, Midland Plant - Units 1 and 2, Part III, Seismic Hazard Analysis, Weston Geophysical Corporation, prepared for Consumers Power Company, Revision, May, 1980.
6. This reference has been deleted.
7. Bechtel submittal to NRC, "Service Water Pump Structure Seismic Model Revision 2 for Midland Units 1 and 2 Consumers Power Company", November 24, 1981.
8. Wong, H. L. and J. E. Luco, "Soil-Structure Interaction: A Linear Continuum Mechanics Approach (CLASSI), Report, CE, Department of Civil Engineering, University of Southern California, Los Angeles, California, 1980.
9. This reference has been deleted.
10. Woodward-McNeill and Associates, "Development of Soil-Structure Interaction Parameters Proposed - Units 2 and 3, San Onofre Nuclear Generating Station", San Onofre, California, January, 1974.
11. Richart, F. E., Hall, J. R. and R. A. Woods, Vibrations of Soils and Foundations, Prentice-Hall, Inc., New Jersey, 1970.
12. Kausel, E., and R. Ushijima, "Vertical and Torsional Stiffness of Cylindrical Footings", Massachusetts Institute of Technology, Research Report R79-6, February, 1979.
13. Veletsos, A. S., and Y. T. Wei, "Lateral and Rocking Vibration of Footings", Journal of the Soil Mechanics and Foundations Division, Proceedings of ASCE, EM5, pp 1381-1395, October, 1971.

REFERENCES (Continued)

14. Luco, J. E., and R. A. Westmann, "Dynamic Response of Circular Footings", Journal of the Engineering Mechanics Division, Proceedings of ASCE, EM5, pp 1381-1395, October, 1971.
15. Johnson, J. J., "SOILST - A Computer Program for Soil-Structure Interaction Analyses", General Atomic Company, GA-A15067, April, 1979.
16. Derecho, A. T. et al, "Analysis and Design of Small Reinforced Concrete Buildings for Earthquake Forces", Portland Cement Associations, 1974.
17. Letter correspondence from E. M. Hughes (Bechtel) to R. P. Kennedy (SMA), January 28, 1983, Subject: Midland Plant Units 1 and 2, Consumers Power Company Seismic Margin Review.
18. ACI 349-80, "Code Requirements for Nuclear Safety-Related Concrete Structures", American Concrete Institute, 1980.
19. Cardenas, A. E., et al, "Design Provisions for Shear Walls", ACI Journal, March, 1973.
20. "Tentative Provisions for the Development of Seismic Regulations for Buildings", National Bureau of Standards Special Publication 510, Applied Technology Council.
21. Bechtel Associates Professional Corporation, "Technical Specifications for Forming, Placing, Finishing and Curing of Concrete for the Consumers Power Company Midland Plant - Midland, Michigan", Spec. 7220-C-231Q, Revision 21, September 28, 1981.
22. This reference has been deleted.
23. Park, R. and T. Paulay, Reinforced Concrete Structures, John Wiley and Sons, 1975.
24. Veletsos, A. S., "Seismic Effects in Flexible Liquid Storage Tanks", Proceedings of Fifth World Conference on Earthquake Engineering, Rome, 1974.

APPENDIX IV-A

SERVICE WATER PUMP STRUCTURE IN-STRUCTURE RESPONSE SPECTRA

IV-A-1

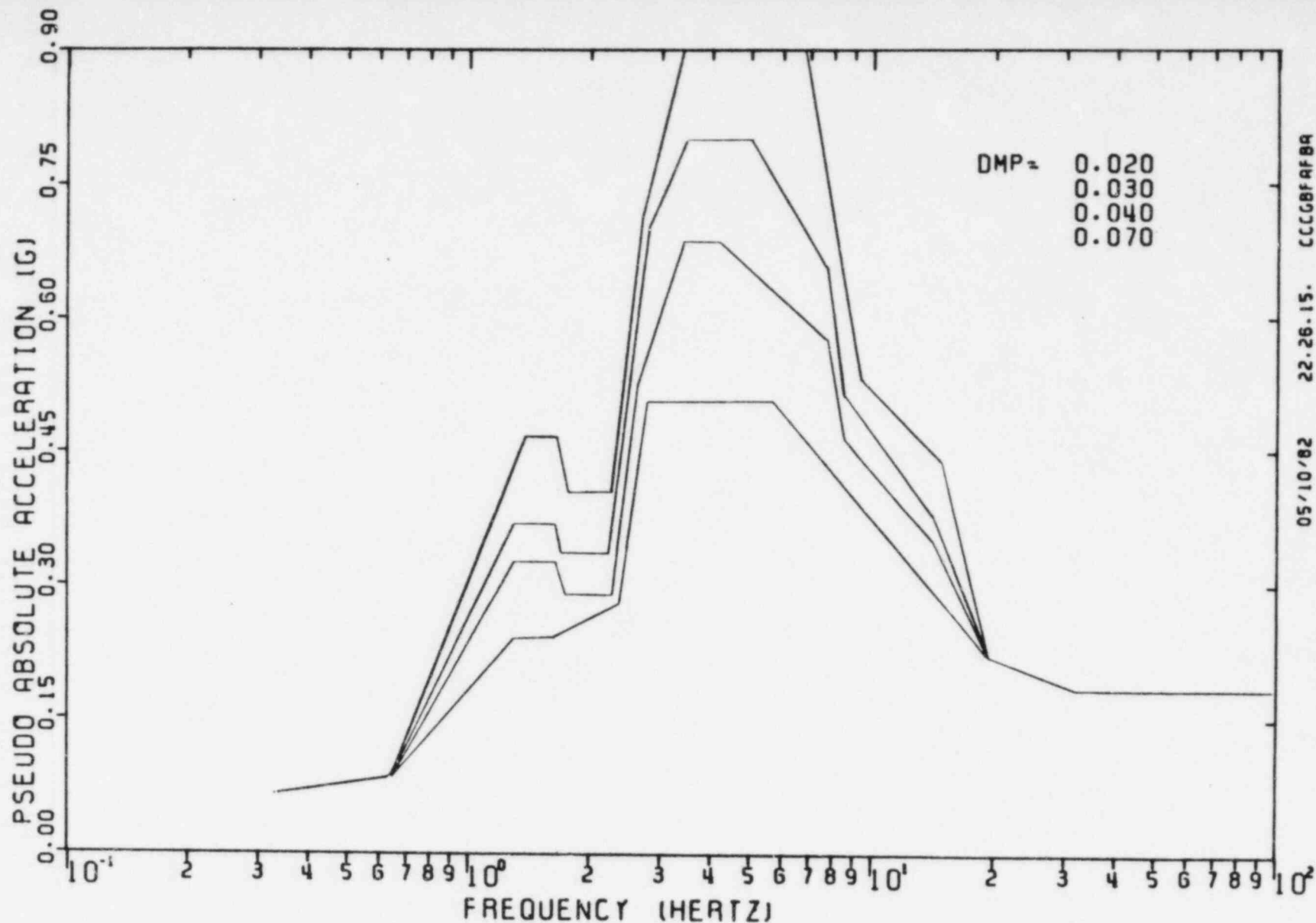


FIGURE IV-A-1. ENVELOPED SRSS COMBINED RESPONSE SPECTRA SW PUMP STRUCTURE, ELEVATION 589'-6", NORTH-SOUTH DIRECTION

05/10/82 22-26-15. CCCCBAFBA

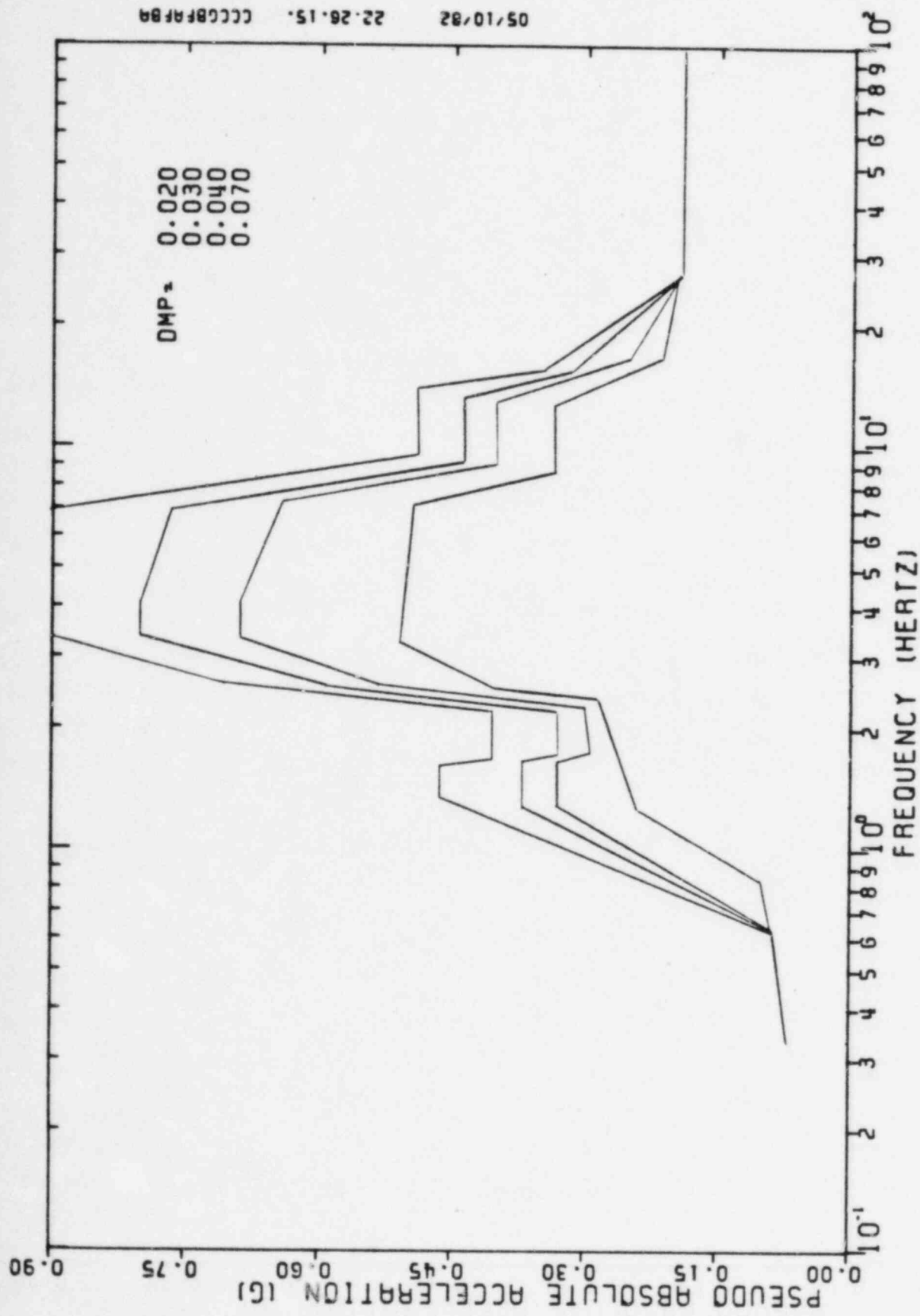


FIGURE IV-A-2. ENVELOPED SRSS COMBINED RESPONSE SPECTRA SW PUMP STRUCTURE, ELEVATION 589'-6", EAST-WEST DIRECTION

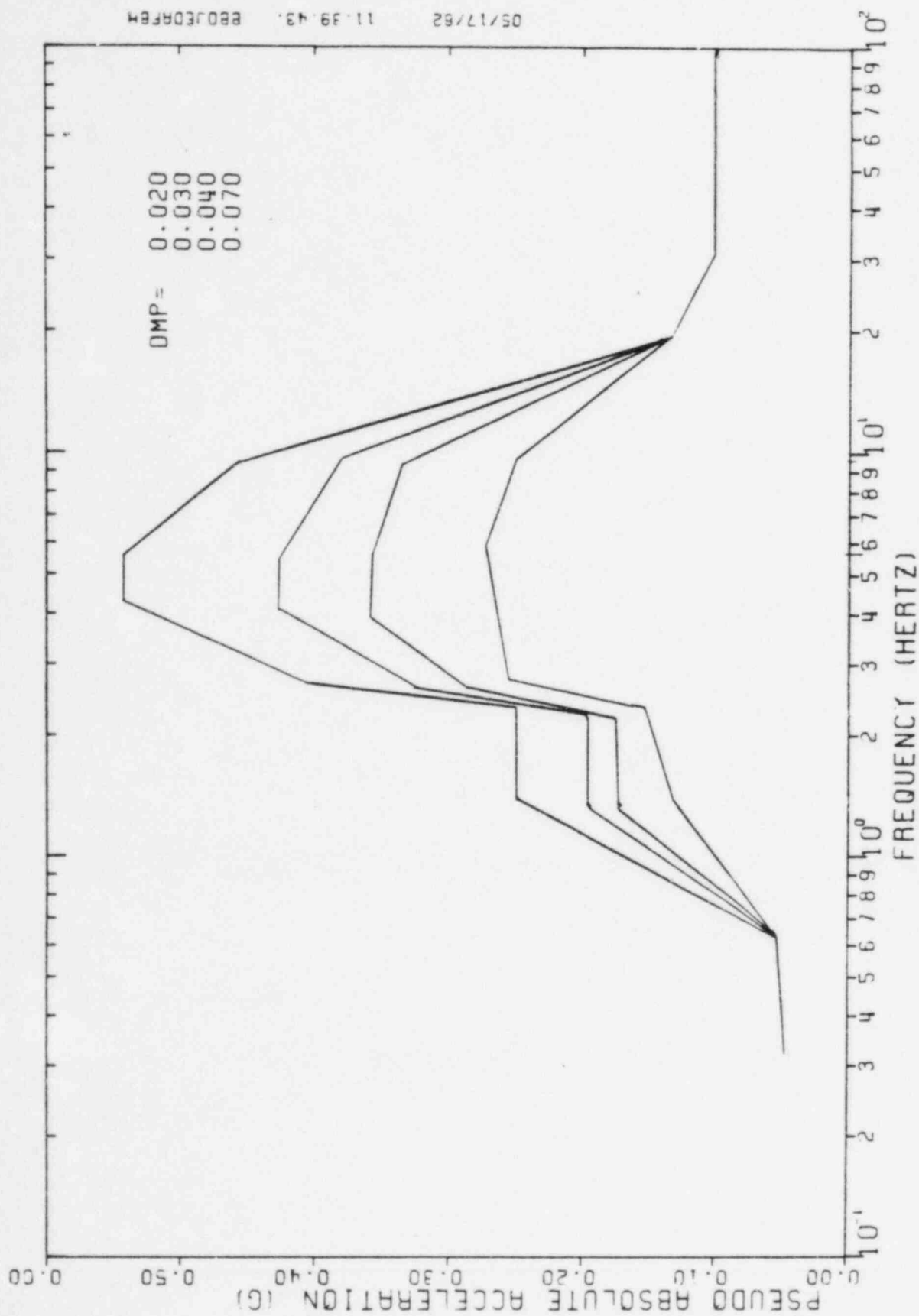


FIGURE IV-A-3. ENVELOPED SRSS COMBINED RESPONSE SPECTRA SW PUMP STRUCTURE,
ELEVATION 589'-6", VERTICAL DIRECTION

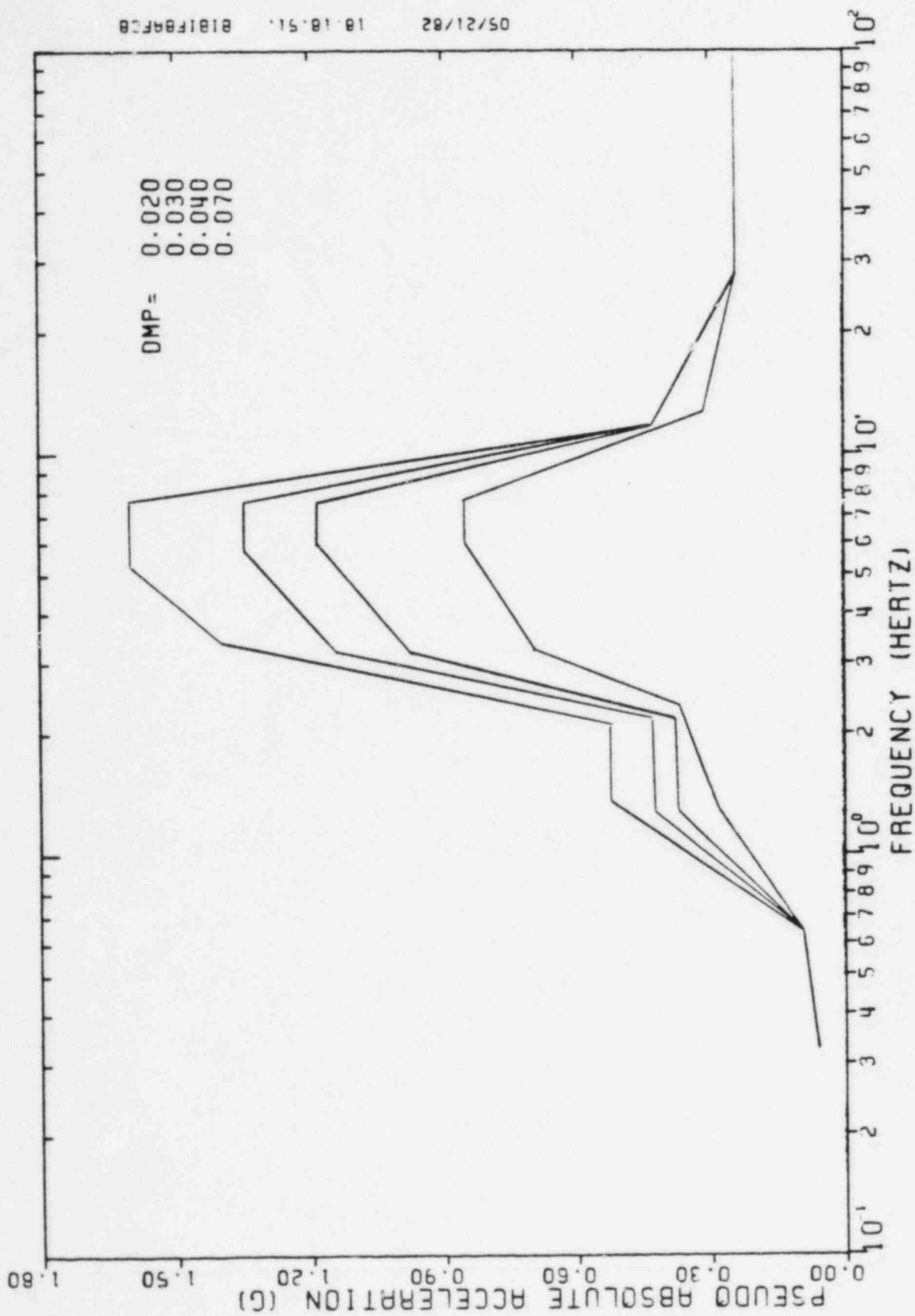


FIGURE IV-A-4. ENVELOPED SRSS COMBINED RESPONSE SPECTRA SW PUMP STRUCTURE, ELEVATION 620'-0", NORTH-SOUTH DIRECTION

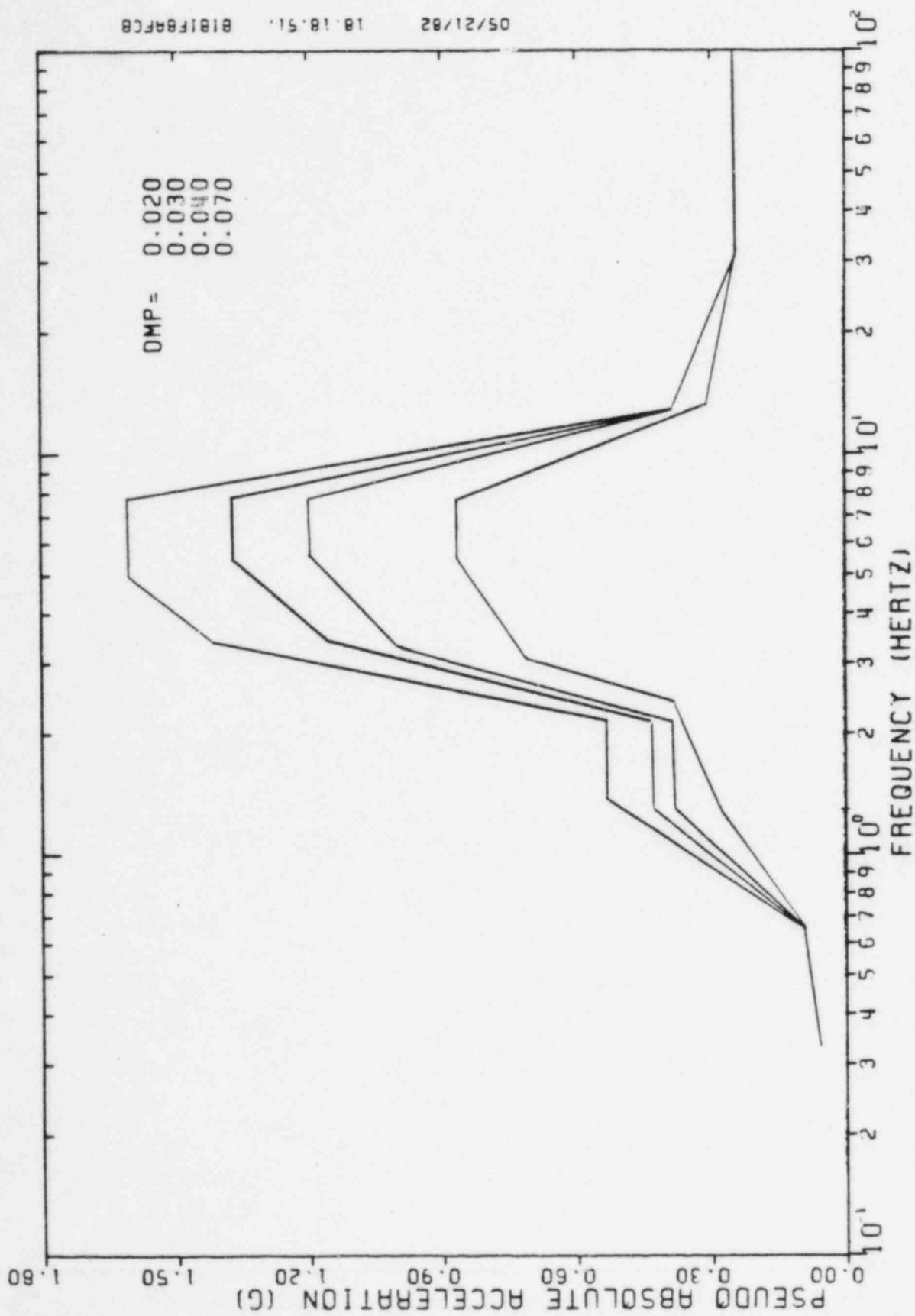


FIGURE IV-A-5. ENVELOPED SRSS COMBINED RESPONSE SPECTRA, SW PUMP STRUCTURE
ELEVATION 620'-0", EAST-WEST DIRECTION

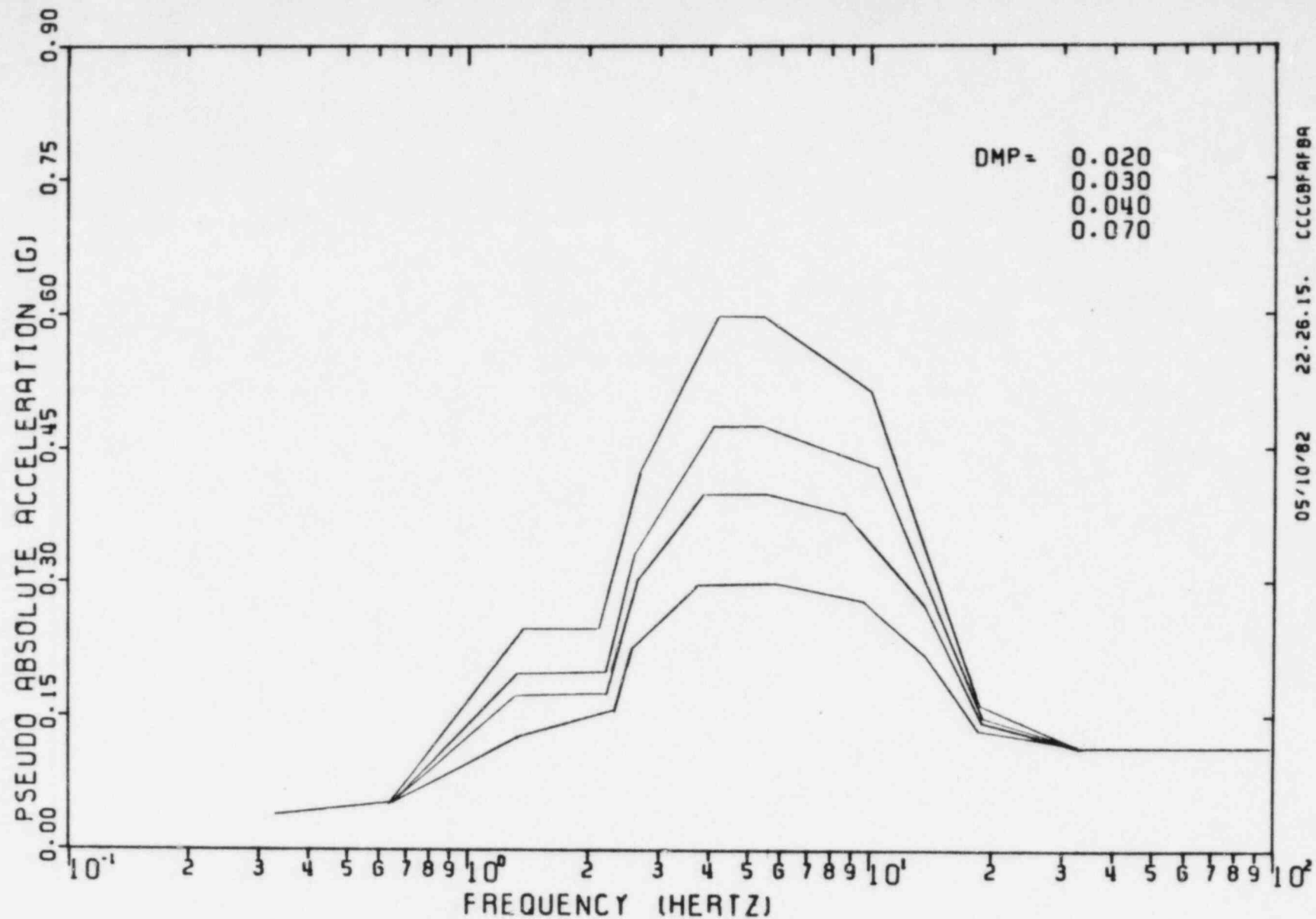


FIGURE IV-A-6. ENVELOPED SRSS COMBINED RESPONSE SEPCTRA SW PUMP STRUCTURE, ELEVATION 620'-0", VERTICAL DIRECTION

IV-A-7

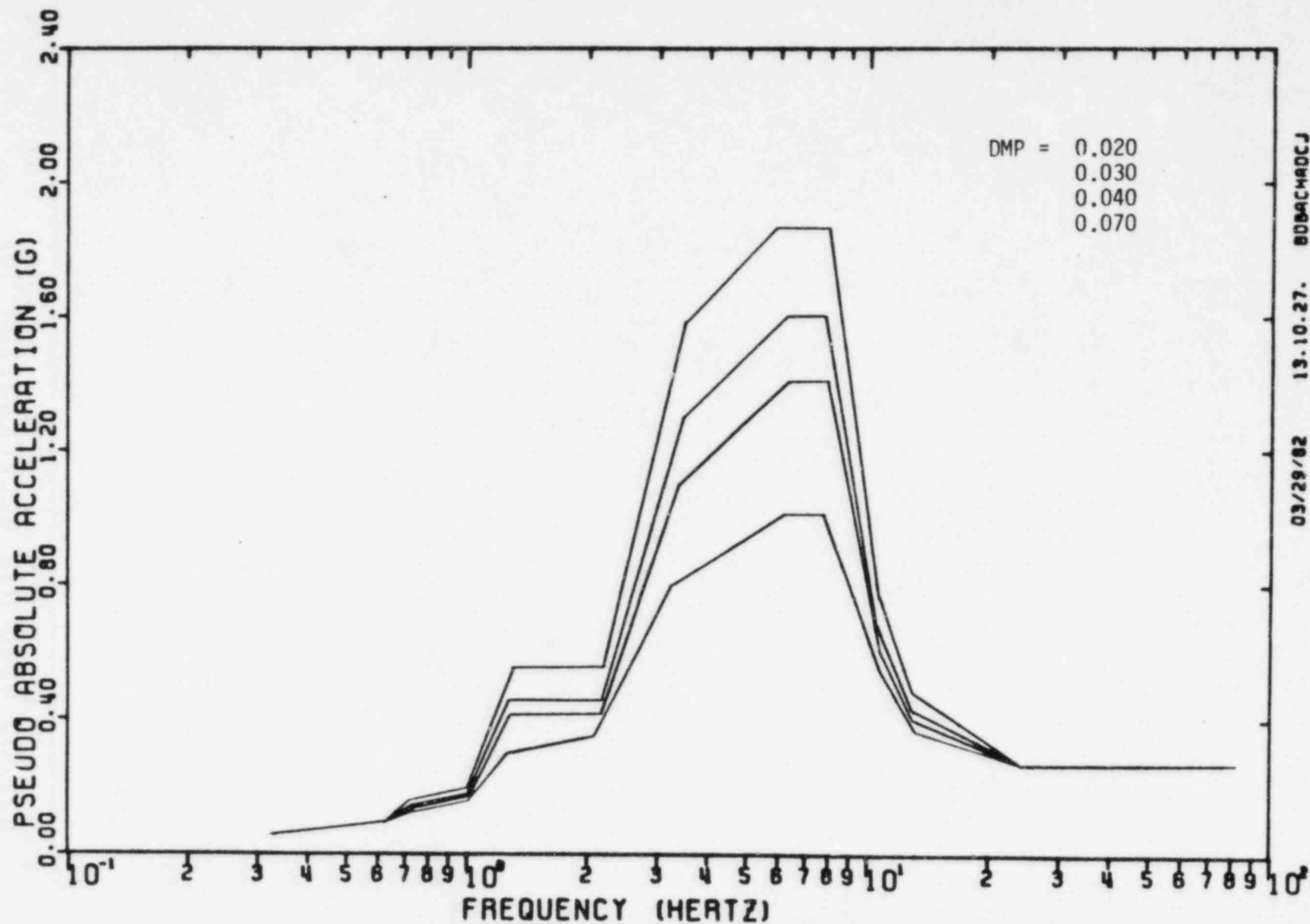


FIGURE IV-A-7. ENVELOPED SRSS COMBINED RESPONSE SPECTRA
SERVICE WATER PUMP STRUCTURE, ELEVATION 634'-6"
NORTH-SOUTH DIRECTION

03/29/82 13.10.27. 80BACHADOCJ

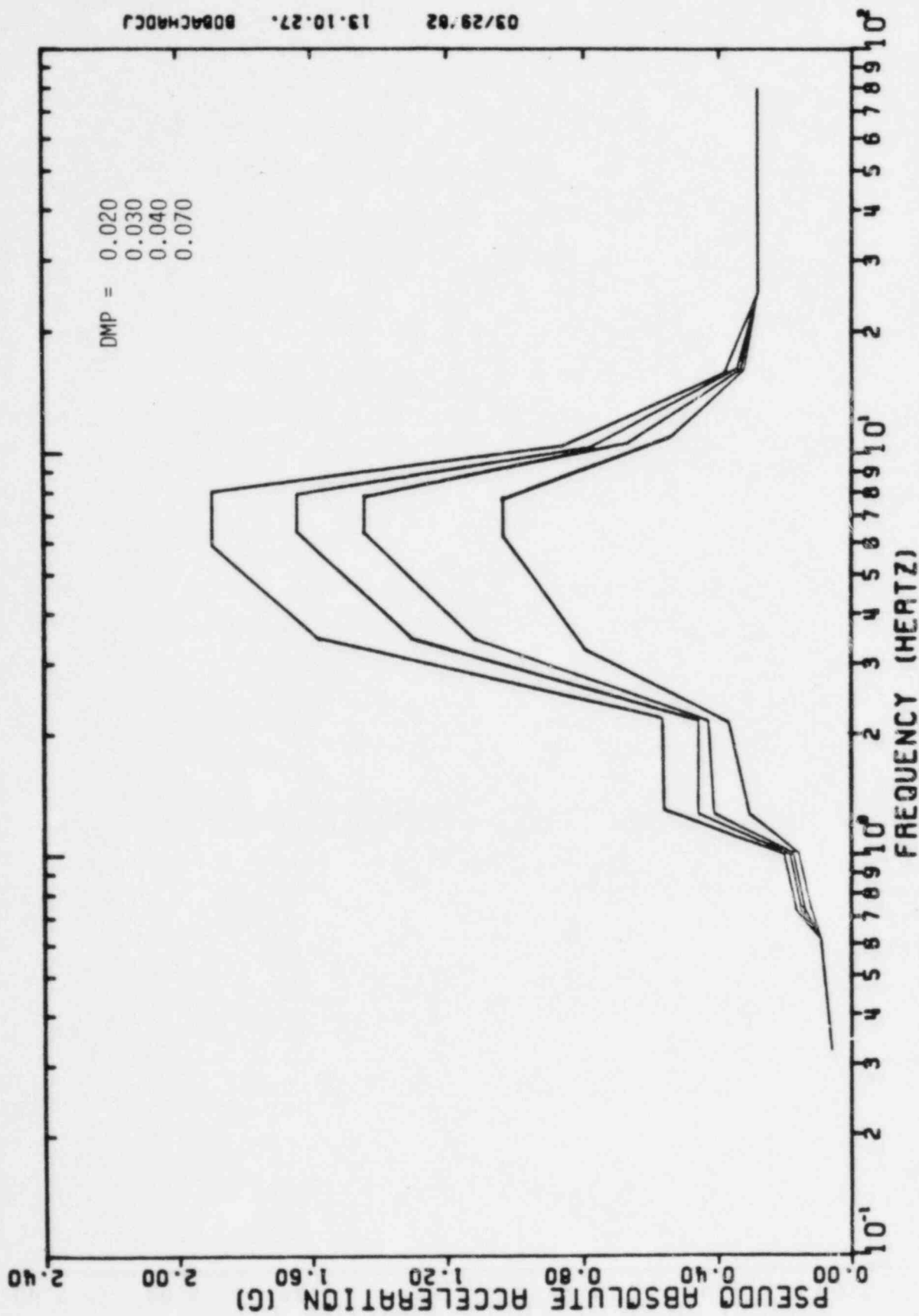


FIGURE IV-A-8. ENVELOPED SRSS COMBINED RESPONSE SPECTRA
SERVICE WATER PUMP STRUCTURE, ELEVATION 634'-6"
EAST-WEST DIRECTION

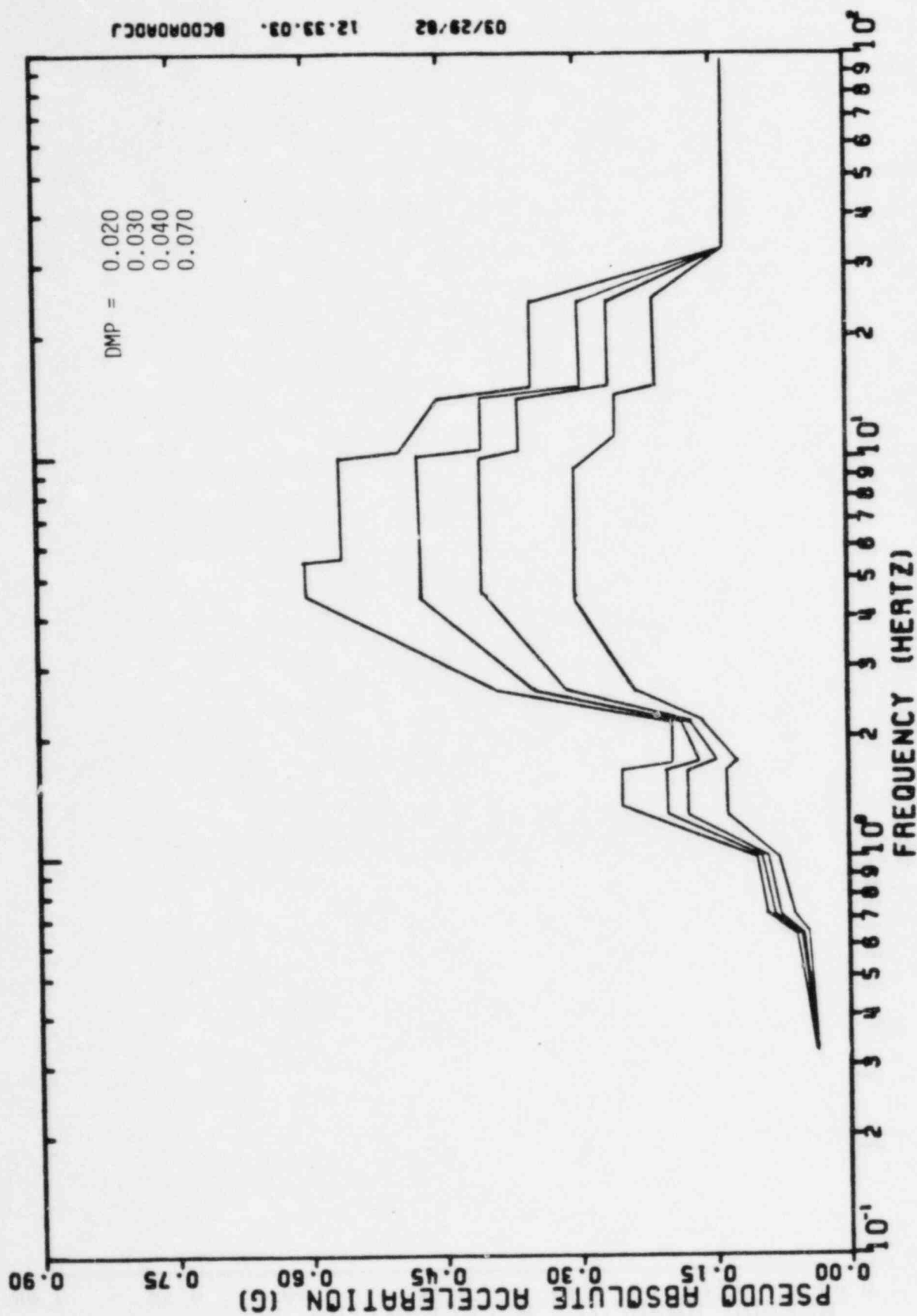


FIGURE IV-A-9. ENVELOPED SRSS COMBINED RESPONSE SPECTRA
SERVICE WATER PMUM STRUCTURE, ELEVATION 634'-6"
VERTICAL DIRECTION

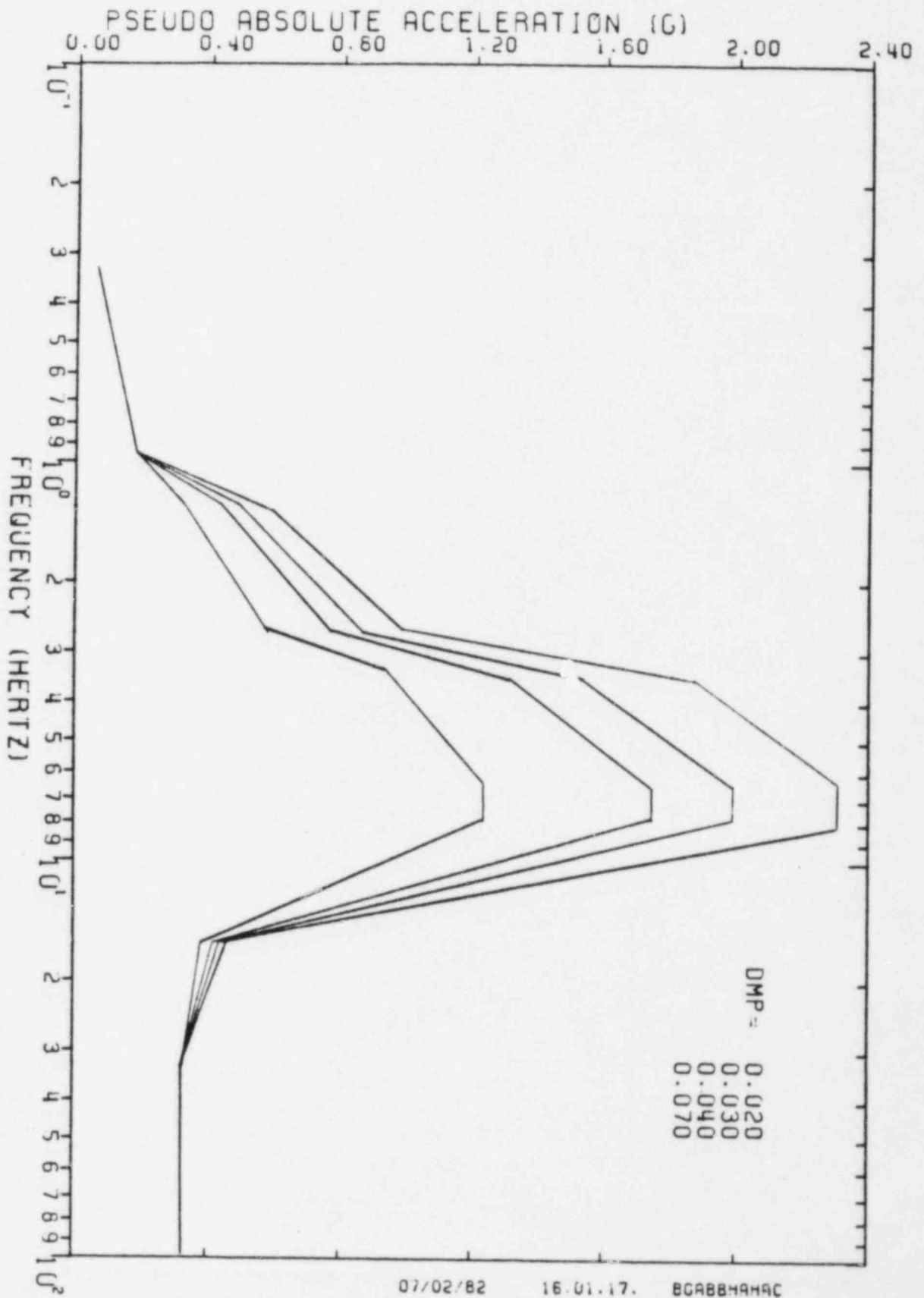


FIGURE IV-A-10. ENVELOPED SRSS COMBINED RESPONSE SPECTRA SERVICE WATER PUMP
STRUCTURE, ELEVATION 656'-0", NORTH-SOUTH DIRECTION

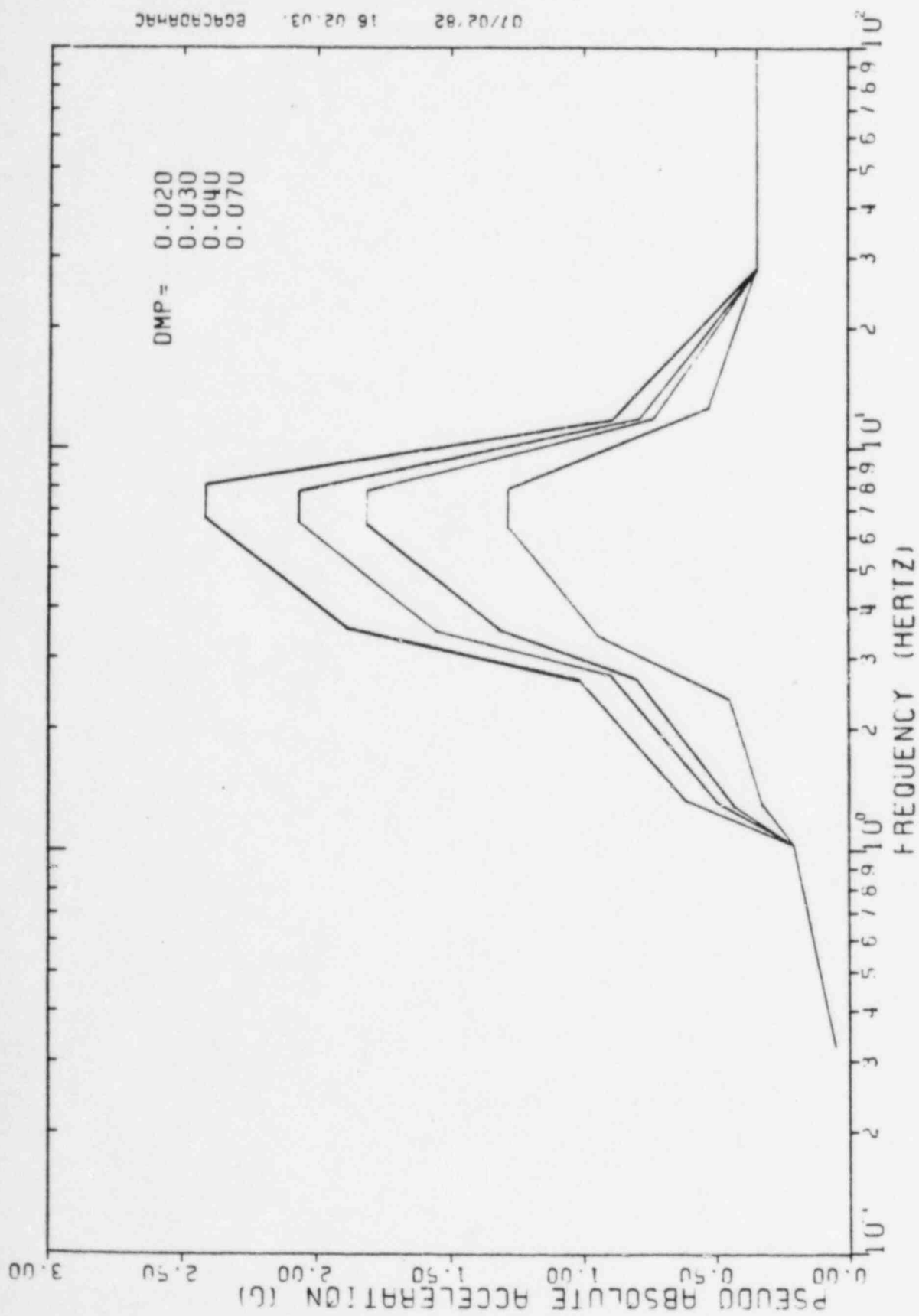


FIGURE IV-A-11. ENVELOPED SRSS COMBINED RESPONSE SPECTRA, SERVICE WATER PUMP STRUCTURE, ELEVATION 656'-0", EAST-WEST DIRECTION

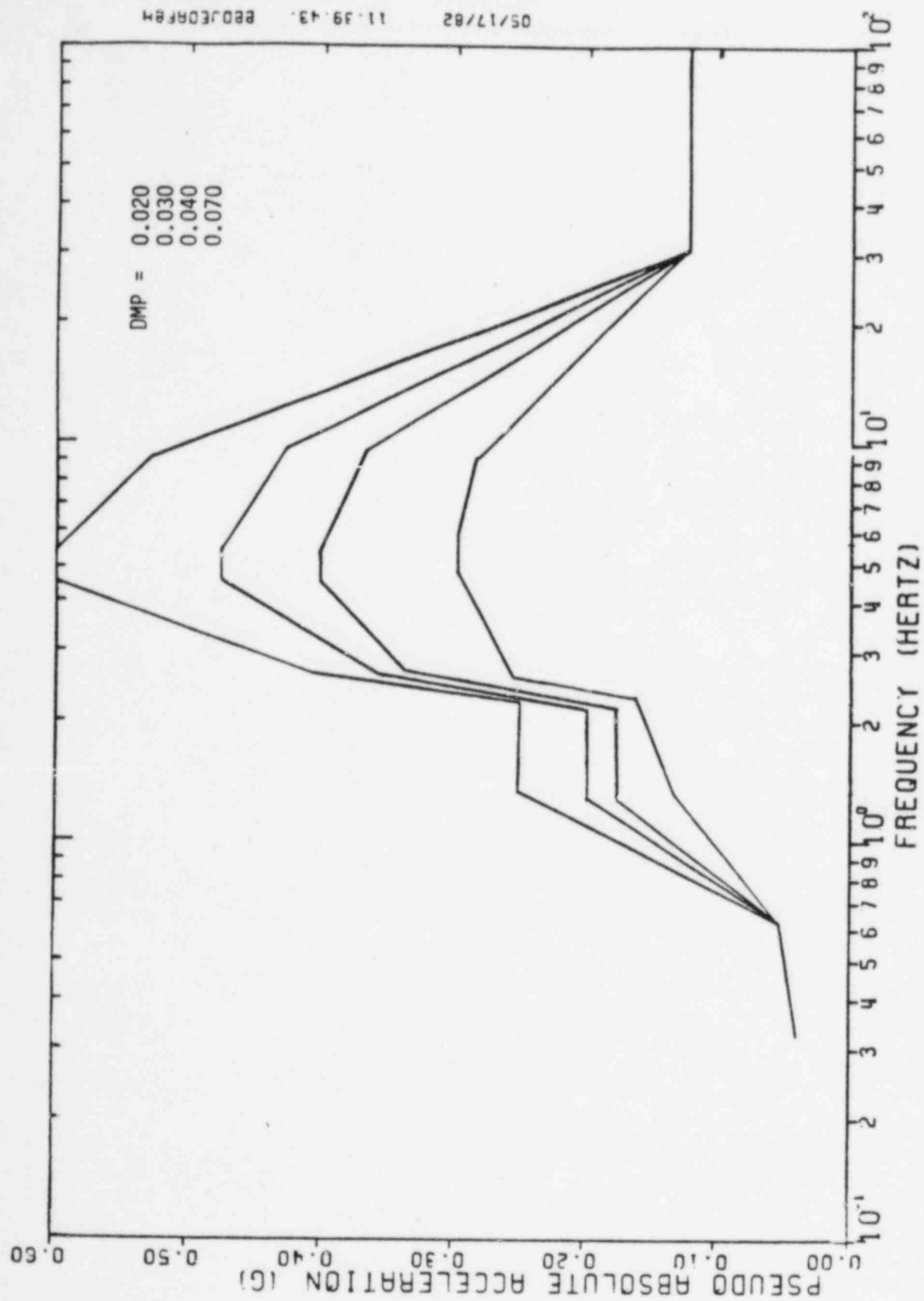


FIGURE IV-A-12. ENVELOPED SRSS COMBINED RESPONSE SPECTRA, SERVICE WATER PUMP STRUCTURE, ELEVATION 656'-0", VERTICAL DIRECTION